

Alma Mater Studiorum – Università di Bologna  
in cotutela con Università di RWTH Aachen

**DOTTORATO DI RICERCA IN**

**CHIMICA**

**Ciclo XXXI**

**Settore Concorsuale: 03/C2**

**Settore Scientifico Disciplinare: CHIM/04**

**DEVELOPMENT OF INNOVATIVE PROCESSES AND CATALYSTS FOR THE  
VALORISATION OF BIO-OIL**

**Presentata da: Aisha Matayeva**

**Coordinatore Dottorato**

**Prof. Aldo Roda**

**Supervisore**

**Prof. Francesco Basile**

**Co-supervisore**

**Prof. Fabrizio Cavani**

**Dr. Daniele Bianchi**

**Supervisore**

**Prof. Regina Palkovits**

**Esame finale anno 2019**

*“Development of innovative processes and catalysts for the valorisation of bio-oil”*

**Der Fakultät für Mathematik, Informatik und Naturwissenschaften der RWTH Aachen  
University vorgelegte Dissertation zur Erlangung des akademischen Grades einer  
Doktorin der Naturwissenschaften**

von

*M.Sc. AISHA MATAYEVA*

aus *QARAGHANDY, KASACHSTAN*

This work was funded by SINCHEM Joint Doctorate Programme-Erasmus Mundus Action (framework agreement N° 2013-0037; specific grant agreement n°2015-1600/001-001-EMJD).



## CONTENTS:

<b><u>ACKNOWLEDGMENTS</u></b> .....	<b>I</b>
<b><u>LIST OF FIGURES</u></b> .....	<b>II</b>
<b><u>LIST OF TABLES</u></b> .....	<b>IV</b>
<b><u>ABSTRACT</u></b> .....	<b>V</b>
<b><u>CHAPTER 1. INTRODUCTION</u></b> .....	<b>1</b>
1.1 MOTIVATION: RECOVERING ENERGY FROM WASTE .....	1
1.2 FUNDAMENTALS OF HTL .....	3
1.3 WASTE BIOMASS COMPOSITION .....	4
1.4 DISTRIBUTION OF NITROGEN IN HTL PRODUCT STREAMS .....	6
1.5 CHEMISTRY OF HYDRODENITROGENATION (HDN) .....	7
1.6 ENI SLURRY TECHNOLOGY (EST) UPGRADING OF HTL OIL .....	10
1.7 AIMS AND A ROADMAP OF THE THESIS .....	15
<b><u>CHAPTER 2. LITERATURE REVIEW</u></b> .....	<b>17</b>
2.1 EFFECT OF OPERATING CONDITIONS ON THE BIO-OIL YIELD AND NITROGEN CONTENT OF BIO-OIL PRODUCED FROM ALGAE HTL .....	17
2.2 MECHANISM STUDY OF HTL .....	21
2.3 HTL OF MICROBIAL BIOMASS .....	25
<b><u>CHAPTER 3. EXPERIMENTAL DESIGN AND PROCEDURE</u></b> .....	<b>29</b>
3.1 HTL OF MODEL COMPOUNDS .....	29
3.2 CATALYTIC LIQUEFACTION EXPERIMENTS .....	33
3.3 HTL OF OLEAGINOUS YEASTS .....	35
3.4 HTL OF LIAMOCINS .....	36
<b><u>CHAPTER 4. RESULTS AND DISCUSSIONS</u></b> .....	<b>38</b>
<b>4.1 HTL OF AMINO ACIDS</b> .....	<b>38</b>
4.1.1 LEUCINE HTL .....	38
4.1.2 PHENYLALANINE HTL .....	47
4.1.3 THE EFFECT OF ACETIC ACID IN IMPROVEMENT OF ENERGY YIELDS .....	55
4.1.4 HTL OF PHENYLALANINE IN BINARY MIXTURES WITH TRIPALMITIN AND GLUCOSE .....	60
4.1.5 CONCLUSION .....	66
<b>4.2 HTL OF ALBUMIN IN BINARY WITH STARCH AND TRIPALMITIN</b> .....	<b>67</b>
4.2.1 BIO-OIL YIELDS, ELEMENTAL ANALYSIS, HHV AND ER OF BIO-OIL PRODUCTS .....	67
4.2.2. BIO-OIL CHARACTERIZATION. ....	70

4.2.3 THE EFFECT OF LIPID DOSAGE ON THE TYPE OF NITROGEN COMPOUNDS OF THE PRODUCED BIO-OIL .....	75
4.2.4 CONCLUSION.....	80
<b>4.3 CATALYTIC HYDROTHERMAL LIQUEFACTION OF AMINO ACID .....</b>	<b>81</b>
4.3.1 HTL PRODUCTS STREAMS YIELDS .....	81
4.3.2 HTL PRODUCT STREAM CHARACTERIZATION .....	82
4.3.3 CONCLUSION.....	85
<b>4.4 HTL OF OLEAGINOUS YEAST .....</b>	<b>86</b>
4.4.1 HTL PRODUCT YIELDS, ELEMENT ANALYSES AND HHV OF .....	86
4.4.2 CHEMICAL COMPOSITION OF BIO-OILS .....	87
4.4.3 CONCLUSION.....	88
<b>4.5 HTL OF LIAMOCINS .....</b>	<b>90</b>
4.5.1 CHARACTERIZATION OF THE LIAMOCINS .....	90
4.5.2 CHARACTERIZATION OF BIO-OIL .....	91
4.5.3 HTL OF LIAMOCINS .....	94
4.5.4 SOLVOLYTIC LIQUEFACTION .....	98
4.5.5 CATALYTIC HYDROTHERMAL LIQUEFACTION .....	100
4.5.6 PURIFICATION OF LIAMOCINS .....	101
4.5.6 CONCLUSION.....	102
<b><u>CHAPTER 5. CONCLUSION AND FUTURE WORK.....</u></b>	<b><u>104</u></b>
<b><u>APPENDIX A. SUPPORTING INFORMATION TO SECTION 4.1.4. ....</u></b>	<b><u>106</u></b>
<b><u>APPENDIX B. SUPPORTING INFORMATION TO SECTION 4.5.3. ....</u></b>	<b><u>107</u></b>
<b><u>REFERENCES.....</u></b>	<b><u>108</u></b>



## Acknowledgments

My sincere thanks go to many people who have helped me and supported me through this study. I would like to express my deepest gratitude to my supervisors, Prof. Francesco Basile and Prof. Fabrizio Cavani (University of Bologna, Italy), Prof. Regina Palkovits (RWTH Aachen University), Dr. Daniele Bianchi (Renewable Energy and Environmental R&D Center, Istituto Eni Donegani). Without their guidance, and support, this study would have not been possible.

I am grateful to the SINCHEM consortium members that made possible this European PhD framework. I have enjoyed three wonderful years and have always been feeling that I am living in a big warm family.

I would like to thank all the people at the University of Bologna, the staff, all my colleagues, for their support and help.

I am very thankful to the staff and colleagues at ENI Donegani for their help and support and a great year of working together. Especially, I would like to express my gratitude to Stefano Chiaberge, Mauro Burattini, Silvia Spera, Alessandro Oldani, Manuela Grande for helping me with the performance of FTICR MS,  $^{13}\text{C}$  solid state NMR, element analysis, and TOC/TN analyses.

I am very grateful to all my colleagues at RWTH Aachen University for their help and training on science as well as German culture. I would like to thank Elke Biener, Heike Fickers-Boltz, Hannelore Eschmann, Wolfgang Falter, and Simon Petring for performing GC, GC-MS, and HPLC-measurements.

I would like to thank all my friends all around the globe that have encouraged me throughout these years. Finally, to my family in Kazakhstan.

## List of Figures

Figure 1. Biomass conversion processes .....	1
Figure 2. Phase diagram of water superimposed with different hydrothermal water technologies. <i>Adapted from</i> [13].....	3
Figure 3. HDN network of pyridine. <i>Adapted from</i> [61].....	8
Figure 4. HDN network of piperidine. <i>Adapted from</i> [42]. .....	9
Figure 5. The HDN reactivity of the types of the nitrogen compounds depending on the severity of the reaction conditions. <i>Adapted from</i> [44] .....	10
Figure 6. Simplified EST process scheme. <i>Adapted from</i> [46].....	11
Figure 7. GC-MS of HTL oil before (a) and after (b) EST upgrading .....	12
Figure 8. APPI+ FTICR MS spectra of HTL bio-oil (a) before and (b) after EST upgrading	13
Figure 9. Cn versus DBE for main N1 and N2 class components in the bio-oil (a) before and (b) after EST upgrading. ....	13
Figure 10. Nature of nitrogen species presented in waste derived oils.....	15
Figure 11. Liamocins structure .....	28
Figure 12. The effect of solvents and catalysts on HTL products stream yields.....	38
Figure 13. The composition of bio-oils from Leucine HTL .....	41
Figure 14. Nitrogen element distribution to products streams of Leucine HTL.....	42
Figure 15. <sup>13</sup> CPMAS NMR analysis of leucine before and after HTL treatment.....	44
Figure 16. Solid residue formation from amino acid HTL .....	44
Figure 17. TOC and TN analyses of aqueous phase.....	45
Figure 18. The effect of solvents and catalysts on the products streams yields of Phenylalanine HTL.....	47
Figure 19. Nitrogen recovery in HTL product streams.....	49
Figure 20. The main components presented in the bio-oil from Phenylalanine HTL .....	50
Figure 21. <sup>13</sup> CPMAS NMR analysis of solid residue from Phenylalanine HTL.....	51
Figure 22. TOC and TN analyses of aqueous phase of Phenylalanine HTL .....	52
Figure 23. Chemical pathway of Glutamine HTL .....	54
Figure 24. Distribution of acetic acid into Phenylalanine HTL product streams .....	55
Figure 25. Carbon element recovery in Phenylalanine HTL product streams, % .....	56
Figure 26. Chemical pathway of Phenylalanine HTL .....	57
Figure 27. Cn vs DBE for main class components in the bio-oil from Phenylalanine HTL: a) in water b) water/acetic acid (95/5 % v/v) .....	58
Figure 28. Chemical pathway of Leucine HTL .....	59
Figure 29. Carbon and nitrogen element distributions in products streams of Leucine HTL, % .....	60
Figure 30. Chemical pathway of Phenylalanine/Glucose binary mixture HTL.....	62
Figure 31. Alkylated pyrazines in the bio-oil from Phenylalanine/Glucose HTL.....	63
Figure 32. Heteroatoms class components of bio-oil derived from HTL of Phenylalanine/Glucose binary mixture .....	64
Figure 33. DBE versus Cn distributions for N2 and O1N1 class compounds in bio-oil of phenylalanine/glucose binary mixture HTL .....	65

Figure 34. The carbon recovery (CR, %) and nitrogen recovery (NR, %) in the bio-oil .....	69
Figure 35. Heteroatom class components of the bio-oil from Albumin HTL. ....	70
Figure 36. Cn vs DBE plots for the main classes found in bio-oil samples from Albumin HTL .....	71
Figure 37. Heteroatom class components of bio-oil from Albumin/Starch HTL.....	72
Figure 38. Cn vs DBE plots for the main classes found in bio-oil produced from Albumin/Starch HTL .....	73
Figure 39. Reaction pathway of Albumin/Tripalmitin binary mixture.....	74
Figure 40. GC-MS chromatograms of bio-oil samples with a) 20 % triolein content; b) 33 % triolein content .....	76
Figure 41. FTICR ESI+ mass spectrum of bio-oil samples from Albumin/Starch/Tripalmitin ternary mixture a) 20 % triolein content; b) 33 % triolein content.....	77
Figure 42. FTICR ESI+ based distribution of the main FAAs species as protonated ions.....	78
Figure 43. FTICR ESI+ Mass spectrum expansion of the mass range 160-230 Da, specific for N, O-containing alkylaromatic compounds (NAs) a) 20 % triolein content and b) 30 % triolein content .....	79
Figure 44. Main NAs components grouped in classes according to their heteroatom content. a) 20 % triolein content; b) 33 % triolein content.....	79
Figure 45. Product streams yields from catalytic hydrothermal liquefaction of Leucine.....	82
Figure 46. Bio-oil composition from catalytic hydrothermal liquefaction of Leucine.....	83
Figure 47. Aqueous phase composition of catalytic hydrothermal liquefaction of Leucine ...	84
Figure 48. Nitrogen species presented in HTL oil from oleaginous yeast.....	88
Figure 49. DBE versus Cn for N2 and O2N1 class compounds in bio-oil products .....	88
Figure 50. TLC of liamocins before and after saponification.....	90
Figure 51. The structure of ML and BHDL.....	92
Figure 52. COSY, HMBC, HSCQ NMR of bio-oil produced form HTL of liamocins .....	93
Figure 53. Reaction pathway of liamocins HTL.....	94
Figure 54. 1H and 13C NMR analyses of ML HTL at 250 °C.....	97
Figure 55. Pictorial view of the solvation of 3,5-DHDA in water and hexane solvents .....	99
Figure 56. The possible formation of GBL and 1,3-octadiene .....	100

## List of Tables

Table 1. Comparison of two thermochemical processes for bio-oil production.....	2
Table 2. The distribution of nitrogen to products .....	7
Table 3. Bond energies (kJ/mol) for commonly encountered bonds [40] .....	8
Table 4. Summary of studies on catalytic liquefaction.....	20
Table 5. Summary of studies on solvolytic liquefaction.....	21
Table 6. Summary of studies on HTL of amino acids .....	22
Table 7. The element analysis, HHV and ER of bio-oils of Leucine HTL.....	40
Table 8. The element analysis, HHV and ER of solid residue of Leucine HTL .....	43
Table 9. Aqueous phase composition of Leucine HTL .....	46
Table 10. The element analysis, HHV and ER of bio-oils of Phenylalanine HTL.....	48
Table 11. The element analysis and HHV of solid residue of Phenylalanine HTL.....	51
Table 12. Aqueous phase composition of Phenylalanine HTL.....	53
Table 13. Phenylalanine HTL main product yield and partition .....	58
Table 14. Bio-oil yields, elemental analysis, HHV and ER of bio-oil products from binary mixtures of Phenylalanine/Tripalmitin and Phenylalanine/Glucose.....	61
Table 15. Bio-oil yields, elemental analysis, HHV and ER of bio-oil products from Albumin in binary mixtures HTL .....	67
Table 16. Bio-oil yields, elemental analysis, HHV and ER of bio-oil products of ternary mixture of Albumin/Starch/Triolein HTL .....	75
Table 17. Bio-oil yields, elemental analysis, HHV and ER of bio-oil products of oleaginous yeasts.....	86
Table 18. Chemical composition of bio-oils from oleagineous yeast.....	87
Table 19. Hydrothermal decomposition of liamocins in water.....	96
Table 20. Hydrothermal decomposition of liamocins in organic solvents .....	98
Table 21. Hydrothermal decomposition of liamocins in THF .....	99
Table 22. Catalytic treatment of liamocins .....	101

## **Abstract**

Hydrothermal liquefaction (HTL) is a process for converting waste biomass to bio-oil by contacting the biomass with water at high temperatures and sufficient pressures in order to keep the water in the liquid state. HTL process has the advantage of being energy efficient and capable of dealing with wet biomass, such as sorted domestic organic waste, sewage sludge, algae, etc.

Despite being a very promising technology economically and environmentally, waste to fuels via HTL has not progressed from pilot scale to industry, primarily due to the issues associated with the recycling of the aqueous phase.

Moreover, waste-derived bio-oil obtained by HTL contains high contents of oxygen and nitrogen because of the initial biomass composition. Therefore, the bio-oil has to be upgraded in order to produce advanced transport fuels.

Information regarding the types of nitrogen compounds present in bio-oil is of major concern of any hydrotreatment, since the low hydrodenitrogenation rate and catalyst poisoning by nitrogen compounds make this process expensive.

Therefore, the main goal of the present study is the investigation of the HTL reaction mechanism, focusing the attention on the nitrogen containing species pathways, with the goal to increase the energy yields and reduce the nitrogen content in the produced bio-oil.

Due to the complexity of the biomass composition, model compounds that encompass all the biochemical components of biomass, namely proteins, lipid and carbohydrates, are emerged to predict important outcomes from HTL of any wet biomass feedstock. Furthermore, several microbial biomass types, such as oleaginous yeast and liamocins, were treated via HTL to produce bio-oil and commercially attractive chemicals.

This work consists of main five parts. In the first part the decomposition behavior of amino acids alone and in binary mixtures with glucose and tripalmitin as representative model compounds of proteins, lipids, carbohydrates, respectively, is investigated. Most attention is paid to the carbon and nitrogen transferring into HTL product streams. Moreover, the effect of homogenous and heterogeneous catalysts, besides the solvents on the HTL product streams is investigated.

The second part includes a comprehensive model study on albumin/starch/tripalmitin mixture in order to mimic a more reliable biomass model and evaluate all the the possible interactions within biomass macromolecular components. Importantly, the effect of biomass composition on the type of nitrogen compounds in the resulting bio-oil is determined.

In the third part deamination of amino acids to produce  $\alpha$ -hydroxycarboxylic acids under hydrothermal conditions is investigated in the presence of heterogeneous catalysts.

The fourth part reports a potential application of the HTL process for the production of bio-oils from oleaginous yeasts.

Finally, in the fifth part hydrothermal decomposition of liamocins, another microbial biomass, to produce commodity chemicals, e.g.  $\delta$ -lactones containing alkyl chains, is reported.

The whole study presented in this thesis helps to better understand the HTL of organic waste biomass and microbial biomass/oils, providing useful insights into the reaction products, pathways, and mechanisms for the production of bio-oils and chemicals.

## **Abstract**

La liquefazione idrotermale (HTL) è un processo che produce bio-olio da biomasse di scarto tramite contatto con acqua ad elevate temperature e pressioni sufficienti a mantenere l'acqua allo stato liquido. I vantaggi dell'HTL sono la sua efficienza energetica e la possibilità di trattare biomasse umide, come residui organici domestici, fanghi di depurazione, alghe, ecc. Nonostante sia una tecnologia molto promettente dal punto di vista economico ed ecologico, l'HTL non è stata applicata a livello industriale a causa di problemi legati al riciclo della fase acquosa, che contiene componenti organici solubili in acqua. Inoltre, i bio-oli ottenuti tramite HTL contengono un'elevata quantità di ossigeno e azoto, a causa della composizione delle biomasse di partenza. Quindi, il bio-olio deve essere idro-trattato per produrre combustibili. Per questo motivo sono necessarie informazioni riguardo alle specie di azoto presenti del bio-olio, in quanto queste possono portare a basse rese di idrotrattamento e avvelenamento del catalizzatore.

Quindi, l'obiettivo principale di questo lavoro è lo studio del meccanismo di reazione coinvolto nell'HTL, con particolare attenzione ai cammini di reazione delle specie contenenti azoto, con l'obiettivo di incrementare le rese energetiche e ridurre il contenuto di azoto nel bio-olio prodotto.

A causa della complessa composizione della biomassa di partenza, sono stati selezionati componenti modello, come proteine, lipidi e carboidrati, che simulino tutti i bio-componenti presenti nelle biomasse umide. Inoltre, diverse biomasse microbiche, come lieviti oleoginosi e "liamocin", sono stati trattati con HTL per produrre bio-oli e molecole commercialmente interessanti.

Questo lavoro è composto principalmente da cinque parti. Nella prima, è stata studiata la decomposizione di amminoacidi e di loro miscele con glucosio e tripalmitina, selezionati rispettivamente come composti modello di proteine, lipidi e carboidrati. Particolare attenzione è stata data alla quantità di carbonio e azoto trasferiti nei prodotti tramite HTL. Inoltre, si è studiato l'effetto sui prodotti ottenuti di catalisi omogenea ed eterogenea e del solvente.

La seconda parte include uno studio modello su miscele di albumina/amido/tripalmitina al fine di simulare meglio una biomassa e valutare tutte le possibili interazioni tra i componenti macromolecolari di essa. In particolare, è stato determinato l'effetto della composizione della biomassa sul tipo di prodotti azotati nel bio-olio prodotto.

Nella terza parte è stata studiata la deaminazione della leucina per produrre acido  $\alpha$ -idrossi-isocaproico in condizioni idrotermali e in presenza di catalizzatori eterogenei.

La quarta parte riporta una potenziale applicazione del processo HTL per produrre bio-oli da lieviti oleoginosi e un confronto con estrazione con solvente in termini di resa e composizione del bio-olio.

Infine, nella quinta parte, è riportata la decomposizione idrotermale del “liamocin”, un'altra biomassa microbica, per produrre prodotti chimici, come  $\delta$ -lattoni contenenti catene alchiliche.

L'intero studio presentato in questa tesi fornisce una miglior comprensione del processo HTL di residui organici, biomasse microbiche e oli microbici, fornendo utili informazioni riguardo al meccanismo di reazione per la produzione di bio-oli ad alto valore aggiunto e prodotti chimici.

## **Abstrakt**

Die hydrothermale Verflüssigung (HTV) ist ein Verfahren zur Umwandlung von Biomasse in Bioöl, bei dem die Biomasse mit Wasser bei hohen Temperaturen und ausreichendem Druck in Kontakt gebracht wird, um das Wasser im flüssigen Zustand zu halten. Die Vorteile des HTL-Prozesses sind die Energieeffizienz und die Fähigkeit mit nasser Biomasse wie sortiertem organischen Hausmüll, Klärschlamm, Algen usw. umgehen zu können.

Obwohl es sich wirtschaftlich und ökologisch gesehen um eine vielversprechende Technologie handelt, ist der Abfall-zu-Brennstoff-Ansatz mittels HTV bisher nicht vom Pilotmaßstab zu industriellen Anlagen übergegangen. Dies ist vor allem auf Frontend-Probleme im Zusammenhang mit dem Recycling der wässrigen Phase zurückzuführen, da diese wasserlösliche organische Verbindungen enthält. Des Weiteren enthält aus Abfällen gewonnenes Bioöl aufgrund der ursprünglichen Biomassezusammensetzung einen hohen Anteil an Sauerstoff und Stickstoff. Daher ist eine Aufwertung des Bioöls nötig, um moderne Kraftstoffe herzustellen.

Informationen über die Art der im Bioöl vorliegenden Stickstoffverbindungen sind bei jeder Behandlung mit Wasserstoff von großer Bedeutung, da niedrige Hydrodenitrogenierungsgeschwindigkeiten der Bioölkomponten und die Vergiftung des Katalysators durch Stickstoffverbindungen während der Veredelung diesen Prozess teuer machen.

Daher ist das Hauptziel der vorliegenden Arbeit die Untersuchung des HTV-Reaktionsmechanismus, wobei die Aufmerksamkeit auf die Reaktionspfade stickstoffhaltiger Spezies gerichtet ist, mit dem Ziel die Energieausbeute zu erhöhen und den Stickstoffgehalt im produzierten Bioöl zu reduzieren.

Aufgrund der Komplexität der Biomassezusammensetzung werden Modellverbindungen entwickelt, die alle biochemischen Komponenten der Biomasse, nämlich Proteine, Lipide und Kohlenhydrate, umfassen, um wichtige Ergebnisse aus der HTV nasser Biomasserohstoffe vorherzusagen. Darüber hinaus wurden mehrere mikrobielle Biomassearten, wie z.B. ölhaltige Hefe und Liamocin, mithilfe von HTV behandelt, um Bioöl und kommerziell attraktive Chemikalien herzustellen.

Diese Arbeit besteht aus fünf Hauptteilen. Im ersten Teil wird das Abbauverhalten von Aminosäuren in reiner Form und in binären Mischungen mit Glucose und Tripalmitin, als repräsentative Modellverbindungen von Proteinen, Lipiden bzw. Kohlenhydraten, untersucht. Die größte Aufmerksamkeit wird hierbei auf die Übertragung von Kohlenstoff und Stickstoff

in HTV-Produktströme gelegt. Darüber hinaus wird der Effekt homogener und heterogener Katalysatoren sowie verschiedener Lösungsmittel auf die HTV-Produktströme untersucht.

Der zweite Teil beinhaltet eine umfassende Modellstudie zu einem Gemisch aus Albumin/Stärke/Tripalmitin, um ein zuverlässigeres Biomassenmodell abzubilden und alle möglichen Wechselwirkungen innerhalb der makromolekularen Biomassekomponenten zu bewerten. Bedeutenderweise wird hierbei der Einfluss der Biomassezusammensetzung auf die Art der Stickstoffverbindungen im resultierenden Bioöl bestimmt.

Im dritten Teil wird die Desaminierung von Aminosäuren zu  $\alpha$ -Hydroxycarbonsäuren unter hydrothermalen Bedingungen in Gegenwart heterogener Katalysatoren untersucht.

Der vierte Teil stellt eine mögliche Anwendung des HTV-Verfahrens zur Herstellung von Bioölen aus ölhaltigen Hefen dar.

Schließlich wird im fünften Teil die hydrothermale Zersetzung von Liamocinen, eine weitere mikrobielle Biomasse, zur Herstellung von Grundchemikalien wie z.B.  $\delta$ -Laktonen mit Alkylketten, erörtert.

Die in dieser Arbeit vorgestellte Gesamtstudie ermöglicht die HTV von organischer Abfallbiomasse und mikrobiellen Biomassen/Ölen besser zu verstehen und liefert nützliche Einblicke in die Reaktionsprodukte, Wege und Mechanismen für die Produktion von Bioölen und Chemikalien.

## Chapter 1. Introduction

### 1.1 Motivation: Recovering energy from waste

Environmental concerns and possible future shortages have boosted research into alternatives for fossil-derived products [1]. Since 2008, the first European regulations regarding biofuels have been defined in the EU's Climate Change Package, which aims to achieve the EU climate targets by 2020 [2]:

- 20 % reduction in greenhouse gas emissions
- 20 % improvement in energy efficiency
- 20 % share for renewable in the EU energy mix.

The waste organic biomass, such as domestic organic waste and sewage sludge, are highly perishable wet materials with a typical moisture content ranging from 50 to 80 % [3]. They often cause serious environmental problems if not properly disposed. They are also readily available: around 800 million tons of organic wastes are annually produced worldwide [4]. Since these feedstocks do not compete with the food, they can be used for sustainable energy production.

The roadmap for biomass conversion into platform chemicals, which is able to substitute petroleum-derived equivalents, is complex and ranges from biological to severe catalytic thermochemical processes (Figure 1).

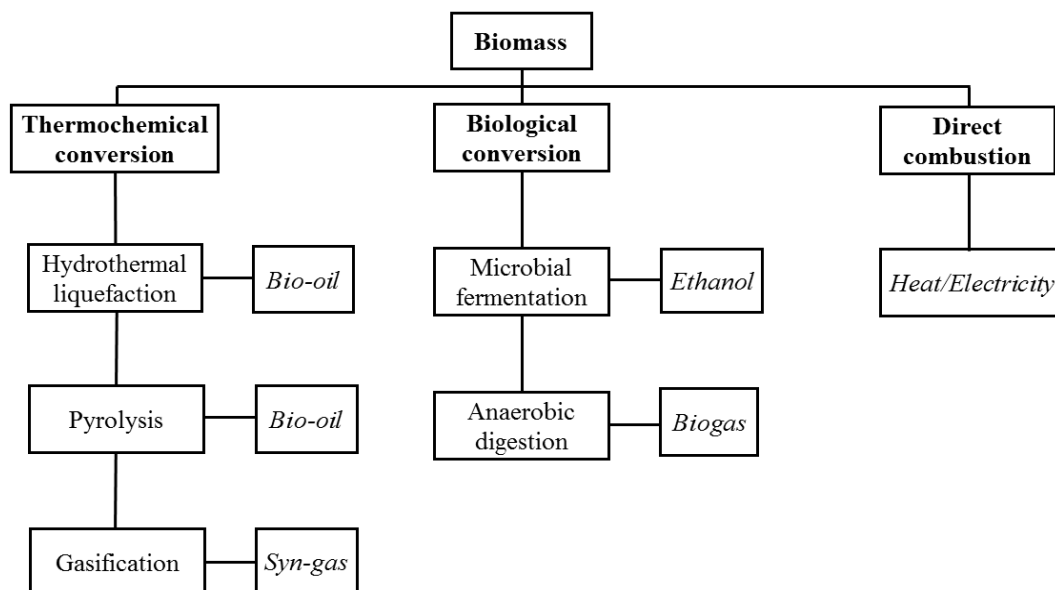


**FIGURE 1.** Biomass conversion processes

Organic waste biomass can be converted to bio-oil, which is a precursor for biofuel, by two main thermochemical routes: pyrolysis and hydrothermal liquefaction (HTL). The characteristics and technical feasibility of the two thermochemical processes for bio-oil production are compared in Table 1.

**TABLE 1.** Comparison of two thermochemical processes for bio-oil production

	<b>Pyrolysis</b>	<b>HTL</b>
<i>Treatment conditions</i>		
Temperature, °C	450-500	300-400
Pressure, MPa	atmosphere	5-20
Pretreatment	Drying is necessary	Drying is not necessary
<i>Bio-oil characteristics</i>		
HHV (MJ/Kg) <sup>-1</sup>	35	22
<i>Elemental analysis, %</i>		
C	70	55
H	8	6
O	12	34
N	10	5

Several studies have been performed on parallel comparative evaluations of the yields and properties of bio-oil obtained by pyrolysis and liquefaction [5], [6], [7]. In most cases HTL resulted in a higher oil yield with superior properties compared to pyrolysis (except fast pyrolysis).

From a technological point of view, HTL proves to be very energy efficient, as it entails temperatures lower than those reached during pyrolysis [8]. Moreover, pyrolysis requires the feedstock with low moisture content, generally less than 30 % [9], while HTL obviates the drying biomass, thus leading to huge energy savings.

However, HTL is a non-selective process due to the complex composition of the waste biomass, containing polysaccharide, lipid and protein fractions (see Section 1.3). Moreover, there is still no description of chemical pathways to explain the bio-oil formation under hydrothermal conditions. It is very challenging to understand the chemistry of HTL if starting directly from the biomass due to its complex composition. To overcome this problem model compounds representing the biomass composition can be used.

When initiating this research, there was very little data in the literature on the model studies relevant to the HTL process of waste biomass. Thus, the present study would provide useful insights into the reaction products, pathways and mechanisms for the bio-oil production during HTL.

## 1.2 Fundamentals of HTL

HTL involves the thermochemical conversion of a broad range of biomass types in the presence of hot compressed water at subcritical conditions into a liquid product known as bio-oil [10]. HTL requires an operating temperature of 300–350 °C at 5–20 MPa for 5–60 min, wherein water is in the liquid form [11]. It produces four phases: a gas-phase, a bio-oil, an aqueous by-product, and a solid residue. Depending on the physical properties (e.g., density and hydrophobicity), the bio-oil is either just gravimetrically separated from the aqueous phase or extracted with an organic solvent [12].

Figure 2 shows temperature/pressure ranges for hydrothermal water processes over the phase diagram of water. Water's triple point and critical point are shown in the phase diagram; the hydrothermal water processes are typically performed in a narrow window just greater than the vapor-liquid co-existence curve or at pressures slightly in excess of water's critical pressure (221 bar).

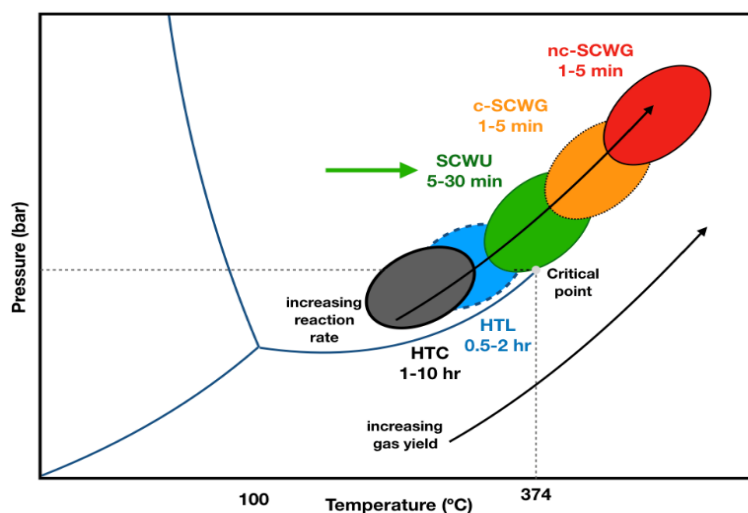


**FIGURE 2.** Phase diagram of water superimposed with different hydrothermal water technologies. *Adapted from [13].*

\*HTC- hydrothermal carbonization, HTL-hydrothermal liquefaction, SCWU-supercritical water upgrading, c-SCWG-catalytic supercritical water gasification, nc-SCWG-non catalytic supercritical gasification.

Subcritical water (<150–374 °C, 0.4–22.1 MPa) and supercritical water (>374 °C, >22.1 MPa) are non-toxic and environmentally friendly media with good mass transfer and heat transfer characteristics. The properties of water, such as the density and dielectric constant, can be continuously controlled between gas-like and liquid-like values by varying the temperature and pressure. For example, at a pressure of 25 MPa, the dielectric constant decreases from approximately 78 at 25 °C to 27 at 250 °C and to 2 at 400 °C [14].

This decrease in dielectric constant increases the solubility of small organic compounds. Thus, the polarity of water, and hence its ability to dissolve various solids, liquids, and gases that are otherwise insoluble or sparingly soluble can be significantly enhanced by transforming ordinary water into supercritical water.

In addition, water under subcritical conditions can act as an acid or base catalyst, whereas supercritical water offers the unique possibility of shifting the dominant reaction mechanisms from free radical to ionic through manipulation of the water density [15].

HTL, which mimics the processing of fossil fuels buried deep inside the earth, occurs in minutes or hours. HTL produces oil with lower oxygen content as opposed to other processes like fast pyrolysis. The HTL process begins with solvolysis of biomass in micellar forms, the disintegration of biomass fractions, and thermal depolymerization into smaller fragments.

Key parameters affecting HTL process include feedstock types, process modes (batch and continuous), process conditions (temperature, retention time, and pressure), and catalysts.

### **1.3 Waste biomass composition**

The major components of waste biomass can be roughly classified to proteins, lipids, carbohydrates, lignin and ash.

**Lipids.** The typical composition of sorted domestic organic waste includes a consistent fraction of lipids as mono-, di-, tri-glycerides and free fatty acids ranging from 10 to 35 % [16]. Microalgae also can have lipid contents as high as 80 %, although this is usually in the range of 15-35 % and is dependent on the growth conditions [17].

In hot compressed water, triacylglycerides are readily hydrolyzed to glycerol and fatty acid. During the HTL process, the conversion of glycerol is inclined to produce water-soluble compounds, such as methanol, acetaldehyde, propionaldehyde, acrolein, allyl alcohol, ethanol

and formaldehyde, with some gas products, mainly CO, CO<sub>2</sub> and H<sub>2</sub> [18]. The lipid content is contributed directly to the HTL oil phase. Therefore, high-lipid biomass produces higher bio-oil yield in comparison to low-lipid biomass.

**Carbohydrates.** As a major component of waste organic biomass, typical carbohydrate contents range between 10-65 wt.% [19]. For instance, the most abundant carbohydrates in algae are cellulose and starch. In addition, depending on the type of species, hemicellulose as well as various other heteropolysaccharides may also be present [20].

Under hydrothermal conditions, carbohydrates undergo rapid hydrolysis to form glucose and other monosaccharides, which are then further degraded. The main liquefaction mechanism is breaking down of carbohydrates to polar water-soluble organics, such as organic acids (i.e. formic, acetic, lactic), aldehydes, and alcohols, all carrying a substantial amount of oxygen [19], [21], [22]. The aldehyde- and benzene-type structures may further produce larger hydrocarbons, which can be then a part of the bio-crude fraction [19]. The degradation of carbohydrates in hot-compressed water has been comprehensively discussed elsewhere [23].

**Proteins.** Higher protein content is a primary difference between organic waste biomass and terrestrial biomass [24] that causes a high content of nitrogen in the bio-oil produced by HTL. The protein content is highly dependent on the type of feedstock and can be as high as about 65-70 wt.% for *Spirulina* [5], [25].

Proteins are polymers of amino acids linked by peptide bonds, which consists of a carbon-nitrogen bond between the carboxyl and amine groups forming long chains [26], which is hydrolyzed in subcritical water [27] to form amino acids. The amino acids can be further converted to amines by decarboxylation and to organic acids by deamination [28]. The degradation products of amino acids may then repolymerize and undergo Maillard-type reactions with the sugars to produce nitrogen heterocyclic compounds, such as indole or pyrroles [29].

Sorted by contributions and tendencies to contribute to the oil yield, the components of biomass are in the following order: lipid > protein > carbohydrate [30]. Although the lipid fraction is typically the main target of oil production, about 1–15 % of the produced bio-oil is converted from carbohydrates and proteins under hydrothermal conditions [22].

Generally, each biomass fraction does not behave independently during the HTL process and their contribution to an overall oil yield depends on an interaction among its components. The

information about the reactions of the most abundant types of biomolecules (e.g., proteins, lipids, and carbohydrates) in hydrothermal water conditions is described elsewhere [31].

Although HTL has a positive economic potential due to a favorable energy balance [32], it produces the bio-oil with a significantly higher oxygen and nitrogen contents, typically 10-20% and 1-8 %, respectively, compared to the conventional crude oil (both elements <1 %) [33]. Bio-oil with a high nitrogen content is undesired, as it has poor storage stability, low energy density and unsuitable for direct application as transportation fuels.

#### **1.4 Distribution of nitrogen in HTL product streams**

The elemental distribution among the HTL product streams can be used to better understand the reaction mechanism of HTL and provide useful information for the process optimization. The nitrogen distribution is considered less by researchers in comparison to carbon distribution, even though it is one of the main influencing factors for sustainable biofuels. The nitrogen could distribute to gas, oil, aqueous, and solid residue phases during the liquefaction (Table 2).

For most of amino acids, the majority of nitrogen was found in the aqueous phase. Y.F. Yang et. al. [34] found that the total nitrogen concentration in the aqueous phase ranged from 998 to 1157 mg/l and half of which was detected as ammonia. Therefore, they proposed recycling the aqueous fraction for algae growth as nutrients.

I. Espinoza-gonzalez et. al. [84] observed that with the temperature increasing from 200 °C to 260 °C, more nitrogen is remained in the bio-oil phase. At higher temperatures ranging from 260 °C to 320 °C a higher amount of nitrogen is released in aqueous fraction or gaseous phase.

Although nitrogen containing gases are not easily detectable in the gas phase, Ross et al. [35] observed that part of nitrogen in algal feedstocks was converted to gaseous products as NO<sub>2</sub>, N<sub>2</sub>O, HCN at the temperature of 300–350 °C for 60 min.

**TABLE 2.** The distribution of nitrogen to products

Feedstock	Operating conditions	Nitrogen distribution, (%)				Ref.
		Gas	Oil	Aqueous	Solid	
<i>Macroalgae</i>						
Derb.	330 °C, 5 min	2	29	65	2	[36]
Ulva		0.5	31	66	2.5	
Chaet		34	19	40	5	
Clad.		11	18	65	5	
Oedog.		8	35	55	2	
Clad.		10	20	55	5	
<i>Microalgae</i>						
Nannochloropsis sp.	350 °C, 10 min	-	4.3	11 g/l*	3.22	[37]
Spirulina platensis	60 min	-	6.3	1.91 g/l*	1.61	[5]
<i>Protein</i>						
Albumin	300 °C	-	2.5	84	0	[38]
Serine	60min	-	2.24	80.5	0	[24]
Valine		-	3.41	84.3	0	
Leucine		-	7.09	69.3	0	
Phenylalanine		-	5.64	84.6	8.4	
Tyrosine		-	50.5	47.5	1.3	

\*N concentration in aqueous phase, g/l was calculated by persulfate method

### 1.5 Chemistry of hydrodenitrogenation (HDN)

Available upgrading techniques for bio-oil include hydrocracking, zeolite cracking, thermal cracking, hydrotreating, etc. Traditionally, cracking reactions (e.g., zeolite cracking) and hydrotreating are two major approaches to upgrade petroleum crude, because they can reform undesired chemicals into hydrocarbons through chemical reactions. Cracking reactions mainly convert heavy molecules into two light molecules, whilst hydrotreating can achieve saturation of olefins, hydrodeoxygenation (HDO), hydrodenitrogenation (HDN) and hydrodesulfurization (HDS).

Organic nitrogen is most commonly removed under high pressure of hydrogen (up to 30 MPa) at 600–670 K. The most well-known catalysts for HDN are sulfided NiMo or NiW supported on alumina [39]. Under industrial conditions, HDN is always accompanied by other hydrotreating reactions, such as HYD, HDS, HDO, HDM, hydrocracking, and coking. Since HDN is less efficient compared to HDS, much more hydrogen is consumed. This can be partially explained by a relative bond strength as shown in Table 3.

**TABLE 3.** Bond energies (kJ/mol) for commonly encountered bonds [40]

Bond	Energy, kJ/mol	Bond	Energy, kJ/mol
H-H	436	N-H	391
C-H	413	C-N	308
C-C	348	C=N	615
C=C	614	C≡N	891
C≡C	839	C-S	259
C-O	358	C=S	577
C=O	799	S-H	347

In general, HDN involves the saturation of the aromatic ring followed by hydrogenolysis of the C–N bonds to yield ammonia and the corresponding hydrocarbon (Figure 3) [41].

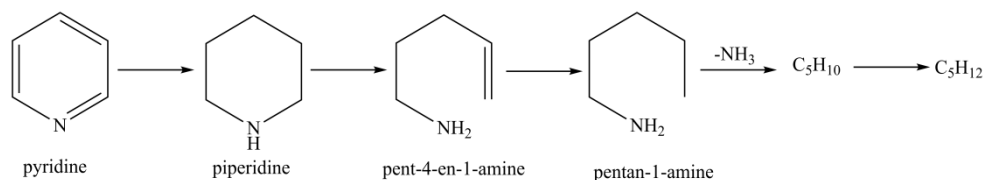


**FIGURE 3.** HDN network of pyridine. *Adapted from [61].*

However, the formation of unsaturated C5 hydrocarbons and ammonia via hydrogenolysis of C–N bonds in the piperidine ring could occur in a lesser extent [42]. Instead, the alkylation of the heterocyclic ring could predominate, resulting in the formation of alkylpiperidines with N-pentylpiperidine (Figure 4). Cyclization reactions resulted in the formation of decahydroquinolines, while dehydrogenation of the latter and of piperidine yielded 5,6,7,8-tetrahydroquinoline and pyridines (tetrahydropyridine and pyridine), respectively.

In other words, during HDN process the formation of secondary nitrogen-containing compounds, which are more resistant to HDN than the original ones, can be observed.

More severe catalyst deactivation is caused by the higher molecular weight-aromatic compounds in the feedstock. With increasing the boiling point of the feeds, the size of molecules of nitrogen-containing compounds increases, which reduces their accessibility to the catalyst surface.

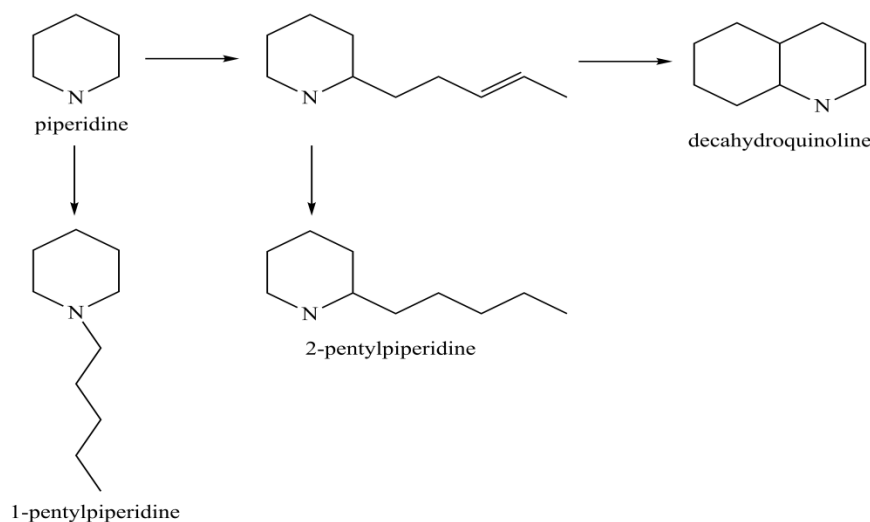


**FIGURE 4.** HDN network of piperidine. *Adapted from* [42].

Most upgrading techniques have been exclusively developed for petroleum, in which nitrogen is not a concern, and there have been only a few studies on the determination of HDN reactivity of nitrogen compounds in fossil crude oils.

T. Zhang et. al. [43] performed FT-ICR MS ESI analyses for the asphaltenes-free vacuum residue derived from deasphalted oils before and after hydrotreating and classified HDN reactivity of nitrogen compounds as easy- and hard-to convert nitrogen compounds. According to their results, N1 compounds were shown to be more hydrotreatment-resistant than compounds with additional nitrogen and oxygen heteroatoms.

Similarly, H. F. Silver and N. H. Wang [44] investigated the relative rates of disappearance of the types of nitrogen compounds presented in shale gas oil using conventional hydrotreatment Co-Mo on  $\text{Al}_2\text{O}_3$  catalyst. At higher temperature (400 °C) the nitrogen removal reached 70%. According to Figure 5, primary and secondary amines and amides were practically missing in the oil after hydrotreatment, while indole and quinolines type compounds were the most difficult to denitrify.

In comparison to fossil fuels, waste biomass-derived oils usually contain much higher concentrations of nitrogen-containing compounds. They are more complex in structure and

more difficult to denitrify. However, till to date no information is reported regarding the HDN reactivity of nitrogen containing components of waste-derived oils.

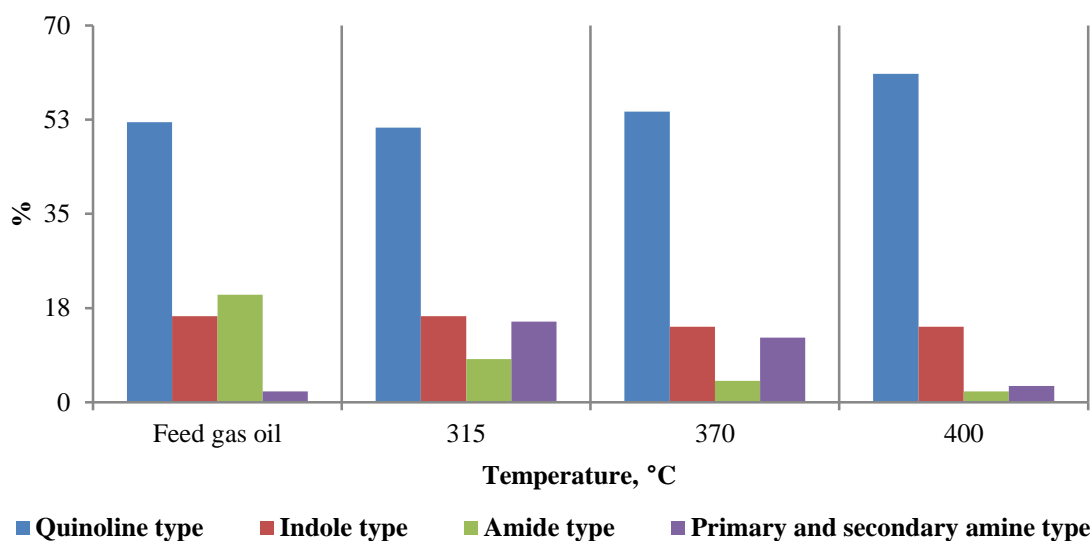


**FIGURE 5.** The HDN reactivity of the types of the nitrogen compounds depending on the severity of the reaction conditions. *Adapted from* [44]

### 1.6 Eni Slurry Technology (EST) upgrading of HTL oil

Eni Slurry Technology (EST) is a hydrocracking process developed by Eni for the upgrading of very heavy feedstock, such as petroleum residues, extra-heavy oils, tars and bitumen (Figure 6). EST provides higher yields over current available conversion technologies. Moreover, EST offers significant advantages in terms of efficiency of hydrogen utilization and catalyst life, achieving longer cycle length compared to hydrocracking solutions currently being marketed [45].

EST is based on a slightly different concept from that industrially applied in the past. A catalyst precursor, consisting of an oleo-soluble molybdenum carboxylate (i.e. naphthenate or octoate), is dissolved in the feedstock and the mixture is fed to the reactor, which operates in the temperatures range 673–723 K under a total pressure of 15 MPa. H<sub>2</sub> is fed through a distributor located at the reactor bottom. Under these conditions, the catalyst precursor is converted to molybdenite, which is crystalline layered MoS<sub>2</sub>, with an average particle size of a few nanometers [46].

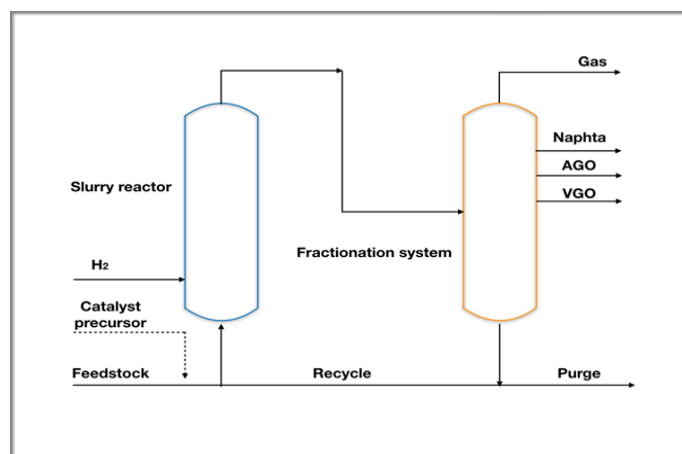


**FIGURE 6.** Simplified EST process scheme. *Adapted from [46]*

Recently EST has been tested for the upgrading of bio-oil produced from HTL of organic domestic waste. Interestingly, for the bio-oil upgrading the metal removal (HDM) (>99%), sulphur removal (HDS) (>85%), and oxygen removal (HDO) (>90%) were efficient, while nitrogen removal (HDN) (>65%) was lower in comparison to HDM, HDS and HDO.

In order to identify the most resistant nitrogen-containing compounds, GC-MS and FTICR MS APPI+ were performed for bio-oils before and after EST treatment.

GC-MS allows the characterization of about 50-70 % of the bio-oil and the upgraded product, since nor heavy or polar nitrogen and oxygen containing compounds are amenable for the detection by GC-MS.

According to GC analysis, fatty acids (FA), fatty acid amides (FAA), and fatty acid esters (FAE) were totally removed (Figure 7 a), as a result, the acidity was reduced and nitrogen content was reduced from 4 % to about 1.5 %. As it can be seen from Figure 7 b, after EST upgrading mainly hydrocarbons were presented in the bio-oil, while, nitrogen containing compounds were not eluted in GC spectra.

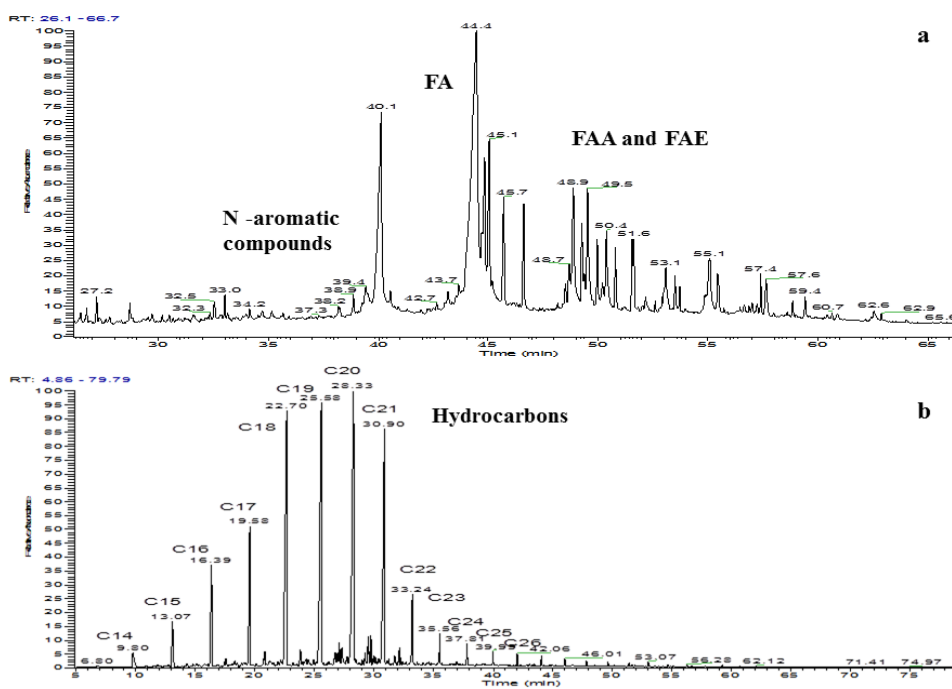


**FIGURE 7.** GC-MS of HTL oil before (a) and after (b) EST upgrading

Petroleomics by ESI-FT-ICR MS have been shown to allow for class attributions of the thousands of polar compounds present in crude oils and to provide crucial data for the oil industry. Data analysis was able to assign hundreds of formulas, which were grouped in several different classes. Appropriate manipulation of this very large data set via specific plots, such as abundance versus class distribution and DBE versus  $C_n$ , permits the identification of patterns and the inference of some important physical and chemical properties of the oil, such as the unsaturation level and aromaticity (DBE= sum of aromatic rings and double bonds). Specific classes can also be observed and semi-quantified. The application of this approach, therefore, allows for a rapid and comprehensive characterization of bio-oil products.

APPI+ FTICR MS analysis showed over 2000 attributed molecular formula for bio-oil and about 2200 molecular formulas for upgraded bio-oil. From normalized data on main classes distribution,  $O_x$  class components are drastically reduced after upgrading, while nitrogen is mainly contained in N1 and N2 classes form (Figure 8).

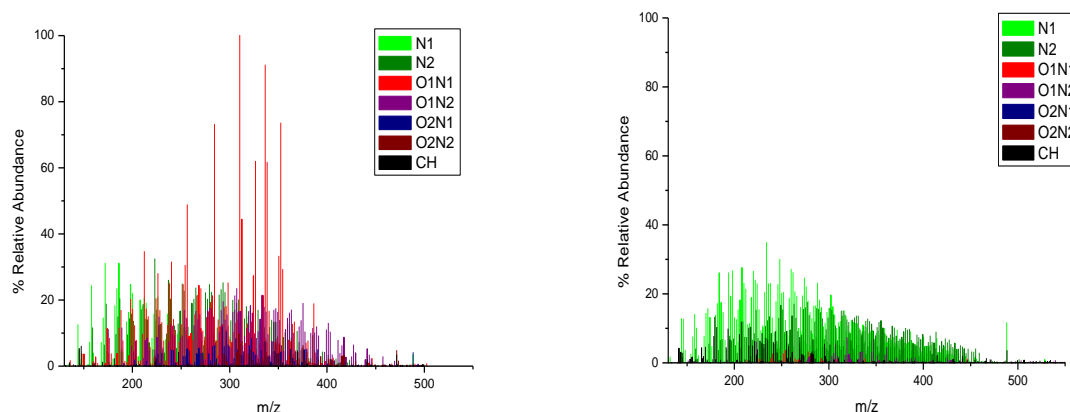


**FIGURE 8.** APPI+ FTICR MS spectra of HTL bio-oil (a) before and (b) after EST upgrading

From Figure 9 it can be seen that wide distributions for nitrogen containing compounds in the aromatic region are at DBE over 4. More abundant compounds in the bio-oil show DBE of 7-10. In the upgraded oil the most abundant compounds show higher DBE values 8-13, that are likely polyaromatic nitrogen containing compounds (PNAHs). Similar behavior is observed for N2 class components. More abundant compounds in the bio-oil show DBE of 7 and 9-12. In the upgraded oil the most abundant compounds show higher DBE values 10-15 (PNAHs).

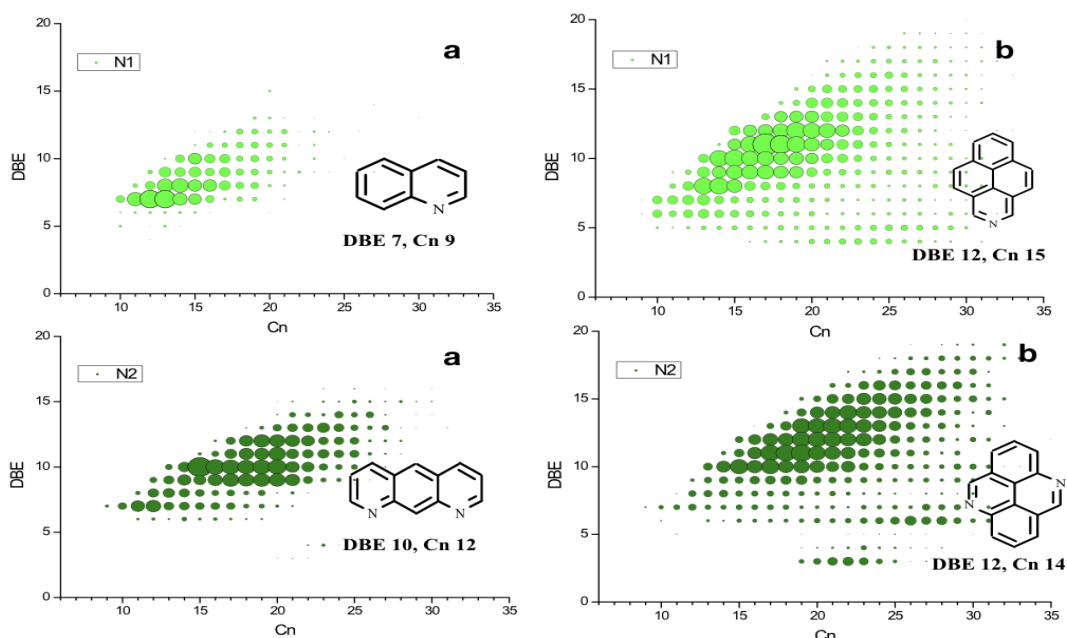


**FIGURE 9.** Cn versus DBE for main N1 and N2 class components in the bio-oil (a) before and (b) after EST upgrading.

Once again, these data suggest that the EST upgrading process is successful in terms of diesel fraction yield and HDO, HDM and HDS; however, nitrogen is not completely removed.

After upgrading, linear saturated hydrocarbons (C14-C30) were the main components of the bio-oil. Regarding petroleomic approach used, the residual nitrogen (1.5 %) is found to be N1 and N2 class components that are attributed to alkylated polycyclic compounds (PNAHs).

To conclude, nitrogen-containing compounds in waste derived bio-oils can be divided into two groups: heterocyclic and non-heterocyclic. Figure 10 lists the various types of nitrogen-containing compounds (without alkyl substitution) presented in the bio-oils. **Non-cyclic nitrogen compounds, such as aliphatic amines and FAAs, are easy to denitrogenate.** Heterocyclic nitrogen-containing compounds can be divided into basic and non-basic compounds. Non-basic compounds consist of five-membered heterocycles, such as pyrrole, indole, carbazole, etc. Basic compounds include six-membered heterocycles, such as pyridine, quinoline, acridine, etc. The lone-pair electrons on the nitrogen atom of non-basic compounds are delocalized around the aromatic ring and are not available for donation to acid sites on catalyst surfaces. In contrast, the lone-pair electrons on the nitrogen atom of basic compounds are available for sharing with acid sites on catalyst surfaces.

**These heterocyclic nitrogen-containing compounds are difficult to denitrogenate during the upgrading.** Moreover, six-membered basic heterocyclic nitrogen compounds cause the deactivation of the hydrotreatment catalysts.

These conclusions are crucial to tune the bio-oil specifications in order to meet the requirements of hydrotreatment process in order to produce advanced transport fuels from organic waste biomass.

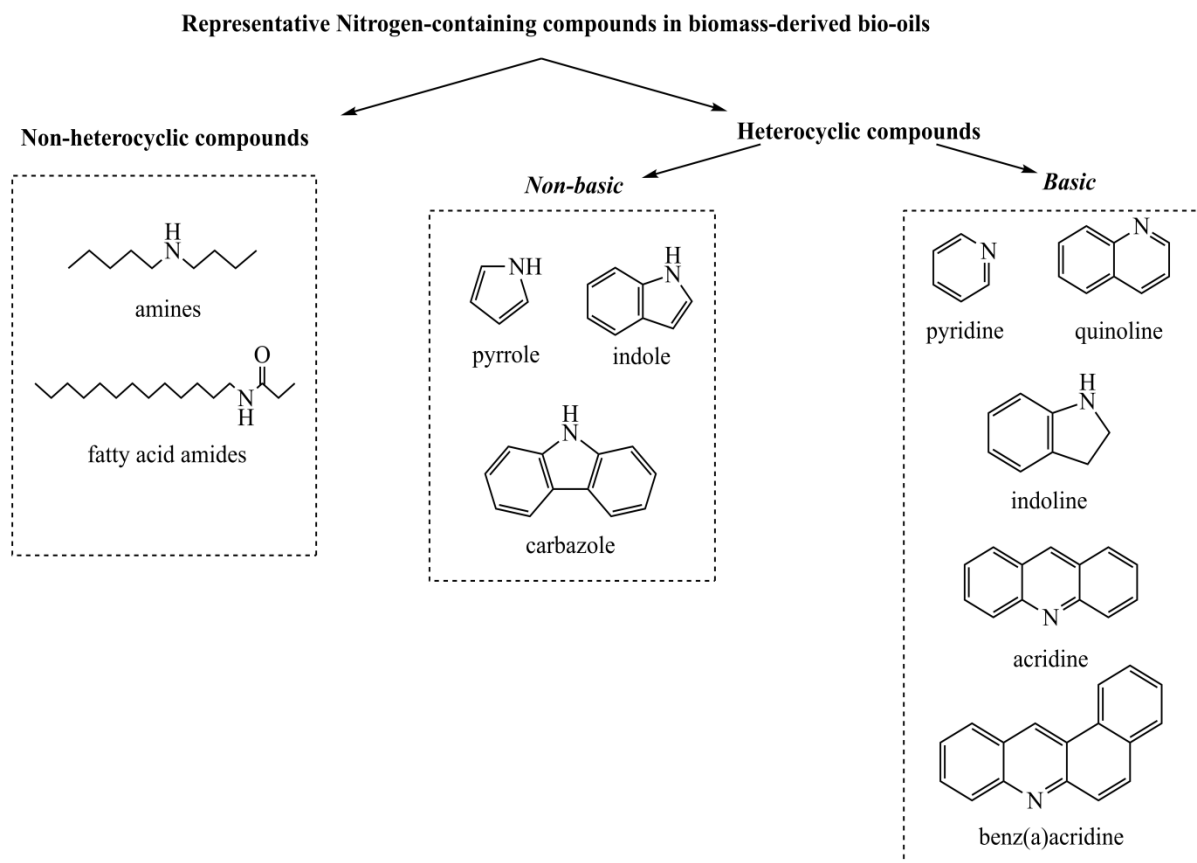


**FIGURE 10.** Nature of nitrogen species presented in waste derived oils

### 1.7 Aims and a roadmap of the thesis

For understanding the degradative phenomena of biomass, which causes the formation of undesirable components (for instance, PNAHs) that are resistant to hydrotreatment, a complete knowledge of the chemical pathway of HTL is required. Therefore, the ultimate goal of this research is to investigate the fundamental mechanisms of HTL, including the elemental transfers during the process, with the emphasis on the nitrogenous species pathways during HTL.

To achieve this goal, the chemical mechanism of HTL of organic waste is extensively investigated starting from monomeric model compounds of protein (leucine, phenylalanine, glutamine) individually and in binary mixtures with carbohydrates (glucose) and lipids (tripalmitin). Then macromolecular model compounds (albumin, starch, tripalmitin, triolein) were employed alone and in binary/ternary mixtures to mimic the real feedstock composition.

Finally, the real microbial biomass feedstocks were treated under HTL conditions to summarize the results of the modelling study.

This whole work is organized as follows. A review of literature on the effect of operating conditions of HTL on the quantity and quality of bio-oil, and the chemical pathway of some model compounds are presented in Chapter 2. Chapter 3 discusses the experimental setup and the methodology used to carry out quantitative and qualitative analyses. Results pertaining to monomeric model compounds are discussed in Section 4.1. Section 4.2 covers the study on HTL of macromolecular model compounds. The possibility of enhancing the deamination route under hydrothermal liquefaction of leucine is demonstrated in Section 4.3. The work carried out with microbial biomass types, including oleaginous yeast and liamocins is reported in Sections 4.4 and 4.5, respectively. Chapter 5 concludes the key findings of this study, and gives directions for future work.

This comprehensive approach can help to better understand the process of organic waste biomass HTL and can be important for tailoring the waste feedstock composition in order to produce the bio-oil with the high standard quality. The whole study is crucial for the optimization of HTL process applied to protein rich biomass and microbial biomass/oils.

## Chapter 2. Literature review

In this chapter a comprehensive literature review on the effect of operating conditions on the bio-oil properties is reported. The chemical pathway of some model compounds under hydrothermal conditions is also reviewed. The existing numerous gaps in the literature on the chemical mechanism of HTL were the motivation of the present study, which aims to establish a foundation for the comprehension of a chemical pathway of HTL process applied to protein rich waste biomass.

### 2.1 Effect of operating conditions on the bio-oil yield and nitrogen content of bio-oil produced from algae HTL

*Effect of temperature.* Temperature is one of the decisive parameters of the HTL process. Most of the HTL studies are performed at a temperature range of 250 °C to 350 °C with 5 to 60 min residence time and majority in a batch reactor. There has been only limited information yet available on continuous-flow tests [47].

When the temperature is in subcritical conditions, a rise in reaction temperature appears to increase the depolymerization of biomass. Consequently, the concentration of free radicals and the probability of repolymerization of fragmented molecular also increase the total yield of bio-oil. When the temperature approaches or exceeds the critical point of H<sub>2</sub>O, the yields of char and gas appear to increase with reaction temperature, thereby indicating that high temperatures promote the repolymerization and redecomposition of intermediate products. As a result, the yield of bio-oil decreases [48].

Moreover, with increment of temperature the nitrogen content of the bio-oil increases. This is attributed to the promotion of protein degradation [49], [50]. Below 250 °C, the extracted bio-oil is mainly derived from lipid, while under higher processing temperature more proteins and carbohydrates are liquefied and become part of the bio-crude oil. Thus, operating parameters for maximum bio-oil yield could not correspond to the desired properties of bio-oil in terms of nitrogen content.

*Effect of heating rate.* X. Peng et. al. [51] reported that the bio-oil yields raised by 13 % when heating rates increased from 5 °C/min to 140 °C/min in HTL of grassland perennials. The

authors found that slow heating rate leads to the formation of char residues because of the repolymerization of intermediates, whereas rapid heating rates lead to the formation of gas products because of redecomposition reactions. So, suitable heating rate is an important parameter in the HTL process. However, the effect of heating rate on product distributions for biomass HTL was lower than those for pyrolysis because of better dissolution and stabilization of fragmented species in a hot-compressed water. Fast pyrolysis is a kinetically controlled process, while HTL is a thermodynamically controlled process.

Effect of residence time. Short residence times are usually expected to produce a large amount of bio-oil, but it cannot always react completely in a short time. On the other hand, long residence time causes the repolymerization of intermediate products, thereby decreasing the bio-oil yield.

Eboibi et al. [52] performed the experiments on HTL of halophytic microalga *Tetraselmis* sp. in a batch reactor at different temperatures (310, 330, 350, and 370 °C) and reaction times (5, 15, 30, 45, and 60 min). Based on their results, the total yield of bio-oil increased with holding times at 310 °C, whereas it decreased with increasing holding times at 350 °C. Therefore, the holding times for obtaining a maximum bio-oil yield were different at various temperatures.

Usually, a high temperature requires low holding times. The group of P. Savage [53] investigated the fast hydrothermal liquefaction of green marine algae *Nannochloropsis* sp. at batch reaction times of 1, 3, and 5 min and set-point temperatures of 300–600 °C. They also performed conventional liquefaction for 60 min at the same temperatures. The bio-oils produced by fast liquefaction had higher carbon contents and higher heating values similar to bio-oils from the traditional isothermal liquefaction process.

These results are fundamental, because such decrease in the reaction time would greatly reduce the reactor volume required for continuous bio-oil production, subsequently reducing the capital costs of processing, while high capital costs is one of the downsides of HTL process. However, it is important to note that bio-oil composition produced from fast HTL differs from that obtained by traditional HTL, so further investigations and optimization are required.

Effect of biomass/H<sub>2</sub>O ratio. In the HTL process, the presence of H<sub>2</sub>O helps enhance the dissolution of intermediates and the repolymerization of small molecules. H<sub>2</sub>O also plays a

significant role in stabilizing free radicals, thereby improving bio-oil quality. However, using much water will greatly increase the cost of HTL process.

*Effect of catalysts.* The use of catalysts in HTL process improves the process efficiency by reducing the char and tar formation. The literature analysis showed that the alkali hydroxides, carbonates, bicarbonates and alkali formates as homogeneous catalysts were intensively studied in the catalytic liquefaction.

A. Demirbaş et. al. showed that the activity and selectivity of alkali solutions placed in the following order:  $K_2CO_3 > KOH > Na_2CO_3 > NaOH$  [54]. They found that alkali carbonates catalytically increased the conversion rate and the generation of bio-oil more than alkali hydroxides due to its secondary reaction with water forming bicarbonates and hydroxides.

A. B. Ross et. al. [35] investigated the influence of alkali catalysts (potassium hydroxide, sodium carbonate) and organic acids (acetic acid and formic acid) on the quality of bio-oil obtained from microalgae and cyanobacteria containing low lipid content. The yields of bio-oil were higher using an organic acid catalyst, bio-oil had a lower boiling point and improved flow properties.

Homogeneous catalysts offer some advantages: decreased solids production, increased bio-oil yield, and improved bio-oil properties. Specifically, alkaline catalysts are able to enhance the bio-oil yield by decreasing the formation of residues, while acid catalysts (e.g. sulphonic acids and sulphuric acid) are capable to reduce the temperature and time required for the liquefaction of lignocellulosic biomass by enhancing the hydrolysis of cellulosic components [55].

However, the separation of these catalysts may become problematic and require additional input energy. The application of heterogeneous catalysts in HTL has also been discussed to improve bio-crude quality [56], [57]. The summary on catalytic liquefaction is reported in Table 4.

**TABLE 4.** Summary of studies on catalytic liquefaction

Feedstock	Set up	Conditions	Catalyst	Oil yield, %	N (%) in feedstock	N (%) in bio-oil	Ref.
Spirulina platensis	1.8 L batch reactor	350 °C, 60 min	Na <sub>2</sub> CO <sub>3</sub>	51.6	10.75	5.44	[58]
			NiO	30.2		6.41	
			Ca <sub>3</sub> (PO <sub>4</sub> ) <sub>2</sub>	34.5		4.74	
D.tertiolect.	100 mL autoclave	360 °C, 50 min	Na <sub>2</sub> CO <sub>3</sub>	25.8	1.99	3.71	[59]
Spirulina	50 autoclave	350 °C, 60 min	Fe(CO)5-S	63.3	4.8	7.5	[60]
Dunaliella salina	500 ml stainless steel autoclave	200 °C, 60 min	Ni/REHY	51.6	7.01	5.82	[61]
			REHY	72		6.69	
Chlorella vulgaris	75 ml batch reactor	350 °C, 60 min	Pt/Al <sub>2</sub> O <sub>3</sub>	38.9	8.2	5.7	[17]
			Ni/Al <sub>2</sub> O <sub>3</sub>	30		5.4	
			Co/Mo/Al <sub>2</sub> O <sub>3</sub>	38.7		5.6	
C.pyrenoid.	58-mL autoclave reactor	400 °C, 4 h, 6MPa H <sub>2</sub>	Ru/C,	63.2-	8.4	1.9-2.8	[62]
			Pd/C, Pt/C.	77.2			
Chlorella pyrenoid.	58 mL autoclave reactor	400 °C, 4h	Ru/C+ Raney Ni	77.2	10.5	2.0	[63]
Nannochl.	316- stainless steel reactor	350 °C, 60 min	Pd/C,	45-	6.32	3.33-	[64]
			Pt/C, Ru/C	50%		4.20	

*Effect of solvents.* At a critical point of water the liquefaction process is operated under challenging conditions and the organic solvents, such as ethanol, methanol, propanol, butanol, tetralin and ethyl acetate, etc. have been studied as alternative reaction solvents to replace water [60]. Moreover, the presence of solvent dilutes the concentration of the products, thus minimizing cross-linked reactions and reverse reactions.

It is generally accepted that protic organic solvents, in particular, methanol and ethanol, are promising solvents for biomass catalytic liquefaction, because they act as hydrogen donor which possess better effectiveness in stabilizing the primary thermal decomposition products, thus preventing coking and resulting in higher yields of bio-oil.

Solvent selection is very important to obtain high liquefaction oil yields and improve the oil properties [65]. However, the use of solvents did not suppress the nitrogen content of bio-oil significantly (Table 5).

**TABLE 5.** Summary of studies on solvolytic liquefaction

<b>Feedstock</b>	<b>Set up</b>	<b>Operating conditions</b>	<b>Solvent</b>	<b>Oil yield, %</b>	<b>N (%) in feeds</b>	<b>N (%) in bio-oil</b>	<b>Ref.</b>
Spirulina	1L GSHA-1 type autoclave	573-653 K, 20 min	Methanol	55	8.87	7.46,	[66]
			Ethanol	54		7.92,	
			1,4-dioxane	56		9.54	
Spirulina	1L GSHA-1 type autoclave,	553 K- 593 K	Ethanol (10- 30%)	35.4- 45.3	8.87	9.38- 10.12	[67]
Chlorella vulgaris	20 mL batch reactor	473 K, 10 min	Formic acid	34.6	11	5.9	[33]
Chlorella pyrenoid.	250 mL batch autoclave	473 K, 60 min	Ethanol/water (80/100 %)	40	9.48	7.99	[51]
Spirulina	50 ml autoclave	473- 698 K, 60 min	Toluene, tetralin,	52,3- 78.3	4.8	6.8-8.4	[60]

## 2.2 Mechanism study of HTL

### HTL of monomeric model compounds

For the potential bio-oil valorization it is significant to unravel the chemical pathway of a protein fraction under hydrothermal conditions. Protein is known to undergo hydrolysis to form its monomers, amino acids. There have been a number of studies devoted to the description of the decomposition of amino acids as a representative model compound of proteins during HTL (Table 6).

**TABLE 6.** Summary of studies on HTL of amino acids

Model compound	Set up	Operation parameters			Main decomposition products	Ref.
		T, °C	P, MPa	T, min		
Alanine, leucine, phenylalanine, serine, aspartic acid	continuous reactor system	200-340	2		Alanine→Ammonia, ethyl amine, pyruvic acid, lactic acid, propionic acid, acetic acid, formic acid Glycine→ammonia, methyl amine, glycolic acid, formic acid, Leucine→ ammonia, acetic acid, formic acid, etc.	[68]
Alanine glycine	continuous high pressure plant	250-450	34 and 24	2.5-35	Alanine→lactic acid, acetaldehyde, propionic acid, ethylamine Glycine→glycolic acid, diketopiperazine, formaldehyde, acetic acid	[28]
Glycine	flow reactor	250, 300, 350, 374	22,2-40	0.25-6	Diglycine, triglycine (trace), diketopiperazine	[69]
Aspartic acid	continuous flow tubular reactor	200-260	20	15-360 s	Ammonia, fumaric acid, maleic acid, pyruvic acid, etc	[70]
Glycylglycine	continuous flow tubular reactor	240-300	20	3-36	Glycine, cyclo(Gly-Gly)	[71]
Glutamate	flow-through hydrothermal reactor	150-250		3-36	Glutaconate, $\alpha$ -hydroxyglutarate, ketoglutarate, formate, succinate, CO <sub>2</sub> , H <sub>2</sub> (aq)	[72]
Phenylalanine	quartz mini-batch reactor	130-340		5-240	Phenylethylamine, styrene	[73], [74]
Tyrosine, serine, threonine, cysteine, aspartic, glutamic acid, lysine, etc.	batch reactor	230-290		2-3	Threonine→glycine, formic acid, acetic acid, carbonic acid Cysteine→glycine, alanine, pyruvic acid, acetic acid Tyrosine→glycine, formic acid, carbonic acid, methylamine, etc.	[75]

Based on previous studies on the amino acids HTL, the predominant reactions involved in the amino acid hydrothermal decomposition are: deamination, decarboxylation, cyclization (e.g. formation of pyroglutamate), lactamization, dehydration, reduction, aldol cleavage (e.g. glycine and alanine formation as thermal transformation products of serine and cysteine through dehydration/reduction and aldol cleavage), dimerization and oligomerization.

Also the formation of simple amino acids, such as glycine and alanine, from higher molecular amino acids was observed by several researchers [28], [68]. That is why, glycine and alanine are the most studied amino acids, as they are like “mirrors” of other amino acids, being their intermediates under HTL conditions.

In spite of a number of studies on the behavior of amino acids in hydrothermal water, there is still a paucity of information to fulfil the following issues:

- The experiments of model compounds HTL with longer holding time that is relevant for real biomass HTL. Only phenylalanine decomposition has been carried out with the water at 130-350 °C with a holding time of 240 min [73], while the rest of the studies have been carried out at shorter holding times.

- Prior works do not provide information about how much carbon and nitrogen of amino acids get actually transferred into bio-oil, gas, aqueous and solid phases.

- None of the studies mentioned above have been carried out in the presence of homogeneous catalysts, while it is known that using alkali and acid catalysts increases the bio-oil yield.

- The information is typically limited to the reactions of individual compounds. Mixture systems are particularly important as they get closer to mimicking the chemistry of HTL of a real biomass providing information about interactions between different molecules.

### **HTL of macromolecular model compounds**

The chemistry involved in the reactions of macromolecular fractions of biomass under HTL conditions have been widely studied for some representative molecules of carbohydrate and lipid macromolecules separately, such as starch [76], [77] and triacylglycerides [57]

For instance, a detailed study of the thermal non-catalytic hydrolysis of sunflower oil with subcritical water illustrated that the fatty acid (FA) yield was found to increase dramatically with the temperature, which then act as acidic catalysts in the hydrolysis reactions [78]. Fatty acid can yield up to 90 wt.% conversion without the use of any catalyst in the hydrolysis reaction in subcritical water [79].

It has been demonstrated that at least 93 % of the starch is converted to soluble products at temperatures ranging from 180 to 220 °C [76]. Starch is found to decompose to sugars, 5-HMF and in very small concentrations to organic acids, such as butyric acid and acetic acid at 200°C [80].

The group of P. E. Savage [81] treated a set of model compounds, such as cornstarch and cellulose as model polysaccharides, soy protein and albumin as model proteins, sunflower oil and castor oil as model lipids, individually and in mixtures at 300 and 350 °C for a batch holding time ranging from 10 min to 90 min. It was found that the lipids produced the highest yield (>90%) of bio-crude and in most cases, the bio-crude yield from HTL treatment of mixtures was very similar to the mass-averaged yield calculated from the results of each individual component separately.

Correspondingly, in the study of P. Biller and A.B. Ross [22] a range of model biochemical components (albumin and a soya protein, starch and glucose, the triglyceride from sunflower oil and two amino acids) and microalgae (*Chlorella vulgaris*, *Nannochloropsis oculata* and *Porphyridium cruentum*) and cyanobacteria *Spirulina* were subjected to HTL at 350 °C, 200 bar in water. The yields and product distribution obtained for each model compound have been used to predict the behavior of microalgae with different biochemical composition and have been validated using microalgae and cyanobacteria. Broad agreement is reached between predictive yields and actual yields for the microalgae based on their biochemical composition.

Although several studies mainly focused on how much lipid, polysaccharide, or protein gets converted into the bio-crude, gas, aqueous-phase, and solid-phase product fractions during HTL, till to date only a few studies on the chemical mechanism of HTL were reported. For instance, A. Croce et. al. [82] described the main reaction pathways involved in the process of bio-oil production from municipal organic wastes using binary and ternary mixtures of cellulose, bovine serum albumin (BSA) and tripalmitin. According to their results, free fatty acids, fatty acid amides and Maillard-type compounds were found to be the main components of the bio-oil.

For the compounds, such as palmitamide, hexadecanenitrile and stearonitrile, hydrodenitrogenation (HDN) is an effectual means for converting them into hydrocarbons, while the rupture of C–N bond in rings is very difficult even under drastic conditions [83].

In this regard, feedstock engineering is a key solution for improvement of the bio-oil yield as well as its quality, making the bio-oil components less critical for the hydrotreatment. However, till to date no available information on the correlation between biomass

composition and the nature of nitrogen containing compounds present in the resulting bio-oil is reported.

### **2.3 HTL of microbial biomass**

The energy and environmental crises, which our population is currently experiencing, are forced to consider efficient and alternative uses for natural, renewable resources. For the sustainable production of chemicals, their precursors should not compete with food and feed use. A promising approach for achieving this goal is to use lignocellulosic biomass for the production of chemicals and fuels [84], as agricultural and agro-industrial wastes are abundant, renewable and inexpensive energy sources [85]. Additionally, these wastes are rich in sugars, which are easily assimilated by microorganisms; therefore, they are very appropriate for use as raw materials in the production of industrially relevant compounds by fermentation. Therefore, future trends will be directed to lignocellulose biotechnology and genetic engineering, by which the huge amounts of lignocellulosic biomass can potentially be converted into different high value products including bio-fuels and value added fine chemicals. In fact, major advances have already been achieved for cellulosic ethanol with corn ethanol [86].

The production of ethanol or any other higher value added products like fine chemicals and bio-fuels from lignocellulosic material involves the breakdown and hydrolysis of lignocellulose-containing materials into disaccharides, such as cellobiose, and ultimately monosaccharides, such as glucose and xylose. Microbial agents, including yeasts, strains, fungi, etc. then convert the monosaccharides into corresponding products (ethanol or acids, etc.) in a fermentation reaction which can occur over several days or weeks depending on the desired product [87].

In order to make cost competitive lignocellulosic biomass derived chemicals or fuels as a high-volume and low-value fuel/chemical, it is essential to encounter stiff competition with the existing market products (fossil fuels, chemicals) by valorising various process intermediates, which could make the entire business model attractive to find a payback for investors [88].

### 2.3.1 Oleaginous yeasts

Biodiesel is mostly produced through transesterification of various vegetable oils and fats using short-chain alcohols with suitable reaction catalyst. The primary feedstock used for biodiesel production are like palm, rapeseed, canola, sunflower, soybean, and coconut oils and they amount to 70–95 % of production cost [89].

These feedstocks can be substituted by microbial oils with a fatty acid profile for the biodiesel production. Moreover, compared with vegetable oil and animal fats, microbial lipids are advantageous because they can be produced in a faster, arable land-independent, continuous and controllable way [90].

Among microbial sources, oleaginous yeasts are very promising since they accumulate lipids in more than 70 % of their cellular dry weight, they offer easy scale-up, and alter their fatty acid composition [91].

*Cryptococcus curvatus* is an oleaginous yeast of particular interest for several reasons. First of all, it requires minimal nutrients for growth and it can accumulate up to 60 % of its cellular dry weight as intracellular lipids. Moreover, the accumulated oil is similar to commonly used plant seed oils in terms of fatty acid composition, which are present mainly as triglycerides (80–90 %). Lastly, it grows in a broad range of substrates including sugars, such as glucose, xylose, galactose, mannose, fructose, ribose, maltose, cellobiose, sucrose, and lactose, and also on glycerol and whey concentrate or permeate [92].

Extracting oil from the cell is a key step in biorefinery of yeast biomass. In recent years, several yeast lipid extraction technologies have been proposed: homogenizers (high pressure), microwaves (followed by enzymes) and solvents [90], [93].

Extracting oil from cells by HTL is a relatively new idea. For the first time I. Espinoza-Gonzalez et. al. [91] cultivated *Cryptococcus curvatus* yeast in a 5L bioreactor and this biomass slurry with a 53 % of lipid content was treated at 280 °C for 1 h with a batch stainless steel reactor. The resulting hexane soluble fraction contained mainly fatty acids and showed a low nitrogen content.

U. Jena et. al. [94] reported the co-solvent HTL of microbial yeast biomass in an isopropanol–water binary system in the presence or absence of Na<sub>2</sub>CO<sub>3</sub> catalyst. They leveraged the experimental results to techno-economic analysis (TEA) of the baseline HTL conversion pathway to evaluate the commercial feasibility of this process. The initial economic evaluation showed that the HTL process could generate a liquid fuel from the yeast biomass at \$5.09 gallon/l.

To the best of our knowledge, no other studies on HTL of oleaginous yeast were reported. This is probably due to the limited availability of this feedstock in the market.

Since HTL of oleaginous yeast biomass is evaluated as an alternative bioprocessing strategy for hydrolysis and lipid extraction for the biofuel production, further research is needed to address several challenges and technical barriers, such as detailed characterization of by-products, process optimization, reactor development, and cost, etc.

### 2.3.2 Liamocins

Yeasts glycolipids are another group of microbial platforms comprising sophorolipids, manno-sylerythritol lipid, cellobiose lipids and polyol lipids that comprise two subgroups: liamocins and polyol esters of fatty acids [95].

Liamocins are structurally unique, heavier-than-water “oils” produced by certain strains of *Aureobasidium pullulans* NRRL 50380. The complete structure of liamocins was determined by Price and co-workers [96]. They found that liamocins have a D-mannitol head group ester-linked to 3,5-dihydroxydecanoate acyl chains, three or four of which are joined together by 1,5-polyester bonds (liamocins Man-A1 and Man-B1), and similar 3'-O-acetylated analogs (Man-A2 and Man-B2) (Figure 11). However, other types of liamocins are produced depending on the choice of strain and growth conditions. The oil is surface active, suggesting that it functions as a biosurfactant. Moreover, oils from these strains were observed to exert an antiproliferative effect on cancer cell lines.

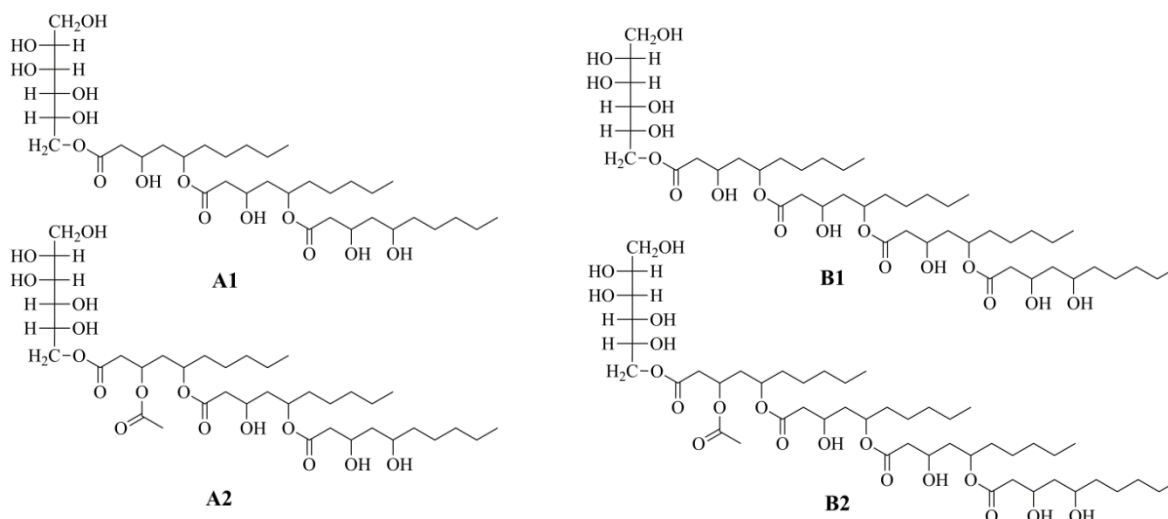


**FIGURE 11.** Liamocins structure

It should be taken into account that liamocins are contaminated and contain some impurities: inorganic salts used for the cultivation, organic solvents employed for the extraction, melatonin and its intermediates produced by microorganisms, etc. As the result, the purity of liamocins in crude oil preparations is uncertain [97]. Therefore, one can consider finding other relevant applications of liamocins. For instance, this microbially produced material could be subjected to additional thermal/chemical treatment serving as precursors. In tandem with the microbial treatment, additional thermal/chemical treatment of liamocins may result in the production of new significant chemicals. However, systematic studies on the HTL of liamocins to produce fuel and chemical products have not been reported yet.

## Chapter 3. Experimental design and procedure

This chapter discusses the experimental setup and procedures used for model compounds and microbial biomass HTL. Since the whole work consists of several parts performed using different approaches in experimental setup and analytical techniques, the chapter is divided into several subsections according to the topics.

### 3.1 HTL of model compounds

**Materials.** Leucine (cas 61-90-55, 98%), phenylalanine (cas 63-91-2, 98%), glutamine (cas 56-85-9, 99%), acetic acid (cas 64-19-7, 99%), formic acid (cas 64-18-6, 95%), glycerol (cas 56-81-5, 99.5%), acetone (cas 67-64-1, 99.5%), Bovine Serum Albumin (cas 9048-46-8, 96%), starch (cas 9005-84-9), tripalmitin (cas 555-44-2, 99%), triolein (cas 122-32-7, 99%), palmitic acid (cas 57-10-3, 99%), oleic acid (cas 112-80-1, 99%), diethyl ether (cas 60-29-7, 99.7%), ethyl acetate (cas 141-78-6, 99.8%) were purchased from Sigma Aldrich used as received. Phenylethylamine (cas 618-36-0, 98%), di(isopentyl)amine (cas 544-00-3, 97%), phenylethylacetamide (cas 103-81-1, 99%), styrene (cas 100-42-5, 99 %), cinnamic acid (cas 140-10-3, 99 %), 3-hydroxy-3-phenylpropionic acid (cas 2768-42-5, 98%) were purchased from Alfa Aesar and used as received.

**HTL experimental setup.** The HTL experiments were performed in a Parr 2L batch reactor (4520 series) up to 300 °C at a heating rate at 2.5 °C/min under 80-85 bar of autogenic pressure and at residence times of 60 min.

In a typical experiment, 300 g of water and 7 g of starting feedstock were loaded into the reactor taking into account the solubility of the feedstock. If needed, 0.7 g of heterogeneous catalyst was added to the reaction mixture. In order to investigate the effect of solvents on the bio-oil yields, 95/5 % v/v water-solvent solutions were prepared. In case of binary and ternary mixtures, equal masses of each component (4g) were used.

After the reactor was sealed, pure nitrogen gas was used to purge the vessel. The reactor was then heated up to the designated experimental temperature and maintained for the given time. At the end of the reaction, the reactor was rapidly quenched at a cooling rate of 11 °C/min by flowing cold water through the cooling coil located inside the reactor. The residence time was defined as the elapsed time between the reaction temperature first achieving and the starting of cooling down procedure.

After the reaction done, the gas yield was calculated by the ideal gas law using the residual pressure (after cooling down the reactor) and the average molecular weight of the gases. The gas composition was then collected and analyzed by Gas Chromatograph (GC). The gas formation was negligible, probably due to the lower heating rate of the reaction. The gas phase was found to consist mainly in CO<sub>2</sub> with the minor amount of CO. The recovery of the bio-oil phase was done by extraction with the diethyl ether (for monomeric model compounds) or ethyl acetate (for macromolecular model compounds). After the extraction of organic phase by the solvent, it was washed with water in order to remove the residual acetic acid partitioned into the oil phase when acetic acid-water binary solvent system was employed. After the evaporation of both bio-oil and aqueous phases from the solvent, they were used for further analytical characterization.

**Gas analysis.** The GC-MS analysis of the gas phase was performed by Gas Chromatograph (Agilent 7890A) equipped with a carboxen 1006 Plot column (30 m x 0.32 mm). The analysis was performed using the following method: 30 °C to 200 °C with 5 °C /min with splitless injection of 1ml of gas. Source Temperature 230 °C, Inlet 250 °C. Scan from 25 to 200 Dalton.

**GC-MS of oil samples.** Bio-oil samples have been first diluted in diethyl ether to a final concentration of 1 mg/ml. About 1 µl of these diluted samples were analyzed by GC-MS with a Finnigan Trace DSQ (Thermo) quadrupole mass spectrometry interfaced to a Finnigan Trace GC Ultra equipped with a DB-5 MS (Agilent J&W) fused silica, non-polar capillary column (30 m x 0.25 mm inner diameter and 0.25 µm film thickness) using helium as carrier gas (1 ml/min), in splitless mode.

Elution was performed using the following protocol: an initial temperature of 60 °C for 2 minutes, and a temperature to 320 °C at a rate of 10 °C min<sup>-1</sup>. Mass spectra were acquired in electronic ionization (EI) mode with a mass range 50-650 Da.

**Quantitative analysis of fatty acids, mono-, di-, and triglycerides.** Quantitative analysis of free fatty acids, mono-, di-, and triglycerides was performed by GC-FID equipped with Supelco Petrocol EX2887 (5m x 0.53 mm ID) using helium as a carrier gas (40 cm/sec constant flow). The analysis was performed using the following method: an initial temperature of 50 °C for 2 minutes, and a temperature to 350 °C with a rate of 10 °C/min. The silylation of oil components was performed using BSTFA (N,O-bis(trimethylsilyl)trifluoroacetamide). About 100 µl of BSTFA and 200 µl of pyridine were added into oil samples and the solutions were heated at 70°C for 40 min. Then the solutions were then diluted with 1 ml of dichloromethane. As internal standard (IS) tetradecan and

tricaprin were used. About 50  $\mu\text{l}$  of IS n-C14 (40.77 mg in 10 ml hexane) and 25  $\mu\text{l}$  of IS (8000 ppm of tricaprin in pyridine) were added to the solutions.

**Elemental analysis.** Elemental analysis of bio-oil products and solid residues was performed by an elemental analyzer Flash 2000 Thermo Fisher. Carbon, hydrogen, nitrogen and sulphur were determined simultaneously by quantitative analysis of their relative combustion gas products (carbon dioxide, water vapor, nitrogen, and sulphur dioxide). About 2-3 mg of each sample was directly weighed in a tin cup. Once inserted into the instrument, a complete combustion at 950  $^{\circ}\text{C}$  was performed. Helium was used as a carrier gas and oxygen as combustion gas.

The analysis of oxygen was done by EA1100 Thermo Fisher. The samples were weighed about 1-2 mg in silver cups and underwent to pyrolysis at 1060  $^{\circ}\text{C}$ .

**Total organic carbon (TOC) and Total nitrogen (TN) analysis.** TOC analysis of aqueous samples was performed by SHIMADZU-TOC-V instrument and TN analysis was done using TNM.

**ESI-FTICR-MS direct flow injection analysis.** Mass spectrometry analysis was performed on a 7 T FTICR MS (LTQ-FT Ultra Thermo Scientific), equipped with ESI (Electrospray) ion source. The mass spectra were collected in positive and negative mode. The sample was infused at a flow rate of 10 L  $\text{min}^{-1}$ ; typical ESI (+) conditions were as follows: source voltage 3.5 kV, capillary voltage 43 V, tube lens voltage 130 V, capillary temperature at 275  $^{\circ}\text{C}$ , sheath gas 10 arbitrary units, auxiliary gas 5 arbitrary units. The spectra were acquired both with a low resolution linear ion trap ( $m/z$  100-144 1000) and with a 7 T ultrahigh resolution FTICR cell with a mass range of 145  $m/z$  100-1000. The resolution was set to 400.000 (at  $m/z$  400). The ion accumulation time was defined by the automatic gain control (AGC), which was set to 106. A minimum of 100 scan was collected and averaged for each analysis to improve the signal to noise ratio. The data were processed by the software Xcalibur (Thermo Scientific), after setting the following restrictions to the element ranges: 0-60  $^{12}\text{C}$ , 0-2  $^{13}\text{C}$ , 10-100 H, 0-6 N, 0-1  $^{31}\text{S}$ , 0-6 O taking into account the elemental analysis, while the error range was set at  $\pm 2.5$  ppm. These restrictions are required because of the great number of possible different combinations of elements that can be generated from a single accurate mass.

The first step of the molecular formula assignment was done below 400 Da, since in this range the assignments are more reliable due to the lower number of possible combinations for a single mass. Secondly, the higher mass peaks (above 400 Da) were assigned through the Kendrick mass [98]. The lists of the masses and the corresponding molecular formulas were

then grouped with a custom designed software (ISOMASS) [99] and the mass peaks relevant to isotopic distributions were identified and deleted.

The relevant signals were categorized according to different parameters, such as the number of heteroatoms (N, O and S) and the number of unsaturations expressed as DBE (Double Bond Equivalents) [100]. For each molecular formula the DBE was calculated according to the following equation (for  $C_cH_hN_nO_oS_s$ ):  $DBE = c - h/2 + n/2 + 1$ . The molecular formulas were assigned to approximately 90 % of the peaks presenting relative intensities higher than 0.1 %.

**LC-MS analysis.** Aqueous phase products were quantitatively determined on a YMC Triart C18 column, using the following LC gradient method: from 60 to 100 % Acetonitrile in 12 minutes followed by isocratic conditions for 4 minutes at a constant flow rate of 0.4 ml/min. The flow was then split with a T union before entering the heated H-ESI ion source operated in positive ion mode with the following conditions: Source voltage 5kV, ESI temperature 100°C, Capillary voltage 43 V, Tube lens Voltage 130 V, Capillary temperature 280 °C, Sheath gas 50, Auxiliary gas 10. The mass spectra were acquired in high resolution in profile mode with the ICR Cell analyzer 176 (200000 RP) with a mass range from m/z 80 to 450. Quantitative determination of the reaction products was done using external standard calibrations in the concentration range between 0.02 and 0.1 mg/ml in acetonitrile.

**Ion exchange chromatography.** For the quantification of the acetic acid, the samples were filtered with 0.45 micron membranes and injected on an ion chromatograph (ICS3000 DIONEX instrument) with a AS11-HC column. The elution was isocratic with NaOH. The detection was conductimetric. Quantification was made with external standards.

**$^{13}C$  solid state NMR spectroscopy.** Solid residue was analyzed by  $^{13}C$  solid state NMR spectroscopy, with a Bruker Avance 400 NMR WB for solid state. Samples were put in 4 mm. zirconia rotors and then analyzed with the following experimental conditions: spectral width: 30 kHz, rotor speed: 12 kHz, Delay: 4.5 s, mixing time (for cross-polarization) contact time  $t_C = 3$  ms, number of scans: 20000.

**Product yield determination.** After all analyses, the product yields of bio-oil and solid residue phases were calculated by the following equations:

$$X_{bio-oil} = Mass_{bio-oil} / Mass_{feedstock} * 100\% \quad (Eq.1)$$

$$X_{solid} = Mass_{solid} / Mass_{feedstock} * 100\% \quad (Eq.2)$$

The carbon and nitrogen recovery in the bio-oil and solid residue were determined by following equations, where C and N are the mass percentages of carbon and nitrogen, respectively:

$$C_{bio-oil} = C(\%)_{bio-oil}/C(\%)_{feedstock} * X_{bio-oil} \quad (Eq.3)$$

$$N_{bio-oil} = N(\%)_{bio-oil}/N(\%)_{feedstock} * X_{bio-oil} \quad (Eq.4)$$

$$C_{solid} = C(\%)_{solid}/C(\%)_{feedstock} * X_{solid} \quad (Eq.5)$$

$$N_{solid} = N(\%)_{solid}/N(\%)_{feedstock} * X_{solid} \quad (Eq.6)$$

The carbon and nitrogen recovery in aqueous phase were determined by TN and TOC analyses. In case of experiments with acetic acid-water solvent system, the carbon fraction which is contributed from acetic acid is subtracted from the total carbon of the system in order to consider amino acid only as a carbon source.

$$TOC_{phenylalanine} = TOC_{total} - TOC_{acetic\ acid} \quad (Eq.7)$$

The High Heating Value (HHV) was calculated by Dulong's formula as below, where C, H and O are the mass percentages of the carbon, hydrogen and oxygen, respectively.

$$HHV(MJ/kg) = 0.338C + 1.428(H - O/8) \quad (Eq.8)$$

Energy Recovery in the bio-oil is calculated by the following formula:

$$ER = X_{bio-oil} * HHV_{bio-oil} / HHV_{feedstock} \quad (Eq.9)$$

### 3.2 Catalytic liquefaction experiments

**Materials.** Leucine (cas 61-90-55, 98%), tri(isopentyl)amine (cas 645-41-0, 95%), diethyl ether (cas 60-29-7, 99.7%) were purchased from Sigma Aldrich used as received. Isopentylamine (cas 107-85-7, 99%), di(isopentyl)amine (cas 544-00-3, 97%), leucic acid (cas 498-36-2, 98%), di(isobutyl)amine (cas 110-96-3, 99%) were purchased from Alfa Aesar used as received.

**Preparation of Titanium dioxide (TiO<sub>2</sub>).** TritonX-100 (*tert*-octylphenoxy-polyethoxyethanol), 1-hexanol (98%, GC), cyclohexane (99%), titanium(IV) butoxide (97%), HNO<sub>3</sub> were purchased from Sigma Aldrich and used as received. All water used was in milliQ grade. The titania synthesis was carried out according to the procedure described in [101], [102] with some modifications and was as follows. First two solutions containing 41.5 g Triton-X (surfactant), 18.9 g 1-hexanol (co-surfactant), and 48.3 g cyclohexane (oil) was prepared. Then the aqueous phase was added to one of the solutions dropwise under stirring, making up the clear microemulsion. 26.4 g of tetrabutyltitanate dissolved in 5 M nitric acid was used as the aqueous phase. Then into this mixture the second solution of Triton-X/1-hexanol/cyclohexane was added and stirred for 1h and was heated to reflux temperature (74 °C) for 5h to complete the reaction. The solid was then separated by centrifugation and washed 5 times with ethanol, dried at 120 °C overnight and calcined at 400 °C for 3h (ramp rate 2 °C/min).

The oxides were generally loaded with Pt 5% wt., Ru 5% wt., Ni 15% wt., Ni/Pt (15%/5% wt.) by incipient wetness impregnation of tetraammineplatinum(II) nitrate, ruthenium nitrosyl nitrate and nickel nitrate salts. Bimetallic impregnation was done by dissolving both the cations in the same aqueous solution to be impregnated. The solution was loaded on the sample avoiding the complete wetting of the solid, following cycles of loading and drying in oven at 100 °C. Finally, the powder was dried at 120 °C overnight, calcined at 350 °C for 3h (ramp 5 °C/min) and meshed 60-80. The metallic phase was obtained by reduction with H<sub>2</sub>/N<sub>2</sub> flow (10 %) at 500 °C for 3h.

**Characterization of the catalyst.** Powders were characterized by P-XRD in a Philips X'Pert X'Celerator, with Cu- $\alpha$  radiation in the range 5-80°2 $\theta$  with a step of 0.1°2 $\theta$ .

Surface analyses were performed on an ASAP 2020 Micromeritics instrument using N<sub>2</sub> as probe gas and pretreating the sample under 30 mmHg, prior at 150 °C (ramp 2 °C/min) for 30 min and then for 60 min at 250 °C (ramp 10 °C/min).

**Experimental set-up.** The experiments were performed in a 300 ml stainless steel Parr autoclave. 50 ml of water and 1.5 g of leucine were loaded into the autoclave. The added catalyst amount was 0.15 g. Then autoclave was charged with the hydrogen of 20 bars. All reactions were carried out at 250 °C for 3 h.

**Product analyses.** Leucic acid was analyzed in an Agilent HPLC over Rezex ROA Organic Acid column (0,0025M H<sub>2</sub>SO<sub>4</sub> eluent, oven temperature 30 °C and 0.5 ml/min flux) with

DAD and RID detector. Isopentylamine was quantified using C18 Poroshell column (5 % Acenotrile/95 % H<sub>2</sub>O isocratic, 0.5 ml/min, 30 °C).

The quantitative analysis of bio-oil was performed on the Agilent Technologies 6890 GC coupled with a mass spectrometer Agilent Technologies 5973 with a non-polar column (5 % Phenyl-95% methyl siloxane, 30m x 250µm x 1.05µm). As internal standard di(isobutyl)amine was used. Helium was used as a carrier gas at a flow rate equal to 1ml/min; the injector was maintained at a temperature of 250 °C in the split mode (50:1); total flow was 23.9 ml/min. The volume of solution injected was 0.5 µL and the standard temperature program was an isothermal step at 50 °C for 5min, ramp 20 °C/min until 280°C, and a final isothermal step for 5min.

The bio-oil and solid residue yields were calculated according to (Eq.1) and (Eq. 2).

### 3.3 HTL of oleaginous yeasts

**Materials.** The biomass obtained from the fermentation of oleaginous yeasts biomass was provided by ENI Donegani in Novara (Italy). The biomass concentration was estimated 76.5g/l, while the lipid fraction -51.5 g/l (67.2 %). There was also a glucose residue (30 g/l) in the yeast biomass that used as a carbon source during the cultivation.

**Processing methodology.** The HTL experiments were performed in Parr 1L batch reactor (Parr instrument) at a temperature of 300 °C and at residence times of 60 min. In a typical experiment, 400 ml of reaction medium consisting of 30g of biomass in water alone was loaded into the reactor. After the reactor was sealed, pure nitrogen gas was used to purge the reactor three times. The reactor was then heated up to the designated experimental temperature (defined as the reaction temperature) and the temperature was maintained for a predetermined time. The gas yield was calculated from the ideal gas law using the residual pressure (after cooling down the reactor) and the average molecular weight of the gases. A typical gas composition was analyzed by Gas Chromatograph and was found to consist mainly CO<sub>2</sub> and in minor amounts of CO. GC-MS, GC-FID, FTICR-MS, TOC/TN and elemental analyses protocols are given in Section 3.1.

### 3.4 HTL of liamocins

**General information.** Liamocins were provided by Biological department of RWTH Aachen University. 6-Pentyl-5,6-dihydropyran-2-one (cas 54814-64-1, 95%), 5-decanolide (cas 705-86-2, 98%), ethyl hexanoate (cas 122-66-0, 98%), ethyl acetate (cas 141-78-6, 99.8%) were purchased from Sigma Aldrich and used as received. 3-Hydroxy-5-decanolide was isolated from the saponification of liamocins.

**Isolation of the liamocins.** The culture broths were centrifuged at 6000 rpm for 30 min. The lipids as heavy oils were then extracted twice with 2-butanone to separate them from the cells. The extract was evaporated to dryness by using rotary evaporator and high-vacuum pump.

**Saponification of the liamocins.** The saponification of liamocins was performed according to the procedure [103] with some modifications. The lipids (about 2 g) were mixed with 2N NaOH (10 ml) and then saponified with permanent shaking overnight at room temperature. After acidification of the reaction mixture with 5N H<sub>2</sub>SO<sub>4</sub> to pH 3, resulting fatty acid components was extracted twice with ether. Removal of the ether gave an oil (about 0.36 g), as a mixture of fatty acid components.

**Experimental set-up.** Reactions were carried out using a 75 ml autoclave (HOKE type). After loading the reactant solution, catalyst, and magnetic stirrer bar into the reactor, the vessel was sealed, purged with and pressurized with N<sub>2</sub> or H<sub>2</sub>. Mechanical stirring was maintained using a magnetic stirrer plate (500 rpm). After the reaction done, the reaction mixture was filtrated in order to separate the solids from the liquid phase. Additional amount of solvent was added to wash the reactor walls and the solids.

**GC-MS analysis.** Measurements were carried out on a Varian CP-3800 gas chromatograph equipped with a CP-WAX-52 column (60 m x 250 µm x 0.25 µm) and a Varian 1200L Quadrupole MS/MS fitted with an electron ionization (EI) source. The volume of injected sample was 1 µL (diluted in methanol 1:10) and the GC signal was recorded with a flame ionization detector (FID). The EI voltage was set at 70 eV with a transfer capillary temperature of 250 °C and an ion source temperature of 250 °C.

**GC-FID analysis.** The analysis of the samples was performed with an Agilent HP6890 gas chromatograph equipped with a CP-WAX-52 column (60 m x 250 µm x 0.25 µm). The volume of injected sample was 1 µL and the signal was recorded by a flame ionization detector (FID). N<sub>2</sub> was used as the inert gas at a flow rate of 1.5 ml/min and an inlet temperature of 250 °C. The split flow was 50 ml/min. The following temperature program

was used for the measurement: 70 °C (5 min) and 200 °C (15 min) with a heating ramp of 8 °C/min.

**HLPC analysis.** The products of oil and aqueous phases were quantified by a high performance liquid chromatograph (LC-20A Prominenc) equipped with a RID and DAD detectors. For the analysis of oil phase a reversed-phase Macherey Nagel-NucleodurC18ec column (250/4) was used on PDA (220 nm). The column temperature was 30 °C. The analysis was performed in isocratic flow at 0.6 ml/min using methanol/H<sub>2</sub>O (50/50 %) in isocratic mode.

For sugars presented in the reaction mixture, when water is used as a reaction medium, were quantified using Organic acid resin column (300 mm X 8.0 mm; 100 mm x 8.0 mm) on RID detector. The column temperature was 40 °C. The analysis was performed in an isocratic flow at 1 ml/min. As a mobile phase 154 µl TFA in 1L H<sub>2</sub>O was used. The quantification of the products was performed using external standards of mannitol, arabitol, acetic acid, glyceraldehyde, 1,3-dihydroxycetone, and butyric acid.

**NMR analysis.** <sup>1</sup>H NMR and <sup>13</sup>C spectra were recorded at 25 °C on a Bruker Avance 400 MHz spectrometer. The data processing was done using the MNOVA software package. Quantitative analysis has been performed using certified Benzoic acid (Sigma Aldrich, 99.9% NMR CRM's) as an internal standard.

**ESI analysis** was performed on LC-MS-2020- Single Quadrupole MS.

## Chapter 4. Results and discussions

### 4.1 HTL of amino acids

In this Section the decomposition behavior of amino acids (leucine, phenylalanine and glutamine) alone and in binary mixtures with glucose and tripalmitin was investigated at 300°C with a batch holding time of 1h. All product streams (bio-oil, solid residue and aqueous phases) were characterized using different analytical techniques. Most attention was paid to the carbon and nitrogen transferring into HTL product streams. The effect of homogeneous and heterogeneous catalysts on the HTL product streams was also investigated. The effect of acetic acid on the improvement of energy yields of HTL oil was comprehensively studied.

#### 4.1.1 Leucine HTL

The bio-oil yield obtained from the blank experiment of Leucine HTL that carried out with the water was 6%. The effect of various solvents and catalysts, which are widely used in biomass valorization, was also investigated on Leucine HTL product streams (Figure 12).

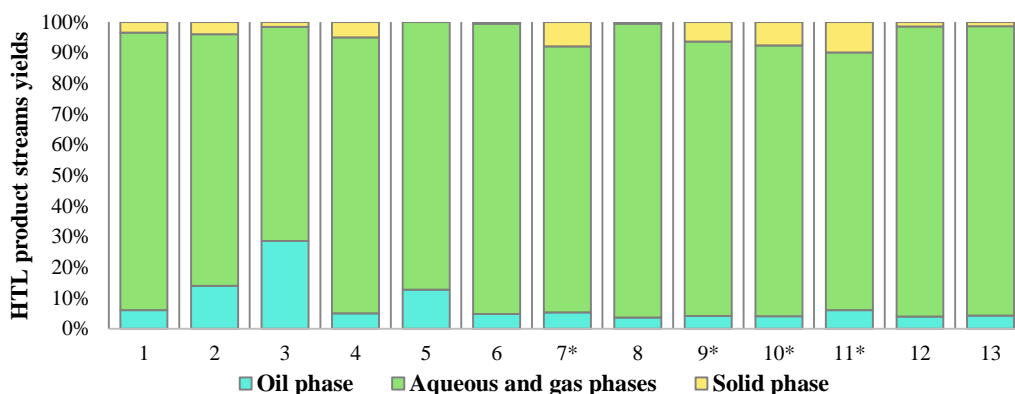


**FIGURE 12.** The effect of solvents and catalysts on HTL products stream yields

**Reaction conditions:**  $T=300\text{ }^{\circ}\text{C}$ ,  $t=60\text{ min}$ ,  $c(\text{leucine})=0.023\text{ g/ml}$ , in **1**) water, **2**) methanol-water (95/5 %, v/v), **3**) acetic acid-water (95/5 %, v/v), **4**) glycerol-water (95/5 %, v/v), **5**) acetone-water (95/5 %, v/v), **6**) formic acid-water (95/5 %, v/v), **7**) water,  $m(\text{Nb}_2\text{O}_5)=0,7\text{ g}$ , **8**) water,  $m(\text{Na}_2\text{CO}_3)=0.7\text{ g}$ , **9**) water,  $m(\text{FeS})=0,7\text{ g}$ , **10**) water (95/5 %, v/v),  $m(\text{FeS})=0.7\text{ g}$ , **11**) methanol-water (95/5 %, v/v),  $m(\text{Nb}_2\text{O}_5)=0.7\text{ g}$ , **12**) methanol-water (95/5 %, v/v),  $m(\text{Na}_2\text{CO}_3)=0.7\text{ g}$ , **13**) methanol-water (95/5 %, v/v),  $m(\text{MgO})=0.7\text{ g}$ .

\*The yield of solid residue can be overestimated due to the presence of catalysts.

The addition of acetic acid, methanol and acetone promoted the formation of bio-oil up to 28.6, 13.9 and 12.69 % respectively, while there was a decrease in the bio-oil yield to 4.74 % when formic acid was used as a co-solvent, respectively. The consistent decrease in the solid residue implies the formation of more water soluble components in the presence of formic acid. Methanol, acetone and acetic acid, on the other hand, could react with the degradation products of amino acid, thus contributing to the bio-oil yield.

The addition of  $\text{Nb}_2\text{O}_5$ ,  $\text{Na}_2\text{CO}_3$  and FeS catalysts lowered the bio-oil yield to 5.2, 3.7 and 4.2%, respectively. In addition, the solid fraction increased from 3.32 (blank experiment) to 7.9 and 10.18 % in the case of  $\text{Nb}_2\text{O}_5$  and FeS, respectively. Since the solid residue was not soluble in the organic solvents, the yield of solid residue could be overestimated due to the incomplete separation of the catalysts from the solids.

The solid residue formation was not observed in the presence of  $\text{Na}_2\text{CO}_3$ . From literature  $\text{Na}_2\text{CO}_3$  is known to accelerate the hydrolysis of macromolecules further decomposition to form water soluble compounds [34], [58], [59], [104], [105]. It is worth mentioning that the effect of  $\text{Na}_2\text{CO}_3$  could be different moving from monomeric model compounds to complex polysaccharides and proteins containing feedstocks. R. Shakya et. al. [105] found that using  $\text{Na}_2\text{CO}_3$  resulted in an increase of the bio-oil yield for high carbohydrate containing algae (Pavlova and Isochrysis) at higher temperatures (300 and 350 °C), whereas for high protein containing algae (Nannochloropsis) the yield was higher only at lower temperature (250 °C). The addition of methanol in the presence of  $\text{Nb}_2\text{O}_5$ , FeS and  $\text{Na}_2\text{CO}_3$  catalysts did not affect significantly on the bio-oil yields.

### **Bio-oil characterization**

Bio-oils having high contents of heteroatoms (O, N, and S) cannot be directly used as a transportation fuel, because they are corrosive and chemically unstable, and they can lead to the emission of air pollutants ( $\text{NO}_x$  and  $\text{SO}_x$ ) upon combustion. In addition, they make catalytic upgrading more challenging [106].

The hydrogen/carbon (H/C), nitrogen/carbon (N/C) and oxygen/carbon (O/C) atomic ratios are important parameters commonly used to characterize the quality of petroleum.

Given these considerations, the heteroatom contents of bio-oil products were carefully analyzed. The elemental analysis, higher heating (HHV) and energy recovery (ER) values of bio-oils are given in Table 7.

As it can be seen from Table 7, there has been a decrease in N/C, O/C and H/C ratios of bio-oils with respect to the leucine standard. This suggests that dehydration, decarboxylation and deamination took place during the HTL treatment.

**TABLE 7.** The element analysis, HHV and ER of bio-oils of Leucine HTL

Reaction conditions	N, %	C, %	H, %	S, %	O, %	N/C	H/C	O/C	HHV, MJ/kg	ER, %
Leucine	10.5	53.6	10.3	0	20.1	0.2	2.3	0.3	29.2	-
1	6.3	72.3	11.3	<0.1	12.9	0.1	2.1	0.1	38.8	8.0
2	5.7	69.9	11.5	<0.1	11.4	0.1	1.9	0.1	37.1	16.5
3	8.9	63.9	10.8	<0.1	15.6	0.1	1.9	0.2	34.2	36.3
4	5.9	61.4	10.4	<0.1	12.5	0.1	2.0	0.2	32.8	5.6
5	6.3	63.0	10.5	<0.1	13.9	0.1	1.9	0.2	33.2	14.3
6	5.9	60.1	10.2	<0.1	11.9	0.1	2.0	0.1	32.2	5.3
7	5.6	61.7	10.4	<0.1	12.7	0.1	2.0	0.2	32.7	5.9
8	6.7	62.9	10.6	<0.1	9.0	0.1	2.0	0.1	33.8	4.3
9	6.3	63.1	10.6	<0.1	13.8	0.1	2.0	0.2	33.4	4.8
10	6.3	62.4	10.6	<0.1	11.4	0.1	2.0	0.1	33.4	4.6
11	6.3	61.3	10.4	<0.1	11.7	0.1	2.0	0.1	32.7	6.7
12	7.7	66.9	11.6	<0.1	10.7	0.1	2.0	0.1	36.3	4.9
13	6.6	65.1	10.9	<0.1	10.8	0.1	2.0	0.1	34.7	5.1

*Reaction conditions: T=300°C, t=60 min, c (leucine)=0.023 g/ml, in 1) water, 2) methanol-water (95/5 %, v/v), 3) acetic acid-water (95/5 %, v/v), 4) glycerol-water (95/5 %, v/v), 5) acetone-water (95/5 %, v/v), 6) formic acid-water (95/5 %, v/v), 7) water, m (Nb<sub>2</sub>O<sub>5</sub>)=0,7 g, 8) water, m (Na<sub>2</sub>CO<sub>3</sub>)=0.7 g, 9) water, m (FeS)=0,7 g, 10) methanol-water (95/5 %, v/v), m (FeS)=0.7 g, 11) methanol-water (95/5 %, v/v), m (Nb<sub>2</sub>O<sub>5</sub>)=0.7 g, 12) methanol-water (95/5 %, v/v), m (Na<sub>2</sub>CO<sub>3</sub>)=0.7 g, 13) methanol-water (95/5 %, v/v), m (MgO)=0.7 g.*

The heteroatoms in the original leucine were significantly removed by HTL, and HHV value was improved. The nitrogen content in the bio-oil produced from the blank experiment was 6.32 %, which is less by 39% in comparison to leucine feed before the treatment. Using the catalysts did not affect the nitrogen content significantly except Nb<sub>2</sub>O<sub>5</sub>, which resulted in the reduction of the nitrogen content by 11% with respect to the blank experiment.

Using Na<sub>2</sub>CO<sub>3</sub> itself, and with the Na<sub>2</sub>CO<sub>3</sub>/MeOH and MgO/MeOH systems declined the nitrogen removal only by 3, 13 and 2%, respectively, compared to the blank experiment; however, these systems resulted in higher carbon and lower oxygen contents of the bio-oil. Based on this, one can assume that using these systems could enhance the energy yields of carbohydrate rich biomass, but not protein rich biomass, since the nitrogen content was not suppressed during the liquefaction process.

It should be pointed out that during the element analysis of bio-oil produced in the presence of acetic acid, the nitrogen content of the bio-oil was 4.2 %, which is less by 34 % with respect to blank experiment. However, this decrease in the nitrogen content was due to mass effect of acetic acid partitioned to oil phase during the extraction. Therefore, the bio-oil was washed with water in order to remove acetic acid residue from the oil and was subjected to elemental analysis. In this case the nitrogen content of bio-oil corresponded 6.5 %.

However, the significantly higher ER value of bio-oil produced in the presence of acetic acid (36.3 %) compared to those from the blank experiment (7.2 %), which was due to the high bio-oil yields obtained. No residual solvent in bio-oil was detected using methanol and acetone, since they were removed by evaporation.

In general, HHV values of bio-oil samples after HTL treatment were significantly higher in all cases in comparison to the original leucine before the treatment. Once again, higher ER values were obtained for the bio-oil products produced in the presence of solvents than that produced in the presence of the catalysts because of higher bio-oil yields.

To provide a detailed chemical characterization of bio-oils, the oil samples were analyzed by GC-MS and FTICR MS. Figure 13 represents the main groups of components presented in the bio-oil normalized by peak area of GC analysis. The bio-oil components can be classified into 4 groups: organic acids, amides, amines, and diketopiperazine (DkP). To the best of our knowledge, secondary and ternary amines and amides are not reported in previous studies that have been performed with shorter residence times.

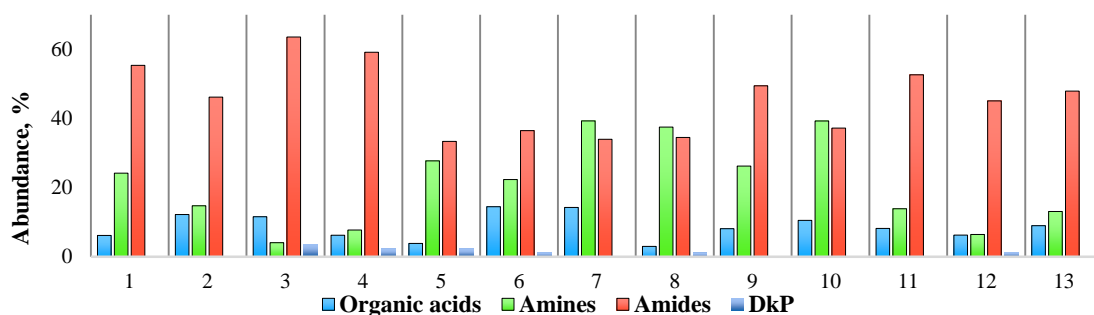


**FIGURE 13.** The composition of bio-oils from Leucine HTL

**Reaction conditions:**  $T=300^{\circ}\text{C}$ ,  $t=60$  min,  $c$  (leucine)=0.023 g/ml, in **1**) water, **2**) methanol-water (95/5 %, v/v), **3**) acetic acid-water (95/5 %, v/v), **4**) glycerol-water (95/5 %, v/v), **5**) acetone-water (95/5 %, v/v), **6**) formic acid-water (95/5 %, v/v), **7**) water,  $m$  ( $\text{Nb}_2\text{O}_5$ )=0,7 g, **8**) water,  $m$  ( $\text{Na}_2\text{CO}_3$ )=0.7 g, **9**) water,  $m$  ( $\text{FeS}$ )=0,7 g, **10**) methanol-water (95/5 %, v/v),  $m$  ( $\text{FeS}$ )=0.7 g, **11**) methanol-water (95/5 %, v/v),  $m$  ( $\text{Nb}_2\text{O}_5$ )=0.7 g, **12**) methanol-water (95/5 %, v/v),  $m$  ( $\text{Na}_2\text{CO}_3$ )=0.7 g, **13**) methanol-water (95/5 %, v/v),  $m$  ( $\text{MgO}$ )=0.7 g.

### Nitrogen element distribution into HTL product streams

Figure 14 shows the nitrogen element distribution into the oil, aqueous, and solid residue phases, calculated on the basis of TN analysis of aqueous phase and elemental analyses of bio-oil and solid residue phases taking account for the product streams yields.

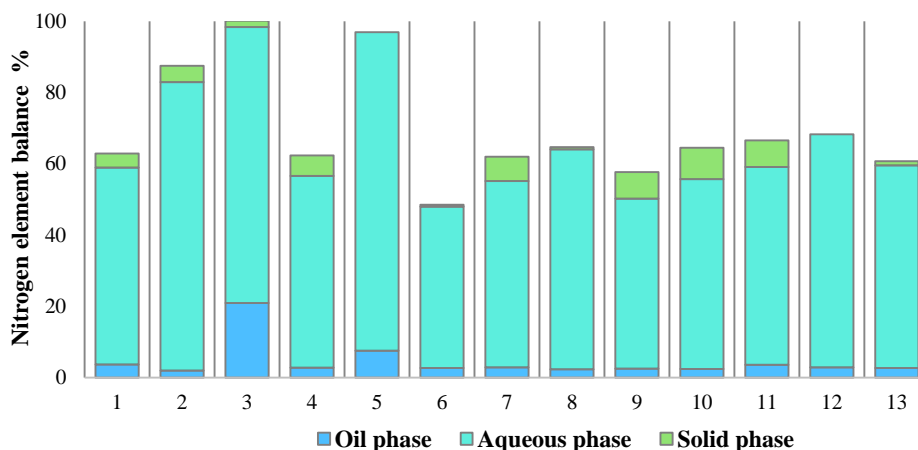


**FIGURE 14.** Nitrogen element distribution to products streams of Leucine HTL

**Reaction conditions:**  $T=300^{\circ}\text{C}$ ,  $t=60$  min,  $c(\text{leucine})=0.023$  g/ml, in **1**) water, **2**) methanol-water (95/5 %, v/v), **3**) acetic acid-water (95/5 %, v/v), **4**) glycerol-water (95/5 %, v/v), **5**) acetone-water (95/5 %, v/v), **6**) formic acid-water (95/5 %, v/v), **7**) water,  $m(\text{Nb}_2\text{O}_5)=0.7$  g, **8**) water,  $m(\text{Na}_2\text{CO}_3)=0.7$  g, **9**) water,  $m(\text{FeS})=0.7$  g, **10**) methanol-water (95/5 %, v/v),  $m(\text{FeS})=0.7$  g, **11**) methanol-water (95/5 %, v/v),  $m(\text{Nb}_2\text{O}_5)=0.7$  g, **12**) methanol-water (95/5 %, v/v),  $m(\text{Na}_2\text{CO}_3)=0.7$  g, **13**) methanol-water (95/5 %, v/v),  $m(\text{MgO})=0.7$  g.

The most nitrogen (55.3 %) is distributed into the aqueous phase in case of the blank experiment. From literature ammonium is known as the main aqueous nitrogen product formed through deamination of amino acid (Section 1.4). Only 3.6 % of the nitrogen is transferred into oil phase and 3.9 % of the nitrogen is recovered in the solid residue.

With the addition of acetic acid and acetone as co-solvents, about 20.9 and 7.5 % of nitrogen element, respectively moved to the oil phase.

$\text{Na}_2\text{CO}_3$ ,  $\text{Na}_2\text{CO}_3/\text{MeOH}$ , and  $\text{MgO}/\text{MeOH}$  resulted in the reduction of nitrogen recovery in the oil phase to 2.3, 2.87, and 2.68 %, respectively, and correspondingly its increase in aqueous phase up to 61.7, 65.4, and 56.9 %, respectively. Once again, this confirms their ability to enhance the further decomposition of bio-oil components to form water soluble compounds.

In comparison, FeS and FeS/MeOH systems did not affect significantly on the nitrogen recovery (NR) in the bio-oil phase; however, the increment of NR in solid residue up to 7.5 and 8.9 %, respectively, was observed. The increase in NR in the solid residue is also

observed in the case of  $\text{Nb}_2\text{O}_5$  and  $\text{Nb}_2\text{O}_5/\text{MeOH}$ . This suggests the further condensation reactions of bio-oil components to form solid residue in the presence of catalysts.

### Solid residue characterization

The elemental analysis, HHV and ER values of solid residue after HTL using different solvents and catalysts are given in Table 8. In comparison to the bio-oil products, the further decrease in H/C and increase O/C ratios of the solid residues implies that dehydration of the bio-oil components could result in the formation of the solid residue, while the increase in N/C ratio suggests that solid residue is mainly formed from nitrogen-containing intermediates of bio-oil.

**TABLE 8.** The element analysis, HHV and ER of solid residue of Leucine HTL

Reaction conditions	N, %	C, %	H, %	S, %	O, %	N/C	H/C	O/C	HHV, MJ/kg	ER, %
1	12.1	62.1	9.7	<0.1	16.5	0.2	1.9	0.2	32.1	3.6
2	12.2	61.8	9.8	<0.1	16.9	0.2	1.9	0.2	32.0	6.5
3	12.3	62.5	9.8	<0.1	15.8	0.2	1.9	0.2	32.3	5.3
4	12.2	62.7	10.5	<0.1	15.2	0.2	2.0	0.2	33.3	5.7
6	12.1	62.5	10.5	<0.1	15.5	0.2	2.0	0.2	33.2	0.5
7	9.1	45.7	7.0	<0.1	12.5	0.2	1.9	0.2	23.4	6.3
8	12.5	62.2	9.7	<0.1	16.6	0.2	1.9	0.2	32.1	0.6
9	12.2	58.0	10.0	1.43	15.5	0.2	2.1	0.2	31.1	6.8
10	12.2	61.3	10.4	0.47	15.7	0.2	2.0	0.2	32.7	8.5
11	7.9	43.0	7.0	<0.1	11.2	0.2	2.0	0.2	22.5	7.6
13	8.8	44.0	8.9	<0.1	18.9	0.2	2.4	0.3	24.3	1.1

**Reaction conditions:**  $T=300$  °C,  $t=60$  min,  $c$  (leucine)=0.023 g/ml, in **1**) water, **2**) methanol-water (95/5 %, v/v), **3**) acetic acid-water (95/5 %, v/v), **4**) glycerol-water (95/5 %, v/v), **5**) acetone-water (95/5 %, v/v), **6**) formic acid-water (95/5 %, v/v), **7**) water,  $m$  ( $\text{Nb}_2\text{O}_5$ )=0.7 g, **8**) water,  $m$  ( $\text{Na}_2\text{CO}_3$ )=0.7 g, **9**) water,  $m$  ( $\text{FeS}$ )=0.7 g, **10**) methanol-water (95/5 %, v/v),  $m$  ( $\text{FeS}$ )=0.7 g, **11**) methanol-water (95/5 %, v/v),  $m$  ( $\text{Nb}_2\text{O}_5$ )=0.7 g, **12**) methanol-water (95/5 %, v/v),  $m$  ( $\text{Na}_2\text{CO}_3$ )=0.7 g, **13**) methanol-water (95/5 %, v/v),  $m$  ( $\text{MgO}$ )=0.7 g.

In order to determine the chemical structure of solid residue,  $^{13}\text{C}$  CP MAS NMR analysis of solid residue from the blank experiment was performed. This technique is considered as the most powerful experimental approach to collect a direct information on structural and conformational characteristics of organic matters.

Regarding to the  $^{13}\text{C}$  CP MAS NMR analysis of the solid, very similar spectra were obtained for leucine before and after the HTL treatment (Figure 15).

The main differences were the shift of COOH-group from 176.6 to 170.8 ppm, which can be

assigned as CONH, and a broadening of the peak at 44.5 ppm after the treatment, indicating that  $-\text{CH}_2$  moiety is more affected by hydrothermal treatment. Supplementary data on element analysis of solid residue allows to conclude that the atomic composition of leucine moved from  $\text{C}_6\text{H}_{13}\text{NO}_2$  to  $\text{C}_6\text{H}_{11}\text{NO}$  that corresponds to  $\text{H}_2\text{O}$  loss.

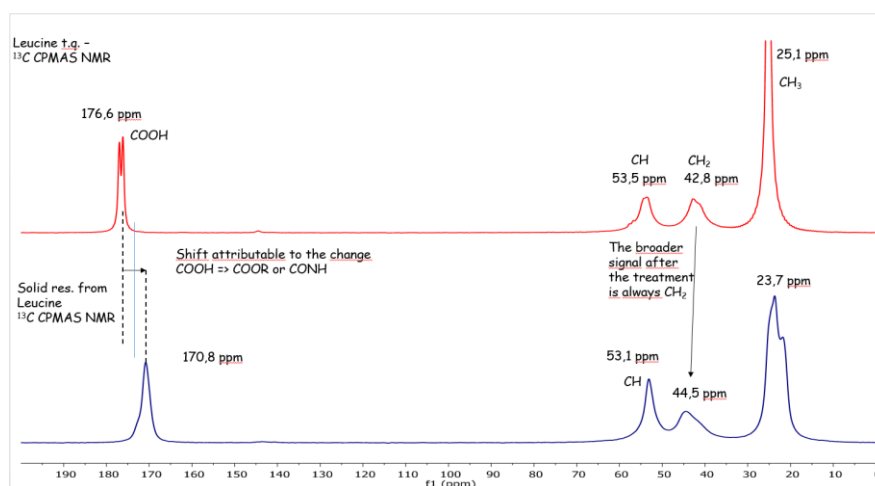


**FIGURE 15.**  $^{13}\text{C}$  CPMAS NMR analysis of leucine before and after HTL treatment

Based on this, one can assume that oligomerization and polymerization reactions took place via multiple dehydration of molecules of amino acids forming high molecular weight insoluble oligopeptide products (Figure 16).

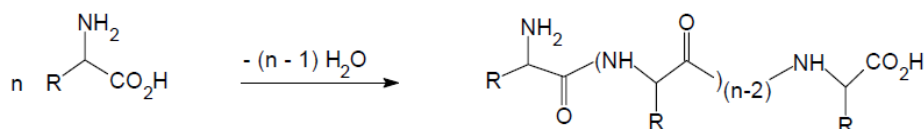


**FIGURE 16.** Solid residue formation from amino acid HTL

### Aqueous phase characterization

The aqueous phase was basic (pH 9–10) after the reaction, which was due to the presence of ammonia and amines. The amount of total organic carbon (TOC) in the aqueous phase indicates that during HTL, a significant portion of the organic products is water soluble (Figure 17). This is not surprising, since the starting model amino acid, leucine, is a small polar molecule.

Higher TOC values in the presence of co-solvents with respect to the blank experiment are due to a possible partition of co-solvents to the aqueous phase during the extraction, making it difficult to obtain reliable information on the water soluble species.

Using formic acid resulted in the reduction of TOC compared to the blank experiment.

Formic acid, in the given reaction conditions, decomposed to gas products ( $\text{CO}_2$  and  $\text{H}_2$ ) and did not contribute to the TOC compared to other co-solvents.

Once again, an increase in TOC value of the aqueous phase in the presence of  $\text{Na}_2\text{CO}_3$  proves the decomposition of bio-oil components to generate more water soluble compounds, while a decrease of TOC in case of  $\text{Nb}_2\text{O}_5$  and  $\text{FeS}$  catalysts is consistent with the increase in solid residue yields, which is due to the condensation of bio-oil components.

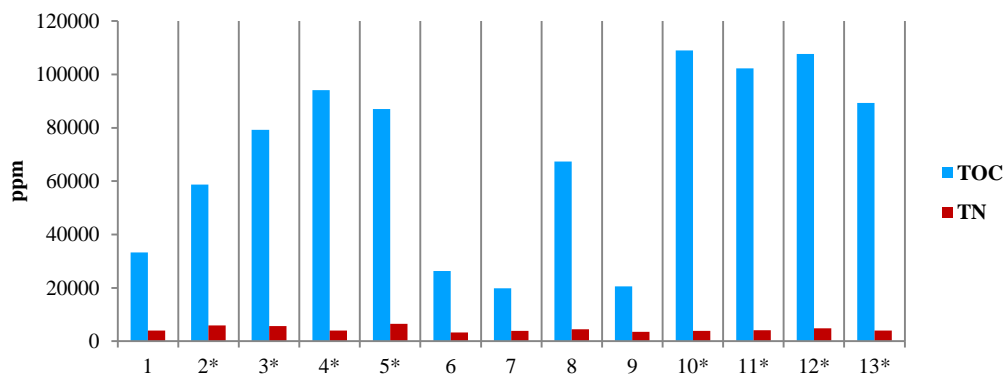


**FIGURE 17.** TOC and TN analyses of aqueous phase

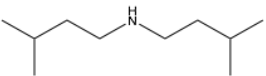
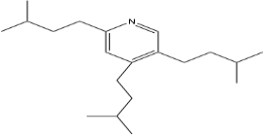
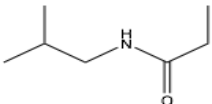
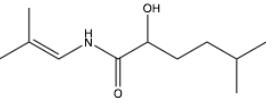
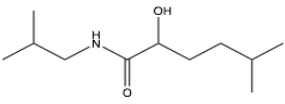
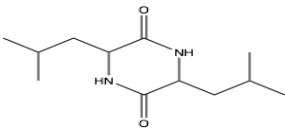
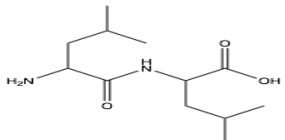
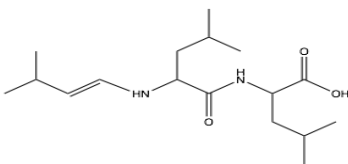
**Reaction conditions:**  $T=300^\circ\text{C}$ ,  $t=60$  min,  $c(\text{leucine})=0.023$  g/ml, in **1**) water, **2**) methanol-water (95/5 %, v/v), **3**) acetic acid-water (95/5 %, v/v), **4**) glycerol-water (95/5 %, v/v), **5**) acetone-water (95/5 %, v/v), **6**) formic acid-water (95/5 %, v/v), **7**) water,  $m(\text{Nb}_2\text{O}_5)=0.7$  g, **8**) water,  $m(\text{Na}_2\text{CO}_3)=0.7$  g, **9**) water,  $m(\text{FeS})=0.7$  g, **10**) methanol-water (95/5 %, v/v),  $m(\text{FeS})=0.7$  g, **11**) methanol-water (95/5 %, v/v),  $m(\text{Nb}_2\text{O}_5)=0.7$  g, **12**) methanol-water (95/5 %, v/v),  $m(\text{Na}_2\text{CO}_3)=0.7$  g, **13**) methanol-water (95/5 %, v/v),  $m(\text{MgO})=0.7$  g.

\*TOC increase due to the water soluble co-solvent

To provide a more detailed information about the chemical composition of the aqueous phase LC-MS analysis is performed. According to results, an isopentylamine as a main product of aqueous phase. Other products with more polar groups, such as  $\text{N}_2$ ,  $\text{O}_2\text{N}_2$ ,  $\text{O}_3\text{N}_2$ , etc. are also present (Table 9). The partition of di(isopentyl)amine ( $\text{C}_{10}\text{H}_{24}\text{N}$ ) is observed in the presence of methanol, acetic acid and glycerol. In the presence of acetic acid, the partition of isopentylacetamide ( $\text{C}_7\text{H}_{15}\text{ON}$ ) is found. Hydroxylated derivatives of amides ( $\text{C}_{11}\text{H}_{21}\text{O}_2\text{N}$  and  $\text{C}_{11}\text{H}_{23}\text{O}_2\text{N}$ ) are also preferred to relocate in the aqueous phase.

The leucylleucine ( $\text{C}_{12}\text{H}_{25}\text{O}_3\text{N}_2$ ) is formed through dehydration of two molecules of leucine. Further dehydration of leucylleucine results in the formation of diketopiperazine (Dkp) of leucine ( $\text{C}_{12}\text{H}_{22}\text{O}_2\text{N}_2$ ).  $\text{C}_{17}\text{H}_{33}\text{O}_3\text{N}_2$  are most likely a condensation product of leucylleucine and methylbutene formed via deamination of isopentylamine. These high molecular weight components in the aqueous phase was observed only in trace amounts.

**TABLE 9.** Aqueous phase composition of Leucine HTL

Compounds	DBE	M.w.	Chemical structure
$C_{10}H_{23}N$	0	157	
$C_{20}H_{35}N$	4	289	
$C_7H_{15}ON$	1	129	
$C_{11}H_{21}O_2N$	2	199	
$C_{11}H_{23}O_2N$	1	201	
$C_{12}H_{22}O_2N_2$	3	226	
$C_{12}H_{24}O_3N_2$	2	244	
$C_{17}H_{32}O_3N_2$	3	312	

To conclude, the aqueous phases from HTL of leucine were found to contain significant amounts of organic compounds. In case of real biomass, it also contains inorganic elements. Therefore, the aqueous phase is not suitable to be discharged to the environment because of the comparatively high level of carbon and nitrogen as well as minerals. Reusing the organic and nutrient rich aqueous phase for algae cultivation is reported to maximize bioenergy production [107].

### 4.1.2 Phenylalanine HTL

The bio-oil yield produced from Phenylalanine HTL carried out with the water was 7.3 %. The effect of solvents and catalysts on product yields of HTL of phenylalanine is given in the Figure 18. The trends were analogous to that described for Leucine HTL.

Also in this case the residual co-solvents in the oil phase were removed by water washing and evaporation. As already observed for leucine, acetic acid dramatically increased the bio-oil yield up to 30.2 %. The addition of other solvents also increased the bio-oil yield slightly (up to 8-9 %). Conversely, the bio-oil yield decreased to 2.1, 2.7, 1.4 % in the presence of  $\text{Na}_2\text{CO}_3/\text{MeOH}$ ,  $\text{MgO}/\text{MeOH}$  and  $\text{Na}_2\text{CO}_3$  systems, respectively. In this case, bio-oil components were not transferred into solid fractions (no solid formation), but relocated into the aqueous phase.

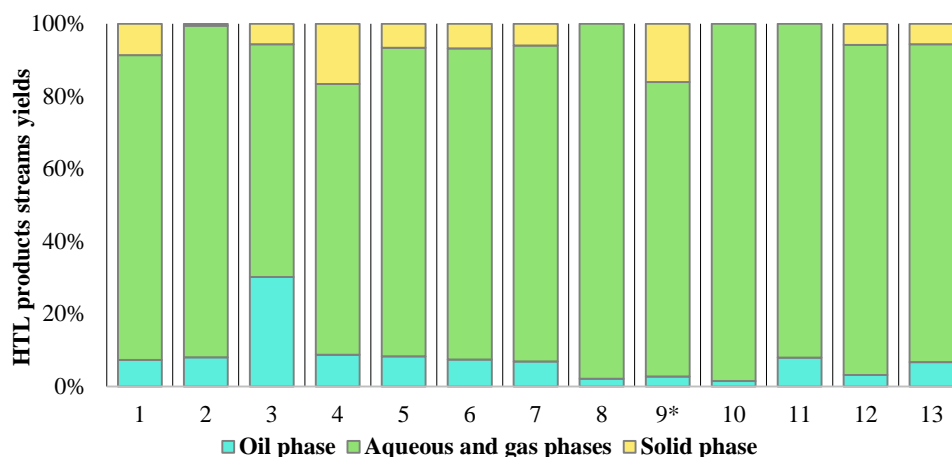


**FIGURE 18.** The effect of solvents and catalysts on the products streams yields of Phenylalanine HTL

**Reaction conditions:**  $T=300^\circ\text{C}$ ,  $t=60$  min,  $c(\text{phenylalanine})=0.023$  g/ml, in **1**) water, **2**) methanol-water (95/5 %, v/v), **3**) acetic acid-water (95/5 %, v/v), **4**) glycerol-water (95/5 %, v/v), **5**) acetone-water (95/5 %, v/v), **6**) formic acid-water (95/5 %, v/v), **7**) water,  $m(\text{Nb}_2\text{O}_5)=0.7$  g, **8**) water,  $m(\text{Na}_2\text{CO}_3)=0.7$  g, **9**) water,  $m(\text{FeS})=0.7$  g, **10**) methanol-water (95/5 %, v/v),  $m(\text{FeS})=0.7$  g, **11**) methanol-water (95/5 %, v/v),  $m(\text{Nb}_2\text{O}_5)=0.7$  g, **12**) methanol-water (95/5 %, v/v),  $m(\text{Na}_2\text{CO}_3)=0.7$  g, **13**) methanol-water (95/5 %, v/v),  $m(\text{MgO})=0.7$  g.

\*The solid phase can be overestimated due to the presence of solid catalyst

The yield of solid residue produced from Phenylalanine HTL (8.6%) was higher than those from Leucine HTL (3.4%). It is interesting to note that the formation of several high molecular weight products was reported in the previous study on Phenylalanine HTL [74]. They reported that styrene formed through the decomposition of phenylalanine can undergo polymerization to produce polystyrene. They also mentioned that phenylalanine could also dimerize at high temperatures and longer batch holding times.

### Bio-oil characterization

The elemental analysis, HHV and ER of bio-oil samples is given in Table 10. Also in this case the decrease in O/C, N/C and H/C ratios in comparison to phenylalanine suggests that the dehydration, deamination and decarboxylation reactions occurred in Phenylalanine HTL.

The nitrogen content in the bio oil from the blank experiment was 4.9 %. Once again, using acetic acid as a co-solvent in the HTL resulted in an increase in nitrogen content up to 6.5%. The addition of other solvents did not affect the nitrogen content, whilst the use of Na<sub>2</sub>CO<sub>3</sub>, Nb<sub>2</sub>O<sub>5</sub> and MgO catalysts reduced the nitrogen in the bio-oil by 28 %, 25 % and 17 % with respect to the blank experiment, respectively.

**TABLE 10.** The element analysis, HHV and ER of bio-oils of Phenylalanine HTL

Reaction conditions	%N	%C	%H	%S	%O	N/C	H/C	O/C	HHV, Mj/kg	ER, %
Phe	H	64.4	7.6	<0,1	20.0	0.1	1.4	0.2	29.8	29.1
1	4.4	80.4	7.5	<0,1	6.5	0.1	1.2	0.1	35.9	8.8
2	5.2	78.4	7.9	<0,1	5.7	0.1	1.2	0.1	36.4	9.9
3	6.5	67.9	9.0	<0,1	14.1	0.1	1.6	0.3	33.2	33.6
4	6.1	74.0	8.0	<0,1	11.5	0.1	1.3	0.1	34.3	11.2
5	5.0	76.3	7.9	0,43	7.1	0.1	1.2	0.1	35.5	9.5
6	5.3	75.6	7.4	<0,1	8.5	0.1	1.2	0.1	34.6	10.1
7	3.7	79.2	6.7	<0,1	5.8	0.1	1.0	0.1	35.2	7.8
8	3.8	83.4	6.3	<0,1	6.8	0.1	0.9	0.1	36.1	1.8
9	4.2	79.5	6.5	0,54	9.7	0.1	1.0	0.1	34.7	3.7
10	5.8	77.6	7.2	<0,1	5.1	0.1	1.1	0.1	35.5	8.8
11	4.4	78.6	6.8	0,14	5.5	0.1	1.0	0.1	35.2	8.1
12	7.9	73.5	7.8	<0,1	8.7	0.1	1.3	0.1	34.4	2.4
13	4.7	79.0	6.5	<0,1	7.9	0.1	1.0	0.1	34.8	3.2

*T=300°C, t=60 min, c (phenylalanine)=0.023 g/ml, in 1) water, 2) methanol-water (95/5 %, v/v), 3) acetic acid-water (95/5 %, v/v), 4) glycerol-water (95/5 %, v/v), 5) acetone-water (95/5 %, v/v), 6) formic acid-water (95/5 %, v/v), 7) water, m (Nb<sub>2</sub>O<sub>5</sub>)=0,7 g, 8) water, m (Na<sub>2</sub>CO<sub>3</sub>)=0.7 g, 9) water, m (FeS)=0,7 g, 10) methanol-water (95/5 %, v/v), m(FeS)=0.7 g, 11) methanol-water (95/5 %, v/v), m(Nb<sub>2</sub>O<sub>5</sub>)=0.7 g, 12) methanol-water (95/5 %, v/v), m(Na<sub>2</sub>CO<sub>3</sub>)=0.7 g, 13) methanol-water (95/5 %, v/v), m (MgO)=0.7 g.*

### Nitrogen element distribution into HTL product streams.

As observed for Leucine HTL, the most nitrogen (76.8 %) was mainly distributed in the aqueous phase. However, in this case a higher nitrogen recovery in the solid residue (12.6%) was observed (Figure 19). The presence of formic acid and methanol resulted in increase in the nitrogen recovery of the solid phase to 16.8 and 16.4 %, respectively. The consistent decrease in the nitrogen recovery of bio-oil and aqueous phases suggest that the condensation

reactions took place.

The nitrogen recovery in the bio-oil phase was increased from 4.2 % from the blank experiment to 20.9% in the presence of acetic acid.

The addition of other solvents and catalysts did not influence substantially on the nitrogen recovery in the bio-oil apart from acetic acid.

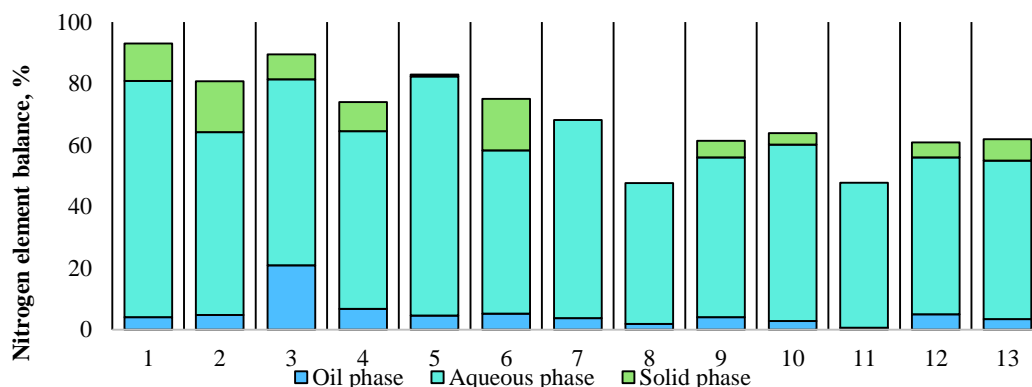


**FIGURE 19.** Nitrogen recovery in HTL product streams

*T=300°C, t=60 min, c (phenylalanine)=0.023 g/ml, in 1) water, 2) methanol-water (95/5 %, v/v), 3) acetic acid-water (95/5 %, v/v), 4) glycerol-water (95/5 %, v/v), 5) acetone-water (95/5 %, v/v), 6) formic acid-water (95/5 %, v/v), 7) water, m (Nb<sub>2</sub>O<sub>5</sub>)=0,7 g, 8) water, m (Na<sub>2</sub>CO<sub>3</sub>)=0.7 g, 9) water, m (FeS)=0,7 g, 10) methanol-water (95/5 %, v/v), m(FeS)=0.7 g, 11) methanol-water (95/5 %, v/v), m(Nb<sub>2</sub>O<sub>5</sub>)=0.7 g, 12) methanol-water (95/5 %, v/v), m(Na<sub>2</sub>CO<sub>3</sub>)=0.7 g, 13) methanol-water (95/5 %, v/v), m (MgO)=0.7 g.*

According to the results obtained from GC-MS and FTICR-MS analyses, the bio-oil components can be classified into 5 groups: organic acids, amides, secondary amines, alcohols and hydrocarbons (Fig. 20). Once again, the formation of amides and secondary amines has not been previously reported. Under hydrothermal conditions phenylalanine undergoes decarboxylation followed by deamination reactions to form styrene which is susceptible to dimerization and trimerization reactions.

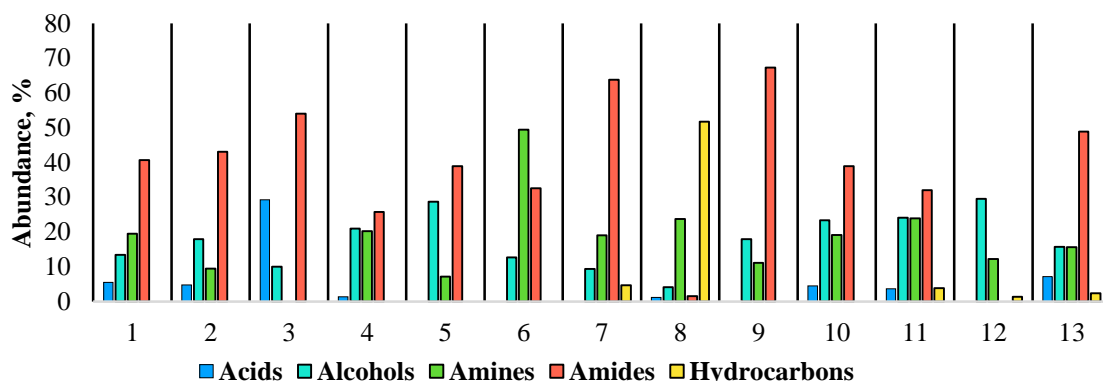


**FIGURE 20.** The main components presented in the bio-oil from Phenylalanine HTL

$T=300^{\circ}\text{C}$ ,  $t=60$  min,  $c$  (phenylalanine)=0.023 g/ml, in **1**) water, **2**) methanol-water (95/5 %, v/v), **3**) acetic acid-water (95/5 %, v/v), **4**) glycerol-water (95/5 %, v/v), **5**) acetone-water (95/5 %, v/v), **6**) formic acid-water (95/5 %, v/v), **7**) water,  $m$  ( $\text{Nb}_2\text{O}_5$ )=0,7 g, **8**) water,  $m$  ( $\text{Na}_2\text{CO}_3$ )=0.7 g, **9**) water,  $m$  ( $\text{FeS}$ )=0,7 g, **10**) methanol-water (95/5 %, v/v),  $m$  ( $\text{FeS}$ )=0.7 g, **11**) methanol-water (95/5 %, v/v),  $m$  ( $\text{Nb}_2\text{O}_5$ )=0.7 g, **12**) methanol-water (95/5 %, v/v),  $m$  ( $\text{Na}_2\text{CO}_3$ )=0.7 g, **13**) methanol-water (95/5 %, v/v),  $m$  ( $\text{MgO}$ )=0.7 g.

### Solid residue characterization

The element analysis of solid residue after HTL using different solvents and catalysts are given in the Table 11. Solid residues, obtained in the presence of the solvents, showed a carbon content (71-73 %) similar to that from the blank test. Conversely, in the catalytic runs an apparent reduction of all carbon, nitrogen and oxygen content was observed, due to the presence of the insoluble catalysts that cannot be separated from the solid reaction product. Comparing O/C and H/C ratios for bio-oils, a decrease of both the ratios suggests that dehydration was involved in the solid residue formation.

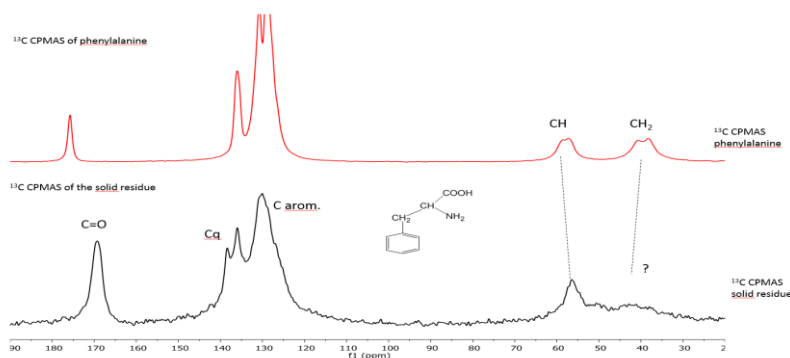
**TABLE 11.** The element analysis and HHV of solid residue of Phenylalanine HTL

Reaction conditions	%N	%C	%H	%S	%O	N/C	H/C	O/C	HHV, Mj/kg	ER, %
1	9.5	73.1	6.5	<0.1	11.1	0.1	1.1	0.1	32.6	9.6
2	9.5	73.0	6.5	<0.1	11.2	0.1	1.1	0.1	32.5	9.5
3	8.4	73.1	6.4	<0.1	12.0	0.1	1.1	0.1	32.4	6.3
4	9.1	72.4	6.0	<0.1	12.7	0.11	1.0	0.1	31.6	9.8
5	9.2	72.0	6.5	<0.1	12.5	0.1	1.1	0.1	32.0	0.6
6	8.7	72.8	5.9	<0.1	10.3	0.10	1.0	0.1	31.8	18.2
7	5.7	43.5	3.4	<0.1	4.8	0.11	1.0	0.1	19.0	3.7
9	7.4	61.5	4.6	4.66	7.7	0.1	1.0	0.1	26.6	5.3
10	7.2	55.5	4.2	<0.1	7.7	0.1	0.9	0.1	23.9	7.0
11	8.9	68.6	5.7	<0.1	9.8	0.1	1.0	0.1	30.2	4.9
13	4.9	45.5	4.9	<0.1	13.3	0.1	1.3	0.2	20.5	11.3

*T=300°C, t=60 min, c (phenylalanine)=0.023 g/ml, in 1) water, 2) methanol-water (95/5 %, v/v), 3) acetic acid-water (95/5 %, v/v), 4) glycerol-water (95/5 %, v/v), 5) acetone-water (95/5 %, v/v), 6) formic acid-water (95/5 %, v/v), 7) water, m (Nb<sub>2</sub>O<sub>5</sub>)=0.7 g, 8) water, m (Na<sub>2</sub>CO<sub>3</sub>)=0.7 g, 9) water, m (FeS)=0.7 g, 10) methanol-water (95/5 %, v/v), m(FeS)=0.7 g, 11) methanol-water (95/5 %, v/v), m(Nb<sub>2</sub>O<sub>5</sub>)=0.7 g, 12) methanol-water (95/5 %, v/v), m(Na<sub>2</sub>CO<sub>3</sub>)=0.7 g, 13) methanol-water (95/5 %, v/v), m (MgO)=0.7 g.*

According to <sup>13</sup>CPMAS NMR analysis of solid residue, a similar trend was observed with respect to that obtained from the solid residue of leucine HTL (Figure 21). Firstly, the -CH<sub>2</sub> moiety at 40.8 ppm was the most affected after hydrothermal treatment. Secondly, the shift of -COOH at 176.6 ppm to -CONH at 170 ppm was detected.

According to the element analysis of solid residue, the chemical formula of solid was C<sub>9</sub>H<sub>9</sub>NO with a loss of H<sub>2</sub>O with respect to the starting amino acid. As already observed for the solid residue from leucine HTL, the dehydration took place, forming peptide bonds between molecules of phenylalanine.

**FIGURE 21.** <sup>13</sup>CPMAS NMR analysis of solid residue from Phenylalanine HTL

### Aqueous phase characterization

As observed for Leucine HTL, the high values of TOC in the presence of solvents were due to the carbons contributed from the solvents, while there was a decrease in TOC when the catalysts were employed except  $\text{Nb}_2\text{O}_5$ . TN values were not changed significantly except acetic acid (Figure 22).

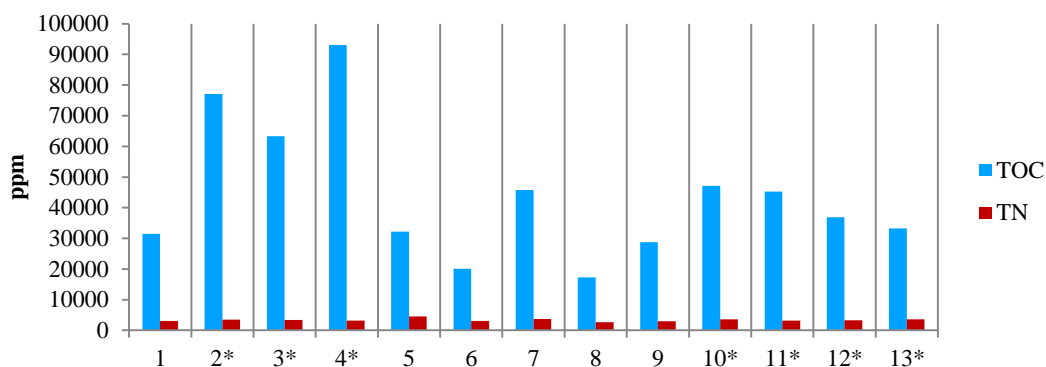


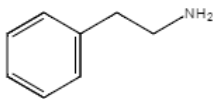
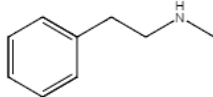
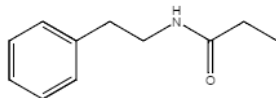
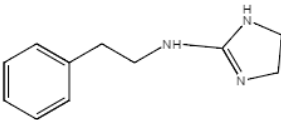
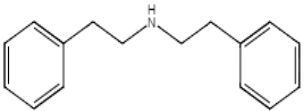
**FIGURE 22.** TOC and TN analyses of aqueous phase of Phenylalanine HTL

$T=300^\circ\text{C}$ ,  $t=60$  min,  $c$  (phenylalanine)=0.023 g/ml, in **1**) water, **2**) methanol-water (95/5 %, v/v), **3**) acetic acid-water (95/5 %, v/v), **4**) glycerol-water (95/5 %, v/v), **5**) acetone-water (95/5 %, v/v), **6**) formic acid-water (95/5 %, v/v), **7**) water,  $m$  ( $\text{Nb}_2\text{O}_5$ )=0,7 g, **8**) water,  $m$  ( $\text{Na}_2\text{CO}_3$ )=0.7 g, **9**) water,  $m$  ( $\text{FeS}$ )=0,7 g, **10**) methanol-water (95/5 %, v/v),  $m$  ( $\text{FeS}$ )=0.7 g, **11**) methanol-water (95/5 %, v/v),  $m$  ( $\text{Nb}_2\text{O}_5$ )=0.7 g, **12**) methanol-water (95/5 %, v/v),  $m$  ( $\text{Na}_2\text{CO}_3$ )=0.7 g, **13**) methanol-water (95/5 %, v/v),  $m$  ( $\text{MgO}$ )=0.7 g.

\*TOC increase due to the water soluble co-solvent

According to LC-MS and FTICR-MS analyses of the aqueous phase, phenylethylamine was the main product of the aqueous phase. The presence N2, N3 class components is observed (Table 12). The possible chemical structures of these components were proposed based on fragmentation patterns and DBE values obtained from FTICR MS analysis.

**TABLE 12.** Aqueous phase composition of Phenylalanine HTL

M.w.	Formula	DBE	Possible structure
121	C <sub>8</sub> H <sub>11</sub> N	4	
135	C <sub>9</sub> H <sub>13</sub> N	4	
163	C <sub>10</sub> H <sub>14</sub> ON	5	
189	C <sub>11</sub> H <sub>15</sub> N3	6	
225	C <sub>16</sub> H <sub>19</sub> N	8	

Generally speaking, among the catalysts, Nb<sub>2</sub>O<sub>5</sub> catalyst seems to be effective in the reduction of nitrogen content of the bio-oil by 11 % in the case of leucine (compared to the blank experiment). In the case of Phenylalanine HTL, the nitrogen content of bio-oil was reduced by 28, 24 and 17 % using Na<sub>2</sub>CO<sub>3</sub>, Nb<sub>2</sub>O<sub>5</sub> and MgO, respectively. However, the bio-oil yield was also decreased significantly.

For both Leucine and Phenylalanine HTL, the addition of acetic dramatically increased the bio-oil yield from 6.02 to 28.6 % and from 7.27 to 30.2 %, respectively. Using acetic acid also increased the nitrogen content in bio-oil by 32.6 % and 41.2 % for phenylalanine and leucine, respectively compared to the blank experiment. However, considerably higher ER values were found.

Since both amino acids tested are hydrophobic ones, the control experiments with the glutamine, which is a hydrophilic amino acid, in the presence of acetic acid was also carried out. As glutamine is a polar compound, there was no bio-oil formation from the experiment performed in a water medium. In comparison, about 6 % bio-oil is obtained with the addition of acetic acid as co-solvent.

Under hydrothermal conditions glutamine undergoes deamidation to form glutamic acid (1 a) (Figure 23). Glutamic acid is then dehydrated to form pyroglutamic acid (2 a) which is the

most abundant product of the aqueous phase. In minor extent glutamic acid undergoes deamination and subsequent hydration to form hydroxyglutaric acid (3 a). The formation of glutarimide (4 a), which is deamination and dehydration product of glutamine, is also observed.

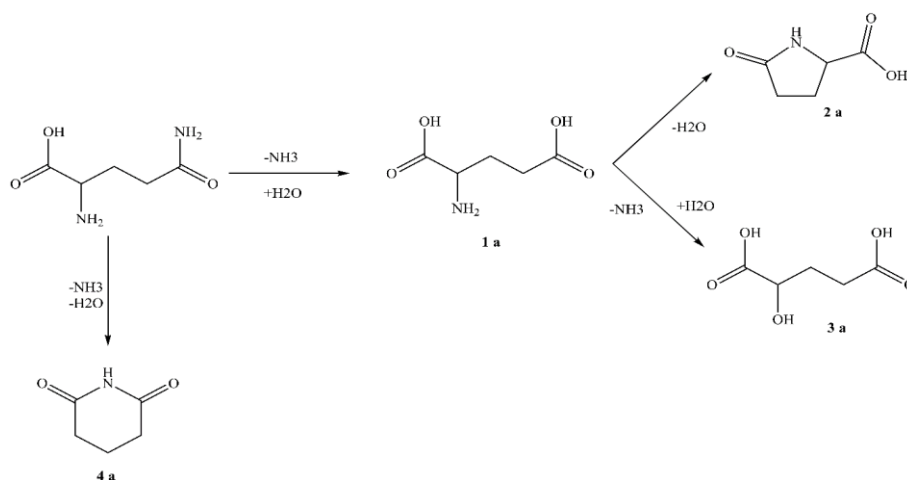


**FIGURE 23.** Chemical pathway of Glutamine HTL

According to TOC/TN and element analyses, all carbon (100%) and nitrogen (100%) elements relocated in the aqueous phase when water was a reaction medium, while an insignificant increase in carbon (6.9%) and nitrogen (0.3%) recovery in the bio-oil phase was observed using acetic acid as a co-solvent.

In this case the carbon balance related to amino acid only was not performed because of the insufficient amount of bio-oil. Therefore, the contribution of carbons of acetic acid to the bio-oil phase has to be considered; however, an increase in nitrogen recovery in the bio-oil phase proves the transferring some water soluble molecules from the aqueous phase to the bio-oil phase.

Apparently, the interpretation of the role of acetic acid in the improvement of bio-oil yield is crucial. This phenomenon is not simply related to a pH effect promoting the formation of more hydrophobic species, since the increase in the bio-oil yield was not observed in the control experiment that carried out at the same pH=5, but using sulfuric acid instead of acetic acid.

### 4.1.3 The effect of acetic acid in improvement of energy yields.

The fate of carbon and nitrogen and its distribution in the product streams is important as it influences the quality of the products. In order to understand the role of acetic acid in the observed yield increase, the standard experiment in water cannot be directly compared to those carried out in water-acetic acid solvent, since the additional mass contribution of acetic acid has to be considered. Therefore, the carbon and nitrogen mass balances related to amino acid only was calculated taking into account of the unreacted acetic acid (mainly in the aqueous phase) and the acetyl moieties (introduced in the bio-oil species).

The elemental balance of carbon and nitrogen was calculated by combining total organic content (TOC) and total nitrogen (TN) analyses of the aqueous phase along with CHN content and yields of the bio-oil products and solid residues. This indirect approach allows to measure the organic molecules presented in the bio-oil and aqueous phases.

The balance of acetic acid during HTL was determined in the gas phase by the difference of CO<sub>2</sub> produced in the experiments with and without the addition of acetic acid; for the aqueous and oil phases- the acetyl moiety containing products and acetic acid residue were quantified (Figure 24).

Then the carbons of the total system subtracted to those contributed from acetic acid in order to obtain the carbons related to the amino acid only.

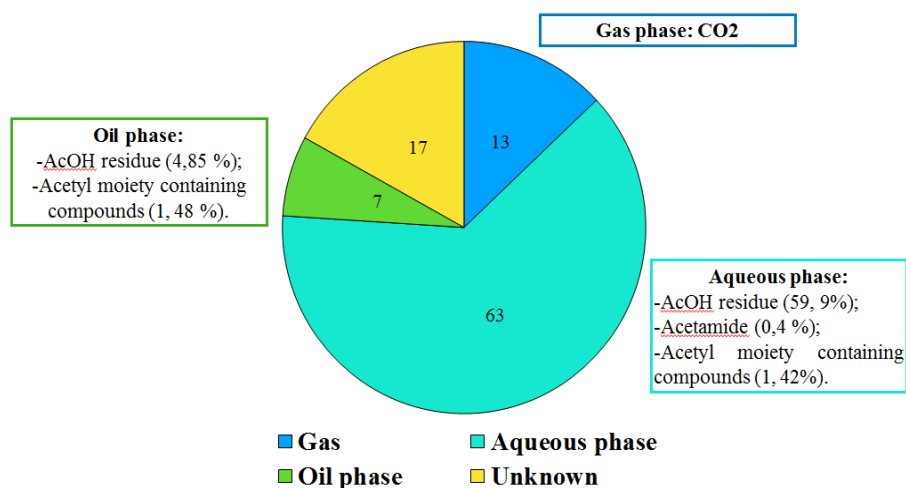


**FIGURE 24.** Distribution of acetic acid into Phenylalanine HTL product streams

According to the results obtained, when water was employed as a reaction medium around 8.5 % of the carbon and 4.2 % of nitrogen were distributed to the oil phase (Figure 25). The

carbon and nitrogen content in the solid residue phase were 12.5 % and 12.6 %, respectively. Both carbon (69.5%) and nitrogen (76.7 %) preferentially accumulated in the aqueous phase. In the presence of acetic acid a threefold increase in the carbon was observed in the bio-oil (28.8%). A significant amount of nitrogen (21.0 %) also moved to the oil phase. This increase is mainly attributed to the migration of water soluble molecules from the aqueous phase into oil phase.

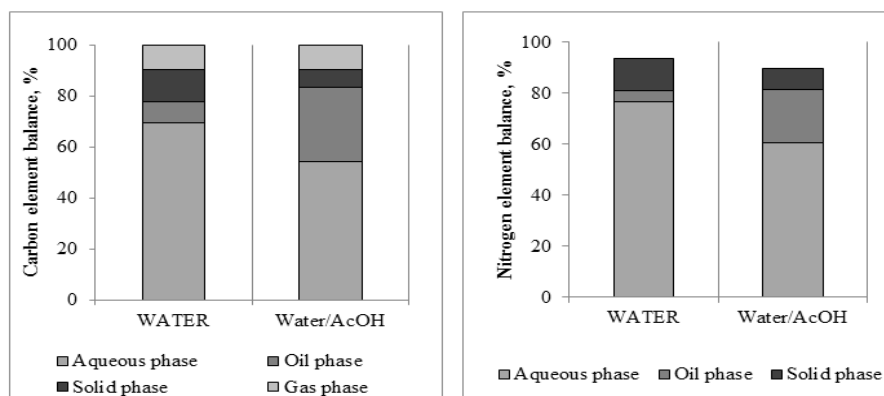


**FIGURE 25.** Carbon element recovery in Phenylalanine HTL product streams, %

Since the main relocations of carbons and nitrogen elements occur between oil and aqueous phases, the detailed characterization and quantification of reaction products in both phases have been done separately in order to reveal the gradual decomposition of the starting feedstock and the subsequent formation of bio-oil.

As shown in Figure 26, decarboxylation and deamination are competitive reactions in the first step of phenylalanine hydrothermal degradation, forming cinnamic acid (1 b) and phenylethylamine (2 b) respectively. Cinnamic acid further reacts with water to form 2-hydroxyphenylpropionic acid (3 b). Both 2-hydroxyphenylpropionic and cinnamic acids react with phenylethylamine to form the corresponding 2-hydroxy-N-phenylethyl-3-phenylpropanamide (4 b) and N-phenylethyl-3-phenylpropanamide (5 b), respectively.

In addition, phenylethylamine undergoes dimerization and deamination reactions to form di(phenylethyl)amine (6 b) and styrene (7 b), both partitioned into the bio-oil phase. Styrene further reacts to form minor amounts of hydration (8 b) and oligomerization (9 b) products.

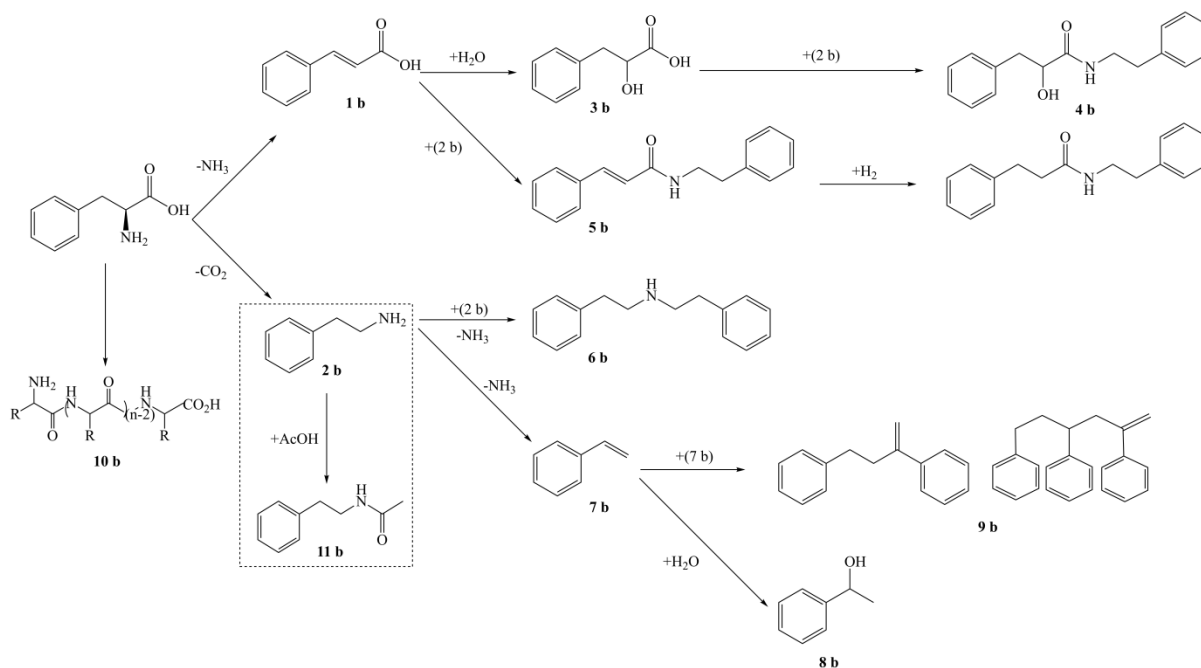


**FIGURE 26.** Chemical pathway of Phenylalanine HTL

In contrast, a different pathway was observed in water/acetic acid binary solvent, since phenylethylamine (2 b) reacts with acetic acid to form phenylethylacetamide (11 b) which is predominantly partitioned in the oil phase, as shown in Table 13, reporting the main reaction product yields and phase partitions. A large amount of carbons of phenylalanine is transferred into the oil phase as phenylethylacetamide (yield 15.6 mol. %) and that result matches with a reduced yield of phenylethylamine (from 61 mol. % to 46 mol. %), thus implying the formation of more hydrophobic compounds than hydrophilic ones.

In this case the acetyl moiety ( $C_n=2$ ) is also incorporated into the oil phase; however, the additional carbon recovery because of phenylethylamine ( $C_n=8$ ) transferring is the main reason for the increased yields as well as the energy recovery in the bio-oil. This explains the effect of acetic acid on the relocation of carbons from the aqueous phase into oil phase and the consequent improvement of mass and energy recovery from the substrate.

**TABLE 13.** Phenylalanine HTL main product yield and partition

Products, (mol, %)	Water		Water/AcOH	
	Aqueous phase	Oil phase	Aqueous phase	Oil phase
1 a		0.20		0.23
2 a	61.4		46.2	
3 a		0.61		2.06
4 a		0.89		1.43
5 a		0.25		0.24
6 a		1.72		2.27
7 a		0.70		0.82
8 a		0.15		0.4
9 a		0.07		0.05
10 a			1.42	15.6

All these products were identified and quantified with an overall molar balance up to 70 % on the basis of GC-MS and LC-MS analyses. The missing fraction of products in bio-oil that were not detectable by GC were identified by FTICR-MS ESI analysis.

According to the results, in the reference water solvent the presence of 6 b and 4 b as the main products of the bio-oil was confirmed. In addition, minor amounts of higher molecular weight N1- and N2- containing species were detected with  $C_n$  from C25 to C40 and DBE ranging 15-25 (Figure 27 a). The high carbon content and unsaturation degree (DBE) of these species suggests that they can be formed by further reactions of styrene intermediates.

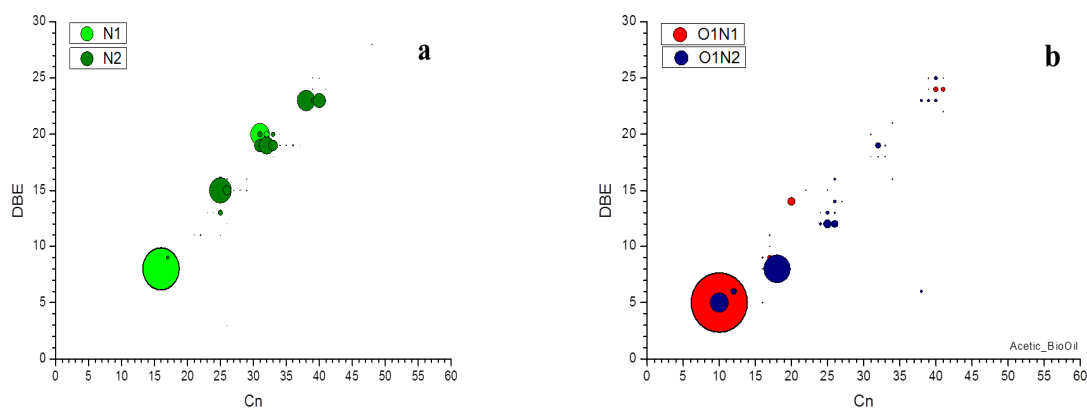


**FIGURE 27.**  $C_n$  vs DBE for main class components in the bio-oil from Phenylalanine HTL:  
a) in water b) water/acetic acid (95/5 % v/v)

In the presence of acetic acid, O1N1 and O1N2 class components with the main product distributions at  $C_n=10-20$  and  $DBE=3-10$  are observed (Figure 27 b). Lower  $C_n$  and DBE of

the components suggest that addition of acetic acid as a co-solvent prevents the condensation reaction, thus decreasing the amount of heavy molecular weight components.

As shown in Figure 28, the similar reaction pathway was also observed for Leucine HTL. According to GC-MS and LC-MS analyses, the decarboxylation pathway was confirmed to be predominant over the deamination route, being isopentylamine (2 c) as the most abundant specie, as already determined for Phenylalanine HTL. The amine (2 c) also undergoes dimerization reaction to form the secondary amine (6 c), while minor amounts of 4-methylpentanoic acid derivatives (1 c and 3 c) produced by the deamination of leucine reacted with 2 b to form the corresponding amides (4 c and 5 c).

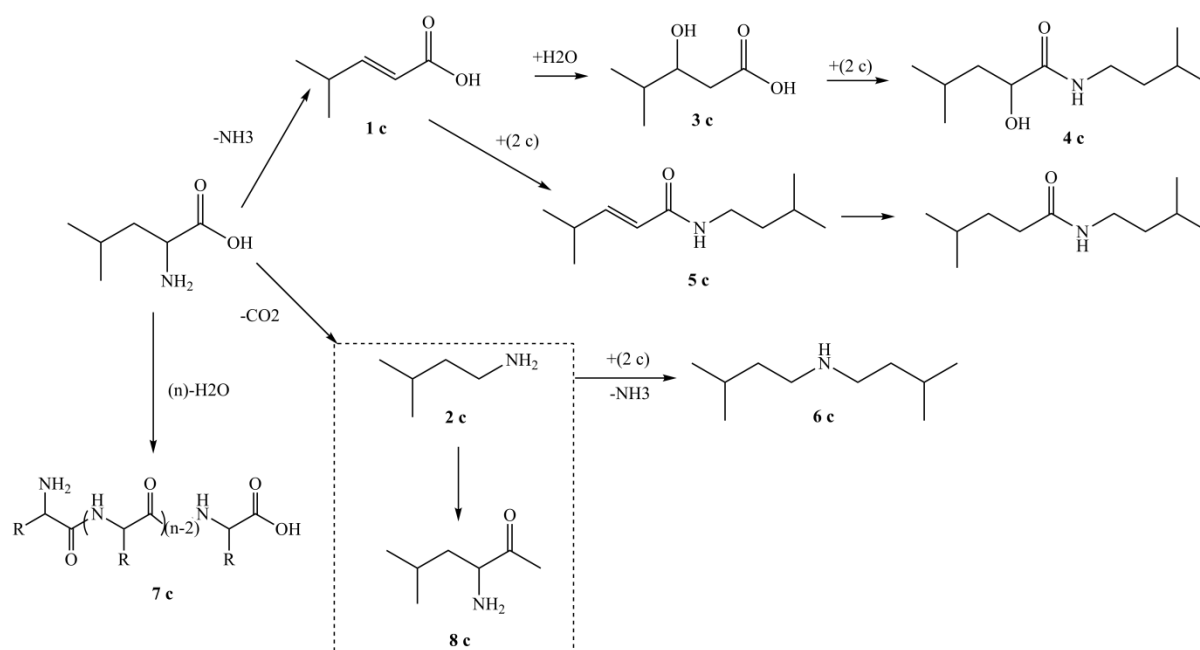


**FIGURE 28.** Chemical pathway of Leucine HTL

Also in this case the significant relocations of carbons from the water phase into bio-oil phase (up to 25 % with the respect to 7.4 % measured in the water medium) is observed (Figure 29).

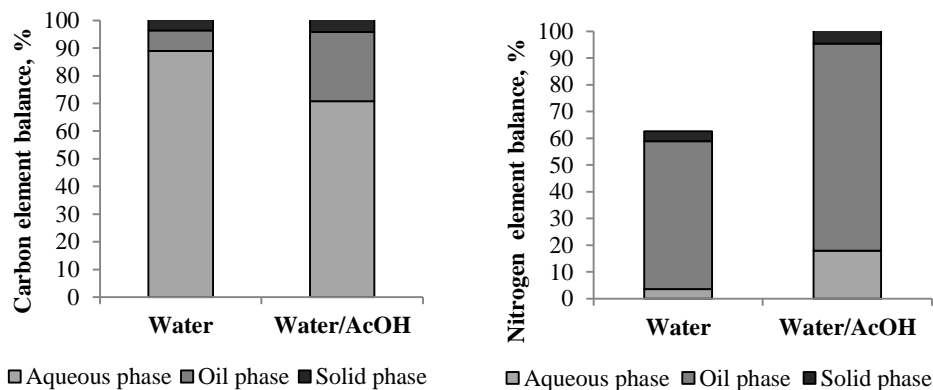


**FIGURE 29.** Carbon and nitrogen element distributions in products streams of Leucine HTL, %

#### 4.1.4 HTL of Phenylalanine in binary mixtures with Tripalmitin and Glucose

The bio-oil yields, elemental analysis, HHV and ER values of bio-oils obtained from HTL of Phenylalanine/Tripalmitin and Phenylalanine/Glucose binary mixtures are shown in Table 14. As expected, the bio-oil amount depends strongly on the initial feedstock composition. A dramatic increase in bio-oil yield from Phenylalanine/Tripalmitin Binary mixture is due to a quantitative contribution of fatty acid to bio-oil yield. This explains why biomass with a high lipid content has been preferred in HTL process, since all lipid content contributes to the bio-oil yield.

The bio-oil yield obtained from the binary mixture of Phenylalanine/Glucose (1:1 by weight) was similar to that measured for Phenylalanine alone, suggesting an equivalent contribution from the two components. Since HTL of glucose leads to highly oxygenated polar molecules that are transferred in aqueous phase, its contribution to the bio-oil yield is supposedly related to the formation of more hydrophobic species formed by reaction with the phenylalanine degradation water soluble products.

This phenomenon was indirectly confirmed by the increased nitrogen content in the bio-oil from 4.4 % measured for phenylalanine alone, up to 5.2 % for the binary mixture, thus indicating a partial relocation of water soluble nitrogenous species from the aqueous into bio-oil phase.

**TABLE 14.** Bio-oil yields, elemental analysis, HHV and ER of bio-oil products from binary mixtures of Phenylalanine/Tripalmitin and Phenylalanine/Glucose

	Phenylalanine		Phenylalanine/Tripalmitin		Phenylalanine/Glucose	
	Water	Water/AcOH	Water	Water/AcOH	Water	Water/AcOH
Bio-oil yield, %	7.9	30.2	68.1	62	7.3	23.5
<i>Element analysis</i>						
C, %	80.4	67.9	77.0	75.0	76.3	69.1
N, %	4.4	6.5	2.1	2.5	5.2	6.9
H, %	7.5	9	11.8	11.2	8.5	8.7
O*, %	6.5	14.1	9.1	11.2	10.0	15.3
Solid residue yield, %	8.6	5.7	1.6	8.2	6.9	10.5
HHV, Mj/kg	36.5	33.2	39.8	38.3	35.9	33.1
ER in bio-oil, %	9.6	33.6	91	79.7	8.8	26.1

\*calculated by difference

The addition of acetic acid seems to be effective in increasing the bio-oil yield for Phenylalanine/Glucose Binary Mixture, while on the other hand, a detrimental effect on the bio-oil yield was observed for Phenylalanine/Tripalmitin Binary mixture HTL. This can be explained by the different reaction pathway.

#### Phenylalanine/Tripalmitin Binary mixture

As shown in Figure 30, in the first step tripalmitin was hydrolyzed to palmitic acid (12 b) and only traces of glycerol mono-palmitate were detected. Phenylethylamine (2 b) formed by decarboxylation of phenylalanine was then acetylated by palmitic acid to form phenylethylpalmitamide (13 b). Palmitic acid (47.0 wt. %) and phenylethylpalmitamide (30.7 wt. %) were the main products in the bio-oil.

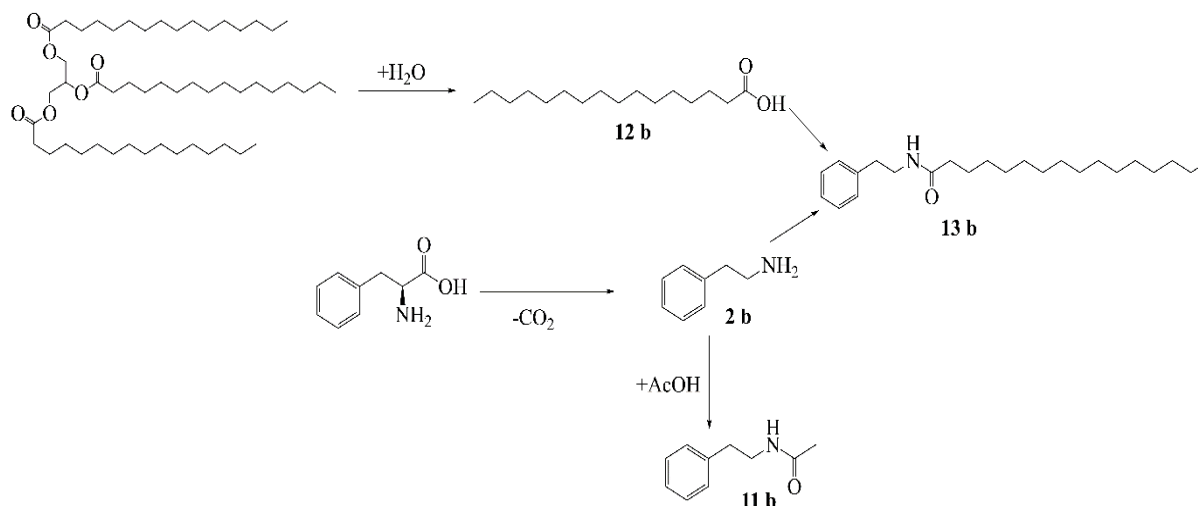


**FIGURE 30.** Chemical pathway of Phenylalanine/Glucose binary mixture HTL

After the subtraction of the total contribution of palmitic acid (3.8 g of free acid and its amides), the fraction of bio-oil deriving from phenylalanine component alone is 1.6 g, thus corresponding to 40 % of the initial mass of amino acid. This value is considerably higher than that obtained with phenylalanine without tripalmitin in water (8 %) and in water/AcOH solvent (30 %), hence suggesting a synergic effect exerted by the lipid fraction on the bio-oil formation chemistry.

In the presence of acetic acid a competition with palmitic acid was observed to form amides 11 b and 13 b, resulting in no beneficial effect on bio-oil yield. On the basis of the bio-oil composition: palmitic acid (70.5 wt. %), phenylethylacetamide (21.5 wt. %), palmitamide (5.2 wt.%), acetic acid turned out to be more effective in the acylation of phenylethylamine.

As shown in Table 14, the nitrogen content in the bio-oil from the binary mixture (2.1 wt.%) was remarkably lower than that measured for Phenylalanine alone (4.9 %) due to the dilution of nitrogen containing species by fatty acid derivatives. The similar dilution effect was observed in the presence of AcOH with the nitrogen content decreasing from 6.5 to 2.5 %.

### Phenylalanine/Glucose Binary mixture

Even if starting from the simple binary mixture of monomeric model compounds, a very broad spectrum of products, each with low relative concentration was displayed by GC-MS analysis of bio-oil. The products of phenylalanine decomposition were also identified in the binary mixture, namely diphenylethylamine (6 b) and the amides (4 b and 5 b), but only as minor components.

According to the EI mass spectrum fragmentation patterns, the main compounds were attributed to the nitrogen containing species with the heterocyclic structures. In particular, the more intense GC-MS peaks showed the ions 108/122 as base peaks in their EI Mass spectra, which are likely related to the alkylated pyrazine cores (ethylpyrazine and propylpyrazine) (Figure 31). In minor extent alkylated pyridines and other N, O containing heteroaromatic compounds were detected

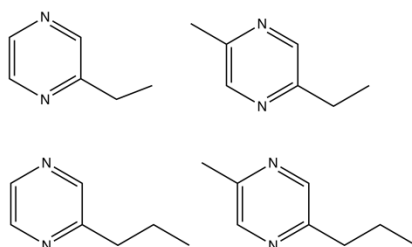


**FIGURE 31.** Alkylated pyrazines in the bio-oil from Phenylalanine/Glucose HTL

The most direct route for pyrazine formation results from the interaction of a  $\alpha$ -dicarbonyls and amines through Strecker degradation [108]. Various types of substituted pyridines can be produced from different combination of aldehydes, ketones, or carbonyl compounds with ammonia, which is degraded from amino acids [109]. In comparison, only in trace amount the presence of pyrroles is found. Authors [109] found that amino acids, which, having no side chain, for example, glycine, aspartic acid, lysine, are more flexible in the formation of pyrroles, while phenylalanine and isoleucine had the least contribution to the formation of pyrroles.

In contrast, a completely different product distribution was obtained in the presence of acetic acid, where the main species were the same as identified in the case of the reaction with Phenylalanine alone HTL. Phenylethylacetamide (11 b) was confirmed to be the most abundant peak, while the formation of a smaller amount of nitrogen containing heterocyclic species was also detected in this case with a broad structural differentiation.

This considerably different behavior can be explained by the greater reactivity of the amines towards the acylation rather than the condensation with carbonyl species leading to amides instead of nitrogen containing heterocyclic products.

This is a key point in the rationalization of HTL mechanism, since the reactivity of amides and nitrogen containing heterocyclic compounds in the hydrodenitrogenation (HDN)

processes is dramatically different, being the latter more recalcitrant and making the upgrading of bio-oils to fuels problematic.

It also should be pointed out that the ratio of feedstock loading to the amount of acetic acid has a significant effect on the bio-oil yield. From the supplementary experiments (Supplementary Appendix A) it was found that the effect of acetic acid on increase in the bio-oil yield is less prominent with the higher loading of the feedstock.

In addition to the products identified via GC-MS, other heavier and more polar compounds have been detected by (ESI+) FTICR MS analysis.

On the basis of these results, N2 is the most abundant heteroatom class, followed by O1N1, N1, and N2 classes, while in the presence of acetic acid the reduction of N2, N1 and N2O1 components was observed and N1O1 class becomes predominant (Figure 32).

This is in agreement with the formation of acetylated nitrogenous species, such as phenylethylacetamide. Only negligible amounts of products were detected for the fully oxygenated O, O1 and O2 classes, confirming that these polar species are predominantly partitioned into the water phase and contribute to the bio-oil formation only after the reaction with the nitrogen containing intermediates.

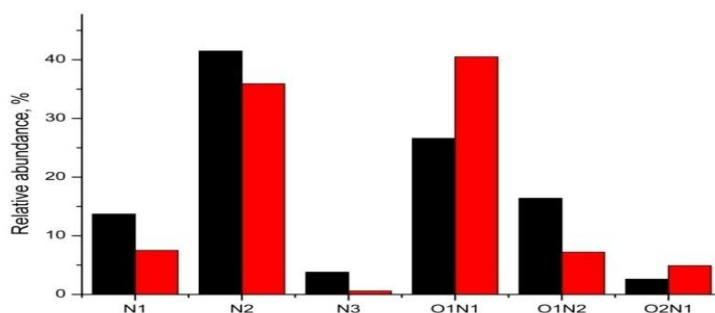


**FIGURE 32.** Heteroatoms class components of bio-oil derived from HTL of Phenylalanine/Glucose binary mixture

The compounds that belong to the most abundant classes (N2, O1N1) were then plotted in DBE versus C<sub>n</sub> plots according to their C<sub>n</sub>, DBE value and relative abundance in the mass spectrum (size of the spots in the plot) (Figure 33).

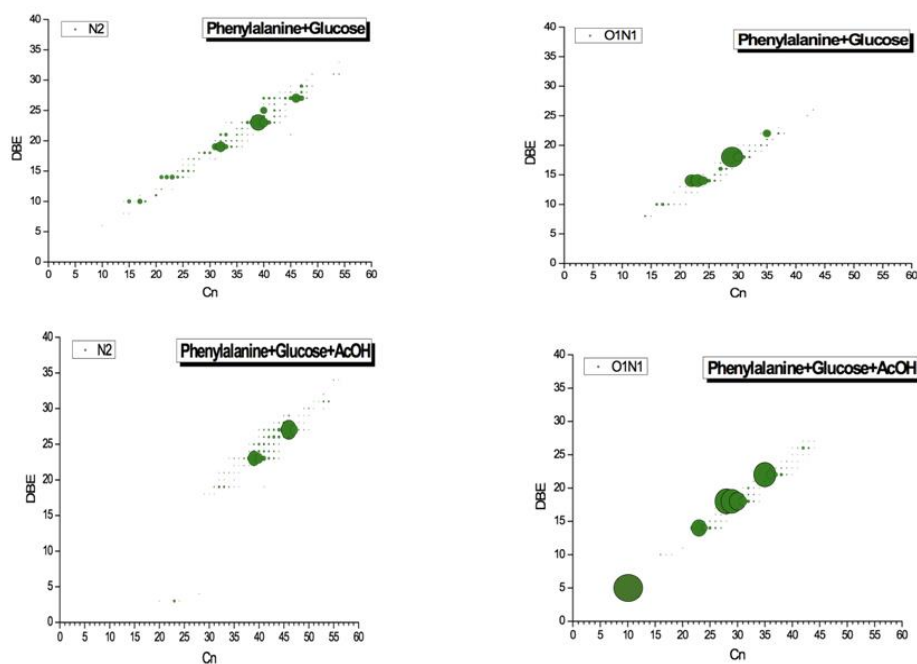


**FIGURE 33.** DBE versus  $C_n$  distributions for N2 and O1N1 class compounds in bio-oil of phenylalanine/glucose binary mixture HTL

Concerning N2 class, a broad distribution of species ranging from  $C_n=15-50$  and DBE 10-30 was determined in the bio-oil. The main N2 class compounds in the bio-oil are related to  $C_n =15-17$  and DBE=10,  $C_n =21-23$  and DBE=14,  $C_n =31-33$  and DBE 19,  $C_n =39-41$  and DBE=23,  $C_n =46-47$  and DBE=27.

Remarkably, this distribution shows discreet differences of benzene or alkylated benzene rings (DBE 4) between the more abundant species. Each of these species could be tentatively assigned to the pyrazine derivatives formed by the successive addition of aromatic rings (likely related to styrene) to the pyrazinic core (DBE=3). The same distribution was observed in the presence of acetic acid; however, the regions of highest abundance are located to higher values of carbon number and DBE ( $C_n =39$  and DBE=23,  $C_n =47$  and DBE=27), indicating the higher abundance of the more unsaturated species.

For the N1O1 class the main peaks correspond to  $C_n=22$  and DBE=14,  $C_n =28-30$  and DBE=18,  $C_n =35-36$  and DBE=22. Here again discreet differences (DBE 4) are found between the more abundant species supposedly formed by the successive addition of the aromatic rings (likely related to styrene).

The N1O1 class compounds in the bio oil obtained from binary mixture HTL in the presence of acetic acid showed similar DBE regions shifted by one or two units of  $C_n$ , suggesting the higher degree of alkylation. Moreover, the presence of phenylethylacetamide at  $C_n=10$  and DBE=5 was also observed.

In both bio-oil samples (with and without acetic acid) N1, N2, O1N1 compounds show high values of DBE, indicating the presence of high unsaturated nitrogen containing compounds. These results prove that the phenylalanine pathway to oligomerization products is significant in the bio-oil from the binary mixture of phenylalanine and glucose HTL. At higher temperatures (100 °C) styrene is reported to auto-polymerize up to 300 °C [110], so oligomerization products containing a vinyl group can undergo addition reactions with phenylalanine derivatives to form nitrogenated polycyclic aromatic hydrocarbons.

#### 4.1.5 Conclusion

The choice of monomeric substrates, representative of protein, polysaccharide and lipid biomass components, has made possible to simplify the spectrum of the products, thus allowing the identification of the main metabolic pathways. In particular, the key role of the acetylation reaction of nitrogen containing compounds was highlighted in the case of biomass feedstock containing protein and acyl donor components, such as acetylated sugar in the hemicellulose and fatty acid chains in the lipid fraction.

The main experimental results from this study can be summarized as follows:

- lipids are the main contributors to the bio-oil yield;
- in addition to the direct input, lipids also display the synergistic effect on the protein contribution into bio-oil yield by the reactive extraction of hydrophilic species (amines);
- lipids also exert the reduction of nitrogen content in the bio-oil by mass effect, thus making the resulting product less critical for the co-feeding in the refinery upgrading processes;
- in the presence of lipids, amides formation is in the competition with the generation of nitrogen containing heterocyclic species, observed in the presence of carbohydrates.

This is a crucial point that determines the bio-oil specifications for the subsequent upgrading by HDN, being conventional catalysts poorly efficient in removing heterocyclic nitrogen.

The result of this model-based study represents a useful tool to design proper waste biomass blends, tuning its composition to produce bio-oils with the standard quality suitable for co-feeding in refinery processes.

## 4.2 HTL of Albumin in binary with starch and tripalmitin

In order to mimic the complex composition of the real organic waste feedstock, albumin was chosen as model compound of the protein macromolecular fraction of biomass and subjected to HTL alone and in binary mixtures with starch and tripalmitin. The previous results obtained from monomeric substrates (leucine, phenylalanine and glutamine) HTL are verified using macromolecular model compounds used herein. All experiments were carried out in water and water/acetic acid (95/5 % v/v) solvent systems.

Since no prior research has been done on the effect of biomass composition on the distribution of nitrogenous species of the bio-oil produced from protein rich biomass, in the present study the effect of the lipid dosage on the ratio of fatty acid amides (FAA) to nitrogen containing heterocyclic and aromatic compounds (NAs) is determined.

### 4.2.1 Bio-oil yields, elemental analysis, HHV and ER of bio-oil products

Table 15 represents the bio-oil yields, element analyses and HHV and ER values of bio-oil products obtained from binary mixtures HTL.

**TABLE 15.** Bio-oil yields, elemental analysis, HHV and ER of bio-oil products from Albumin in binary mixtures HTL

	Albumin		Albumin/Starch		Albumin/Tripalmitin	
	Water	Water/AcOH	Water	Water/AcOH	Water	Water/AcOH
Bio-oil yield, %	7.9	29.4	6.5	20.92	73	66.46
<i>Element analysis, %</i>						
C	72.6	65.8	71.02	60.02	74.3	72.37
N	6.75	7.69	6.23	8.49	2.2	2.62
H	9.07	9.89	7.5	7.88	11.4	10.82
O*	7.95	14.84	12.66	19.89	12.1	14.89
S	3.54	0.43	2.57	<0.1	<0.1	<0.1
Solid residue, %	0.12	2.63	0.2	2.5	0	2.6
HHV (Mj/kg)	35.6	33.4	32.67	28.6	38.2	36.53
ER, %	12.9	44.39	10.0	28.4	89.9	72.2

\* calculated by difference,%

As shown in Table 15, the HTL of albumin resulted in 8 % bio-oil yield, comparable to that obtained with phenylalanine (Table 14). The nitrogen content (7.0 %) was higher with respect to that measured for phenylalanine (4.4 %) and leucine (6.3 %) due to the presence of a fraction of smaller fragments with a higher N/C ratio formed by short chain amino acids.

The formation of solid residue was negligible (about 0.12 %), thus indicating a complete hydrolysis of albumin under the hydrothermal conditions at 300 °C to amino acids and their derivatives. When the peptide bonds in albumin are broken, some hydrophobic amino acids (e.g. phenylalanine, tryptophan, etc.) derivatives can contribute to the oil formation, while hydrophilic amino acids (glutamic acid, aspartic acid, etc.) derivatives are preferentially partitioned in the aqueous phase. Therefore, the bio-oil yield produced from proteins HTL may vary according to the amino acid distribution.

In the case of the binary mixture Albumin/Starch, the lower bio-oil yield (6.5 % vs 8 % obtained with albumin alone) suggests a lower contribution of the starch fraction to the formation of hydrophobic products. Conversely the nitrogen content in the bio-oil (6.4 %) did not decrease proportionally to the protein content in the mixture (50 % vs 100 %). This phenomenon is probably due to the reaction of starch decomposition products bearing carbonyl groups with water soluble amines forming oil-soluble species.

A. A. Peterson et. al. [111] found the dosage of glucose increased the conversion of glycine under hydrothermal conditions, while glycine itself was not so reactive. It is known that nitrogen containing heterocyclic compounds, such as pyrroles, pyridines, etc. are formed by the interaction of carbonyl group of sugars and amine groups generated from amino acid decarboxylation. Moreover, not only reducing sugars, but also the degradation products of glucose, such as pyruvaldehyde, etc., containing carbonyl group also reacts vigorously with the amines.

Albumin/Tripalmitin mixture afforded the highest bio-oil yield (73.0 %), as already observed for the phenylalanine model amino acid, due to the direct contribution of fatty acids and the formation of hydrophobic fatty acid amides, partitioned into the oil phase. The consistent reduction of nitrogen content (2.2 % vs 7 %) can be explained by a simple dilution effect of the protein fragments by the lipid fraction that is quantitatively partitioned into the bio-oil.

The addition of acetic acid (5 % by volume) in the reaction medium resulted in a dramatic increase of the bio-oil yield up to 29.4 and 20.9 % for albumin alone and albumin/starch mixtures, respectively. As already observed (Section 4.1.3) with phenylalanine and leucine model amino acids, this is the consequence of the acylation of water soluble amines derivatives forming more hydrophobic oil soluble amides products. In both cases an

increased amount of nitrogen was detected in the bio-oil-due to the transfer of nitrogenous species from the aqueous phase. Conversely, in the case of the albumin/tripalmin mixture, acetic acid exerted a detrimental effect on the yield due to the competition with fatty acids in the acetylation of amines.

The carbon recovery (CR, %) and nitrogen recovery (NR, %) in the product streams is given in Figure 34.

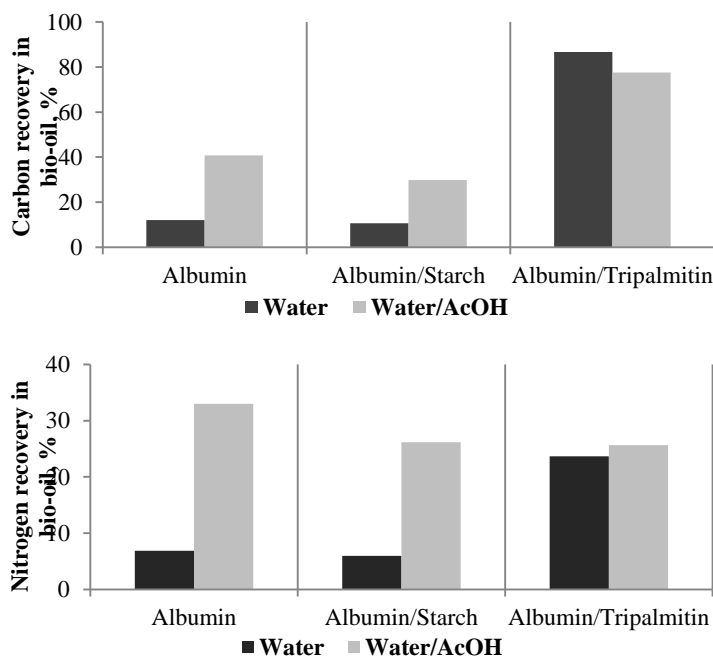


**FIGURE 34.** The carbon recovery (CR, %) and nitrogen recovery (NR, %) in the bio-oil

Only 12.07 % of carbon and 6.9 % nitrogen recovered in the bio-oil produced from HTL of albumin. The presence of starch decreased the CR to 10.6 %, while NR was not reduced significantly (5.97 %), thus affecting negatively on the bio-oil composition. With the addition of acetic acid, the CR as well as NR increased due the transferring of water soluble amines to oil soluble amides after acetylation reaction.

The CR of 86.6 % and NR of 23.68 % are obtained in the bio-oil produced from Albumin/Tripalmitin Binary mixture. The addition of acetic acid resulted in the reduction of CR due to the formation of water soluble acetamides. The increase in NR implies that long chain acids are more beneficial for reducing the nitrogen content due to the mass effect.

These results suggest that each fraction of biomass does not behave independently and the bio-oil yield is strongly affected by the composition of biomass. Instead, the specific interactions between biomass macromolecular fractions determine the bio-oil quality.

### 4.2.2. Bio-oil characterization.

#### Albumin HTL

The bio-oil produced from Albumin HTL contains mainly diketopiperazines (dKP) and secondary amines in small amounts. According to the FTICR MS analysis, N2, N1 are the most abundant heteroatom class in the resulting bio-oil products (Figure 35).

The degradation of proteins can produce a variety of N1 compounds, such as alkyl and aromatic amines, nitriles and imines, whose structures depend on the nature of amino acids and most of them, should be relocated in the aqueous phase. Some amines can undergo self-condensation to form secondary amines that were detected in the oil phase.

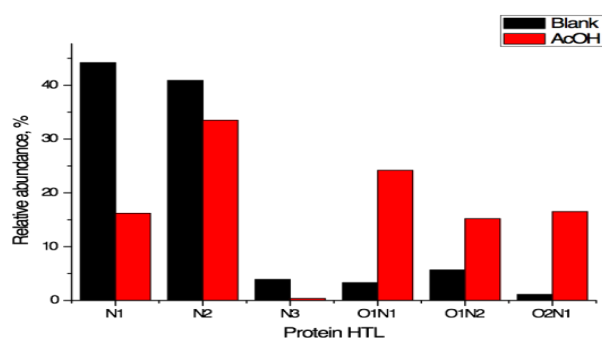


**FIGURE 35.** Heteroatom class components of the bio-oil from Albumin HTL.

To further visualize the compositional structure of components in bio-oil abundance-contoured plots of double bond equivalents (DBE=rings and double bonds) versus carbon number ( $C_n$ ) for the main heteroatom classes are depicted in Figure 36.

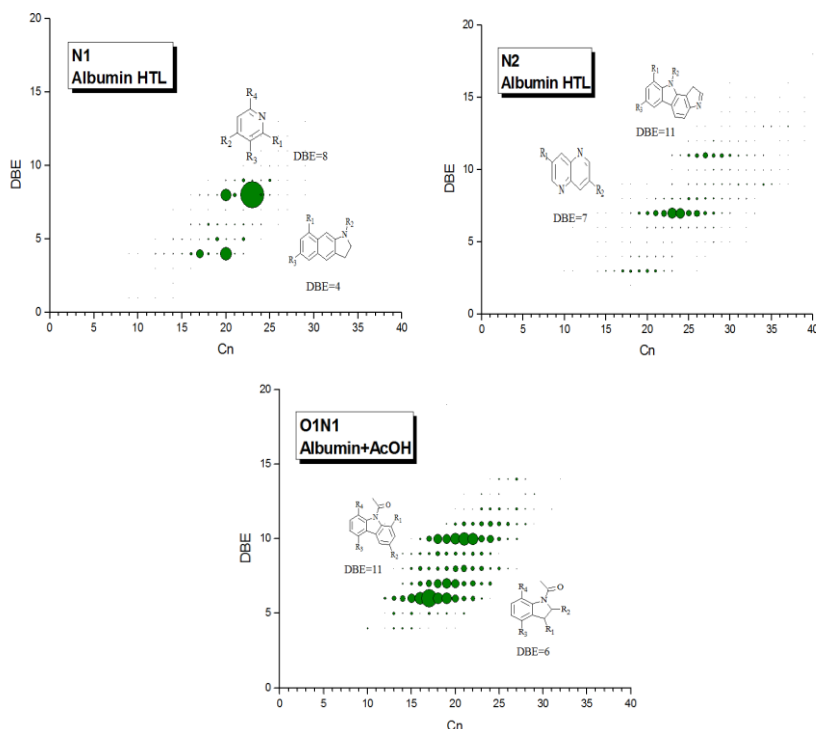


**FIGURE 36.** Cn vs DBE plots for the main classes found in bio-oil samples from Albumin HTL

The main homologous series (elemental formulas with the same DBE value and different C<sub>n</sub>) correspond at DBE of 4 and 8 with C<sub>n</sub>=17 and 24, respectively. Based on the supplementary fragmentation spectra by GC-MS, the observed N1 class components with DBE=4 are likely alkylated pyridine derivatives (tri(isopentyl)pyridine, etc.).

For N2 class components, the main species in the bio-oil are related to DBE=7 with the extensive variation of C<sub>n</sub>=20-27, indicating a large degree of alkylation present for these DBE values. N2 species at DBE=7 might be indicative of benzopyrazine or 2 pyridinic rings. Generally, pyridine and pyrazine compounds are formed by Maillard reaction between amino acids and sugars; however, the formation of nitrogen containing cyclic/aromatic compounds (NAs), such as piperidines, indoles, and pyrrolidinones, was observed from HTL of the protein model compound, such as soy protein concentrate [112].

Alternatively, it was shown that decarbonylation and dehydration of amino acids can occur in such a way that pyrazines are formed from the thermal degradation of only the amino acid without a carbohydrate source [113]. The degradation of serine in the absence of sugars could lead to the formation of different  $\alpha$ -aminocarbonyl intermediates that are the common precursors to pyrazines and pyrroles [114].

Generally, the alkylated pyridine rings can be formed through a condensation reaction of aldehydes, ketones with ammonia or ammonia derivatives [115]. Based on this, tri(isopentyl)pyridine might be generated from the reaction of methylbutanal or methylbutanol with the methylbutylamine that are degradation products of leucine.

Conversely, the bio-oil derived from the HTL of Albumin in acetic acid-water binary solvent system showed a different distribution of products. Some amides (phenylethylacetamide, pentylacetamide, etc.) were detected. Similarly, the presence of amides is also confirmed by FTICR-MS analysis showing a high abundance of O1N1 and ON2 compounds and lower distribution of N1 and N2 classes. The highest relative abundances are observed at DBE=6 and Cn=16-18 and DBE=10 and Cn=20-23 and they are likely related to aromatic amides. This confirms N-acylation effect of acetic acid.

### Albumin/Starch HTL

The N2, N1 are the most abundant heteroatom classes in the bio-oil produced from a binary mixture of albumin and starch (Figure 37). However, N2 class components were predominant in comparison to N1. The formation of O1N2, O2N2, O2N1 class components is also detected in small amounts.

N1 and N2 class component distribution of bio-oil resembles similar product distribution produced from HTL of Albumin, suggesting that these components are mainly related to the degradation of albumin itself and their subsequent rearrangement reactions.

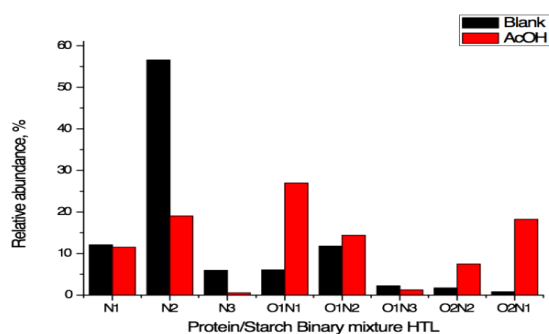


**FIGURE 37.** Heteroatom class components of bio-oil from Albumin/Starch HTL

The O1N2, O2N2, O2N1 are likely related to alkylated heterocyclic and aromatic compounds because of the high unsaturation degree. For instance, the main O1N2 class distribution corresponded at DBE=7 and Cn=19-24; DBE=11 and Cn=25-27 (Figure 38). The numerous variations of the structures are possible for these molecules because of high

DBE and  $C_n$ . These components are likely formed through Maillard reaction between protein and starch degradation products.

In the presence of acetic acid an increment of O2N1 and O1N1 class components is observed in the bio-oil. O1N1 species range from DBE=1-15 and  $C_n$ =10-25. The non-aromatic species (below DBE 4) most likely correspond to the amides family, whereas the aromatic species ( $DBE \geq 4$ ) probably contain a combination of different nitrogen and oxygen functionalities.

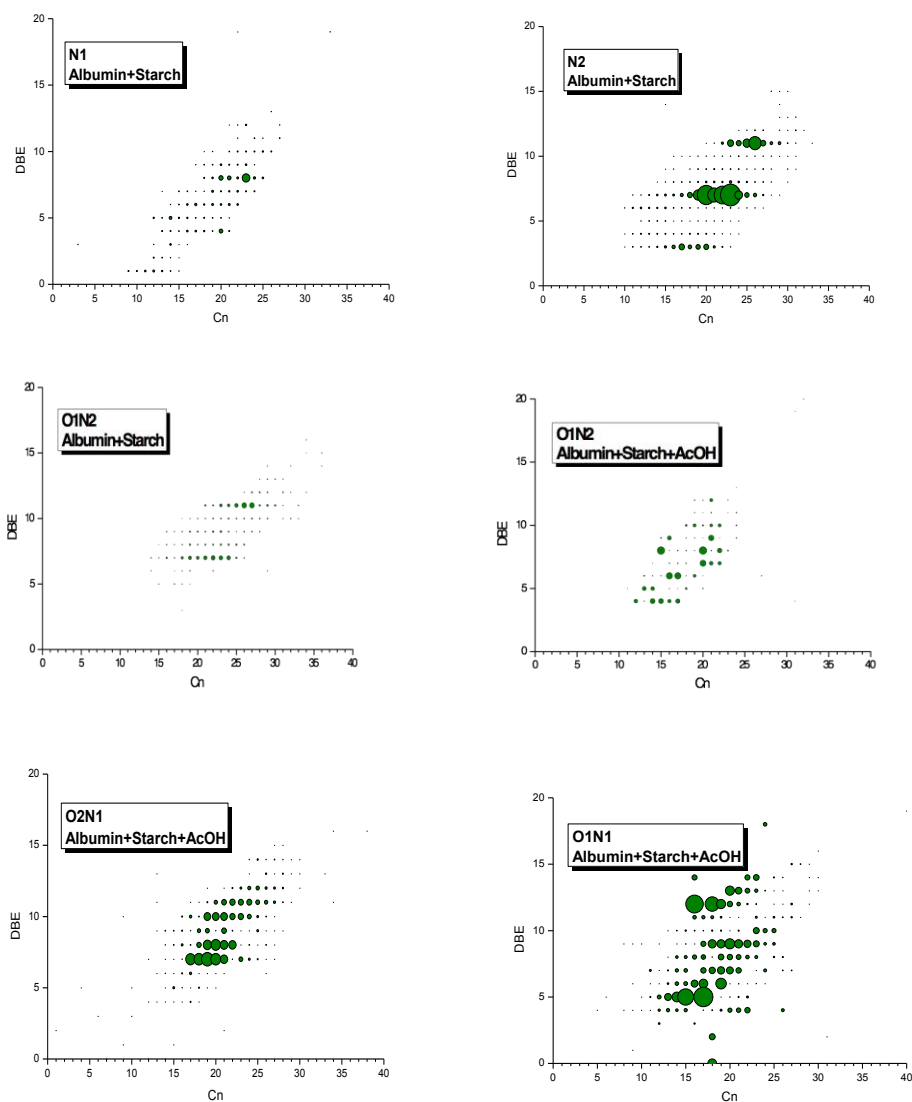


**FIGURE 38.**  $C_n$  vs DBE plots for the main classes found in bio-oil produced from Albumin/Starch HTL

### Albumin/Tripalmitin Binary mixture

The bio-oil produced from Albumin/Tripalmitin binary mixture was analyzed by GC-MS and GC-FID analyses. According to the results, in Albumin/Tripalmitin binary mixture tripalmitin was hydrolyzed to form palmitic acid (accounting to 71.6 wt.% of bio-oil) that further reacted with the ammonia or amines forming fatty acid amides (total 3.81 wt.%) (Figure 39). In the presence of acetic acid, the yield of fatty acid amides was lower (1.21 wt.%), because amines reacted predominantly with the acetic acid forming light molecular weight amides that were partitioned into the aqueous phase with the unreacted acetic acid.

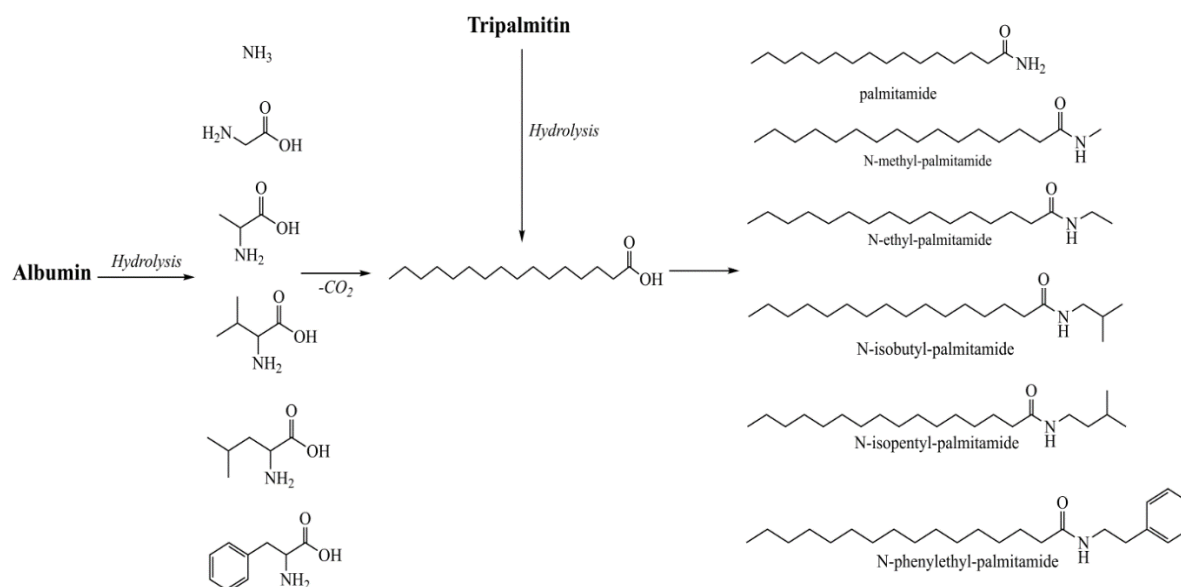


**FIGURE 39.** Reaction pathway of Albumin/Tripalmitin binary mixture (Main products were identified by GC-MS and GC-FID)

Although FA and its derived FFA are abundant in the bio-oil, they do not affect negatively its properties as they can be converted easily into more valuable products through upgrading step.

However, the determination of the ratio between nitrogen containing heterocyclic and aromatic compounds and fatty acid amides in the bio-oil is crucial in order to prove the hypothesis about the effect of lipid dosage on the inhibition of Maillard reaction between carbohydrate and protein.

### 4.2.3 The effect of lipid dosage on the type of nitrogen compounds of the produced bio-oil

In order to confirm the competition between the formation of heterocyclic products, by Maillard-type mechanism, and the formation of fatty acid amides, a comparative experiment was carried out using ternary Albumin/Starch mixtures with two different triglyceride contents. In this case, triolein was used as a lipid model compound.

The Albumin/Starch/Triolein ternary mixtures with a relative ratio 1:1:0.5 and 1:1:1, respectively, were treated under the same HTL operating conditions in order to replicate 20 % and 33 % lipid content of the biomass composition. The yields of bio-oil, HHV and ER values are presented in Table 16.

**TABLE 16.** Bio-oil yields, elemental analysis, HHV and ER of bio-oil products of ternary mixture of Albumin/Starch/Triolein HTL

	Albumin/Starch/ 20% Triolein <sup>a</sup>	Albumin/Starch/ 33% Triolein <sup>b</sup>
Bio-oil yield, %	25	36
Solid yield, %	2.1	1
Element analysis		
C%	74	74,5
N %	3,8	3,0
H, %	10,5	11,1
O, %	11.4	11.4
S, %	0,3	0,1
HHV, MJ/kg	36.7	38
ER, %	37.17	51.19

As expected, the higher yield of bio-oil is produced with higher content of lipid of 33 %. The nitrogen content also decreased with the higher lipid content; however, it might be due to the lower protein content 33 % vs 40 % in the mixture with 20 % of triolein.

#### Bio-oil composition

The GC-MS chromatograms of both bio-oil samples are very similar, showing the IS at 25.1 min.; and wide peaks corresponding to oleic and palmitic acids in minor amount at 35 and 39 min, respectively. Fatty acid amides are detected at higher retention times (43 to 56 min),

while at lower retention times (7 to 30 min) a wide area of co-elution is found in both samples, mainly related to nitrogen containing heterocyclic compounds, and in the lower extent to FAs (C12-C14) and other oxygenated aromatic compounds (Figure 40).

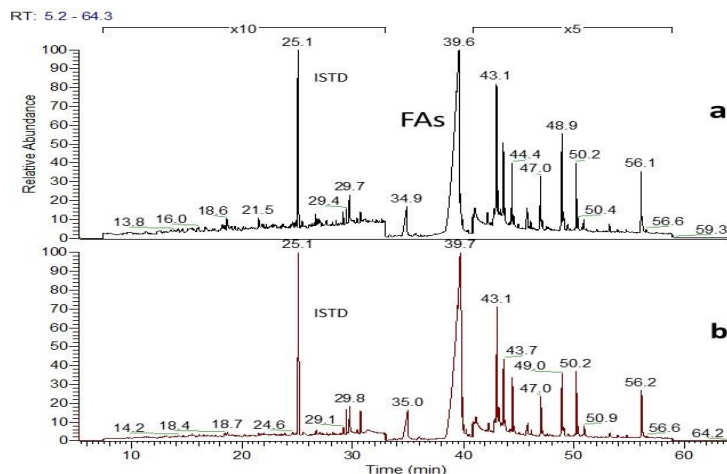


**FIGURE 40.** GC-MS chromatograms of bio-oil samples with a) 20 % triolein content; b) 33 % triolein content

*\*In the section a, the high retention time area (amides area) and the lower retention time area (nitrogen containing heterocyclic area) were amplified 5 times and 10 times, respectively*

Considering the peak areas, normalized with the area of the IS, only a semi-quantitative determination could be obtained, due to the FAs peaks poor resolution and the different quantitative response of the IS with respect to the other classes of molecules.

Given the low reliability of the GC-MS analysis, FTICR ESI+ was employed for the detailed characterization of both FAAs and NAs species in bio-oil, using caffeine as internal standard ( $m/z$  195.09 peak), as shown in Figure 41.

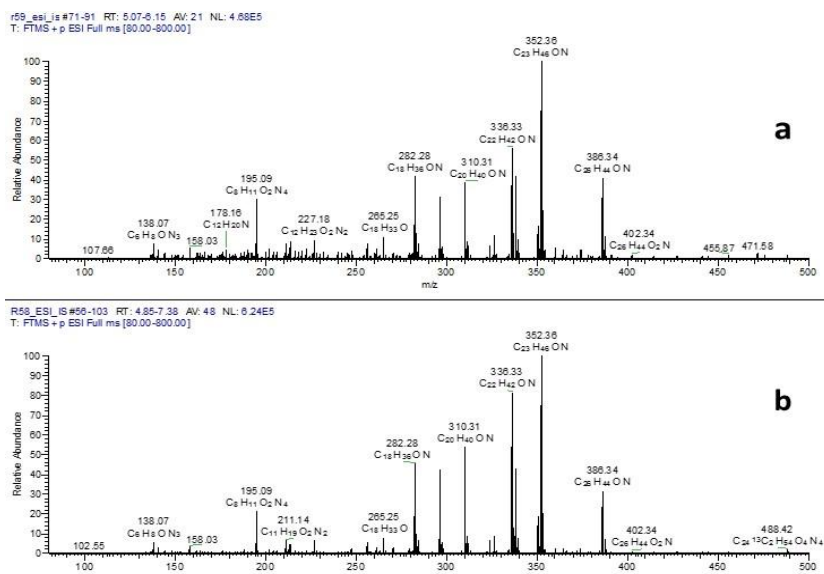


**FIGURE 41.** FTICR ESI+ mass spectrum of bio-oil samples from Albumin/Starch/Tripalmitin ternary mixture a) 20 % triolein content; b) 33 % triolein content.

\*Caffeine was used as IS (m/z 195.09 peak)

According to the ESI+ mass spectra, the main components in both samples are related to FAAs (O1N1 class), with similar qualitative distributions found in both samples. The FAs are not detected by ESI+, since they are selectively detected as ionic species in the ESI- mode. The molecular formula of each FAAs component was confirmed by FTICR MS and their distribution is plotted for the two samples in Figure 42. After normalization with respect to the IS, the ratio between the total FAAs relative peak intensity of the mixture b (33 % triolein) and a (20 % triolein), was estimated as 1.51, indicating a higher FAAs content in the high-lipid mixture.

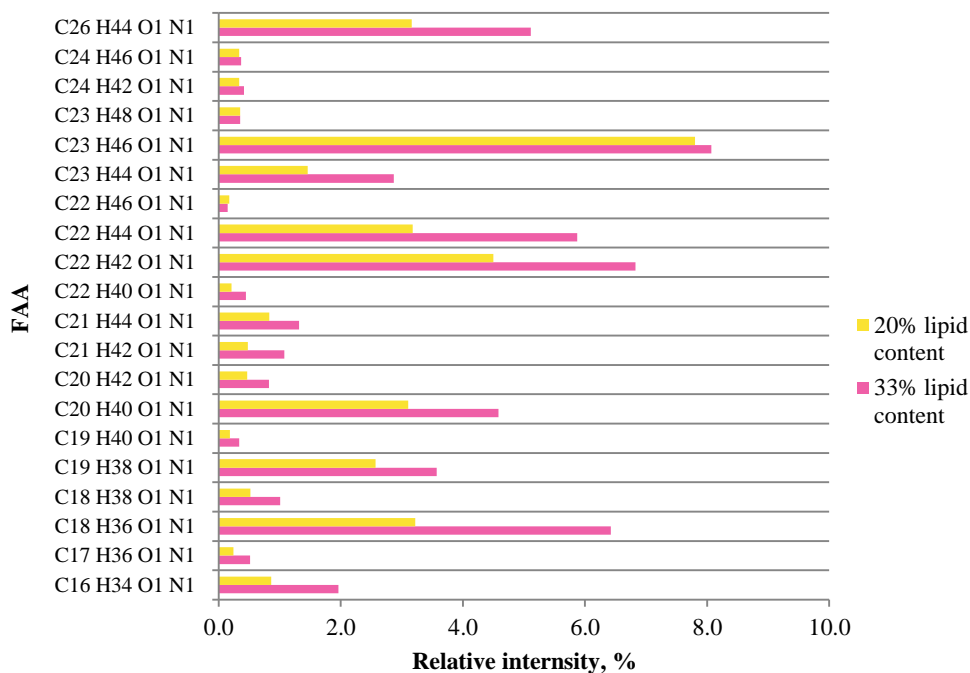
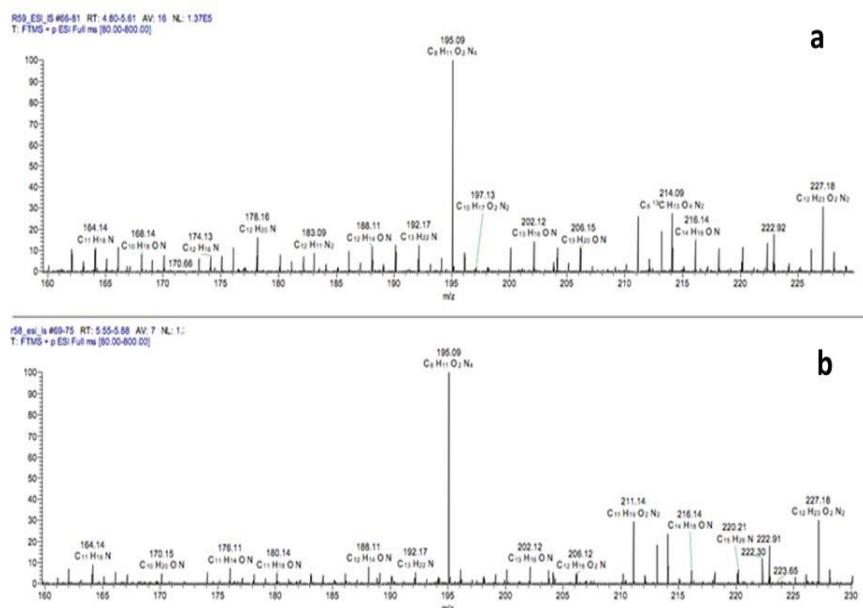


**FIGURE 42.** FTICR ESI+ based distribution of the main FAAs species as protonated ions  
 a) 20 % triolein content; b) 33 % triolein content

\*Relative abundance of FAA is calculated with respect to the response of IS (caffeine)

Concerning the nitrogen containing aromatic compounds (NAs), the FTICR mass spectra have been elaborated, and only the mass peaks related to nitrogen containing aromatic compounds (with a DBE higher than 4) were considered. Their total relative amount was then calculated considering their relative intensity in the mass spectra normalized with the relative intensity of the IS (caffeine), and also considering the dilution of the starting sample (Figure 43). The expansion of the mass range was done at 160-230 da.



After normalization with respect to the IS, the ratio between the total NAs relative peak intensity of the mixture b (33 % triolein) and a (20 % triolein), was estimated as 0.47, indicating the presence of a lower fraction of aromatic and heterocyclic nitrogen compounds of the bio-oil produced from the high lipid mixture.

From these results, a significant conclusion can be highlighted. The two HTL experiments carried out with different amount of lipids provide different bio-oil yields, mainly due to the fact that most of the lipid is converted into the bio-oil fraction. Moreover, higher lipid dosage promotes the formation of FAAs species, reducing the formation of NAs, thus making the bio-oil less recalcitrant and more suitable for hydrotreatment process.

#### **4.2.4 Conclusion**

The previous results obtained from monomeric substrates (leucine, phenylalanine and glutamine) HTL are verified herein, using complex biomass polymers (albumin, starch, tripalmitin), as they are known to provide a more accurate representation of the real biomass composition. It is shown that the synergy existing between lipid and protein results in recovering more energy embedded in proteins.

In comparison, the interactions between albumin and starch showed double-folded effects on the production of bio-oil through HTL conversion. On the one hand, it could generate more bio-oil yield than the starch or albumin alone confirming a positive effect. On the other hand, the introduction of nitrogen into the bio-oil could reduce the bio-oil quality due to potential upgrading or combustion problems.

Most importantly, through two experiments using two different lipid content in the starting feedstock, the existing strong correlation between lipid dosage and FFA/NAs ratio of the resulting bio-oil is found. This finding is crucial for feedstock engineering that can determine the likelihood of success in the conversion of waste biomass to advanced bio-oils.

On the basis of these results, a plausible approach of co-feeding the high-protein waste biomass with the waste cooking oil, oleaginous yeast biomass, is proposed in order to increase the bio-oil yield and prevent the formation of nitrogen containing heterocyclic compounds.

### 4.3 Catalytic hydrothermal liquefaction of amino acid

The previous modelling study on HTL of leucine and phenylalanine (Chapter 4.1) showed that deamination was predominant over decarboxylation under hydrothermal conditions. In this case co-feeding the protein-rich biomass with waste cooking oils or generation of acids in situ directly from the carbohydrate macromolecules of biomass is proposed in order to maximize the energy yields.

On the other hand, this Section is devoted to discussions on how to enhance the deamination rate of amino acids under hydrothermal conditions, thus decreasing the nitrogen content of the bio-oil using catalyst.

#### 4.3.1 HTL products streams yields

From literature the deamination of amino acids is carried out in the presence of enzymes to form  $\alpha$ -keto acids. The deamination of glutamic acid deamination in the presence of montmorillonite saturated with  $\text{Na}^+$ ,  $\text{Mn}^{2+}$ ,  $\text{Cu}^{2+}$  metallic cations to yield  $\alpha$ -hydroxyglutaric acid and traces of butyric acid is also reported [116]. However, kinetic and reaction yields are significantly reduced compared to the biological systems.

To the best of our knowledge, till to date no studies on deamination of amino acids under hydrothermal conditions using heterogeneous catalysts have been reported. Therefore, in order to perform the catalytic hydrothermal deamination of amino acid, leucine is chosen as a model compound, since phenylalanine contains an aromatic ring that can be saturated during the catalytic runs [117]. As catalysts, Pt, Ru, Ni on  $\text{TiO}_2$  were employed, since  $\text{TiO}_2$  is a good metal oxide support due to the strong metal support interaction, chemical stability, and acid-base property. Moreover,  $\text{TiO}_2$  is a recognized heterogeneous catalyst support in petroleum refining industries: hydrodesulfurization, oxidative desulfurization, and biodesulfurization for organo sulfur compounds removal from crude oil and refined petroleum products [118]. In this study  $\text{TiO}_2$  was prepared by microemulsion method and were loaded with Pt 5% wt., Ru 5% wt., Ni 15 % wt., Ni/Pt 15/5 wt. % by incipient wetness impregnation (see Section 3.2). According to XRD analysis, the synthesized  $\text{TiO}_2$  catalysts are dominated by the anatase phase. The catalysts have a higher surface area of  $132.5 \text{ m}^2/\text{g}$  compared to commercial ones ( $90 \text{ m}^2/\text{g}$ ).

The effect of the catalysts on the product yields of Leucine HTL is shown in Figure 45. From the blank experiment about 3.8 % of bio-oil and 29.4 % of solid residue yield was produced. There is an increase in bio-oil yield up to 10.5 and 10.9 % in the presence of Ni Pt/TiO<sub>2</sub> and Ru/TiO<sub>2</sub>, respectively. In contrast, using Pt/TiO<sub>2</sub> and Ni/TiO<sub>2</sub> catalysts resulted in the decrease in the bio-oil yield to 1.9 and 2.5 %, respectively. Moreover, the addition of catalysts significantly decreased the solid residue formation to 17 and 15.7 % using Ni/TiO<sub>2</sub> and Pt/TiO<sub>2</sub>, respectively.

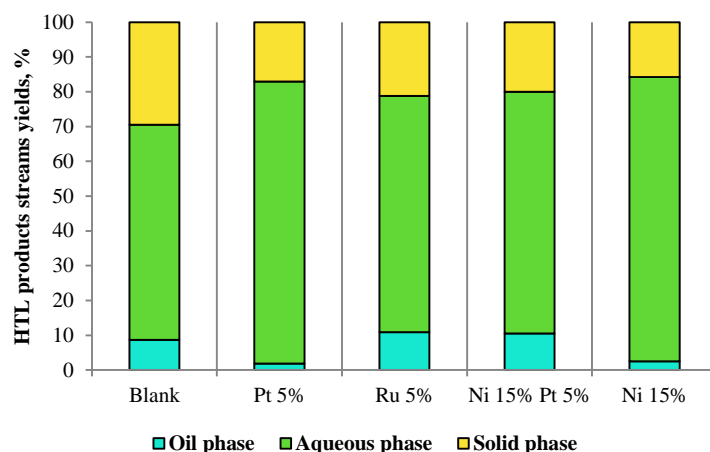


**FIGURE 45.** Product streams yields from catalytic hydrothermal liquefaction of Leucine

*Reaction conditions:*  $T=250^{\circ}\text{C}$ ,  $t=180\text{ min}$ ,  $c(\text{leucine})=0.03\text{ g/ml}$ ,  $V(\text{H}_2\text{O})=50\text{ ml}$ ,  $P(\text{H}_2)=20\text{ bar}$

### 4.3.2 HTL product stream characterization

The composition of bio-oil was analyzed by GC-MS using di(isobutyl)amine as an internal standard. The presence of di(isopentyl)amine, leucyl-glycyl-leucine, 1, 2-dimethylpiperidine was detected by GC-MS analysis in the bio-oil produced from the blank experiment. Using Pt/TiO<sub>2</sub> promotes the formation of di(isopentyl)amine and tri(isopentyl)amine and methylbutanol. In this case the presence of methylpentenoic acid is also observed (Figure 46). It should be pointed out that there were compounds that were not eluted during the GC-MS analysis. Therefore, the bio-oil samples were derivitised using BSA (N,O-bis(trimethylsilyl)acetamide), readily silylating alcohols, amides, amines, amino acids, carboxylic acids, etc. After derivatization a wide distribution of the peaks was obtained; however, not all the peaks were determined because of the complexity in mass spectra interpretation.

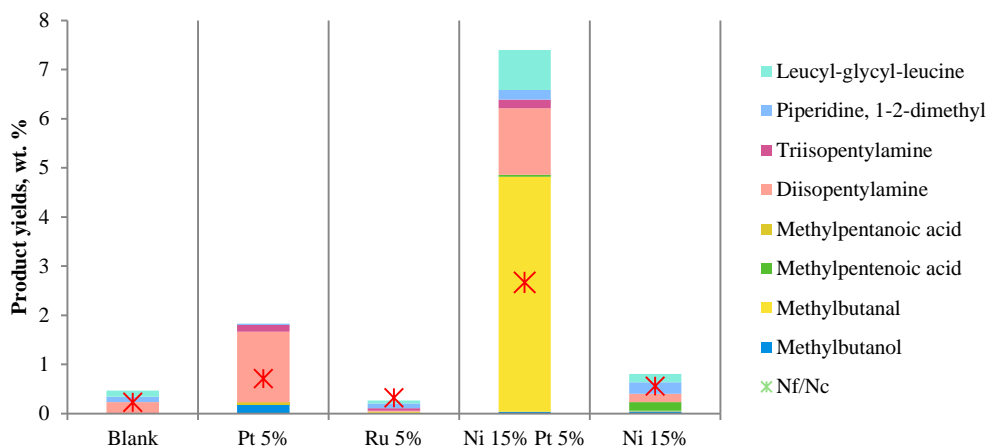


**FIGURE 46.** Bio-oil composition from catalytic hydrothermal liquefaction of Leucine

*Reaction conditions:*  $T=250^{\circ}\text{C}$ ,  $t=180\text{ min}$ ,  $c(\text{leucine})=0.03\text{ g/ml}$ ,  $V(\text{H}_2\text{O})=50\text{ ml}$ ,  $P(\text{H}_2)=20\text{ bar}$

The identified compounds were grouped into deamination, decarboxylation and dehydration products and the ratio of  $N_f/N_c$  (nitrogen containing/nitrogen free) is also calculated, where  $N_c$  is the sum of decarboxylation and dehydration reaction products and  $N_f$  is the sum of deamination reaction products. The ratio of  $N_c/N_f$  products of bio-oil components presumably estimates the nitrogen content of the bio-oil. A higher ratio of  $N_f/N_c$  products indicates the deamination reaction proceeds at a higher rate, as a result, the bio-oil has a lower nitrogen content.

Di(isopentyl)amine is considered as a 2/3 of decarboxylation and 1/3 of deamination product, since it is formed from two molecules of leucine, one of which undergoes both deamination and decarboxylation reactions, another only decarboxylates. Similarly, tri(isopentyl)amine is generated from three molecules of leucine, two of which deaminate and decarboxylate, while the third molecule is the only decarboxylation product. Thus, tri(isopentyl)amine is a 3/5 of decarboxylation and 2/5 of deamination product.

According to the results obtained (Figure 46), using the catalysts increased the ratio of  $N_f/N_c$  with respect to the blank experiment, thus presumably decreasing the nitrogen content of the bio-oil compared to that produced in the absence of the catalysts. The effect of the catalysts in increasing the  $N_f/N_c$  ratio of bio-oil components was in the following order:  $\text{Ru } 5\% < \text{Ni } 15\% < \text{Pt } 5\% < \text{Ni } 15\% \text{ Pt } 5\%$ .

Aqueous phase of the blank experiment contains two main components, leucic acid (16.8 %) and isopentylamine (32 %) (Figure 47). With respect to the blank experiment, using Pt 5% and Ni 15% Pt 5% on  $\text{TiO}_2$  catalyst slightly accelerate the decarboxylation route of amino acid forming isopentylamine to 39.9 and 39 %, respectively. In contrast, Ni/ $\text{TiO}_2$  increased

significantly the deamination rate. Importantly, the yield of leucic acid ( $\alpha$ -hydroxy-isocaproic acid) reached about 53.4 % in the presence of Ni/TiO<sub>2</sub> catalysts.

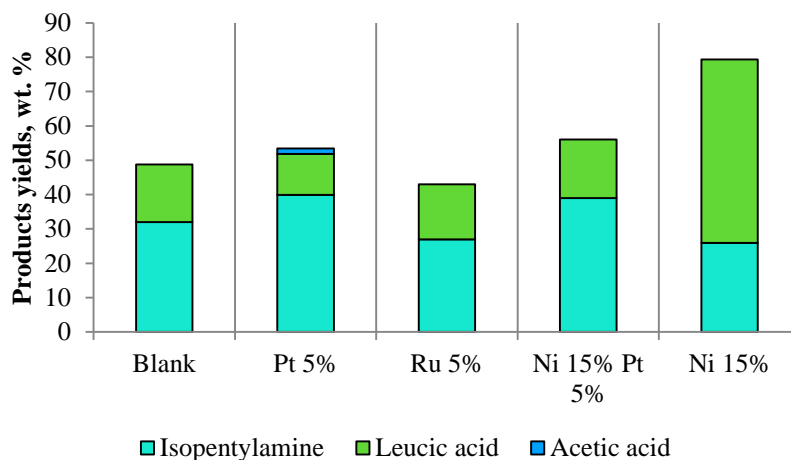


**FIGURE 47.** Aqueous phase composition of catalytic hydrothermal liquefaction of Leucine

*Reaction conditions:*  $T=250\text{ }^{\circ}\text{C}$ ,  $t=180\text{ min}$ ,  $c(\text{leucine})=0.03\text{ g/ml}$ ,  $V(\text{H}_2\text{O})=50\text{ ml}$ ,  $P(\text{H}_2)=20\text{ bar}$

The aqueous phase produced was also analyzed by FTICR MS ESI in positive and negative modes. Apart from isopentylamine and leucic acid, and secondary amines, the presence of hydroxylated amides ( $\text{C}_9\text{H}_{20}\text{O}_2\text{N}$ ,  $\text{C}_{10}\text{H}_{20}\text{O}_2\text{N}$ , etc.) were found, but not quantified because of commercial unavailability.

Using Pt/TiO<sub>2</sub> enhances the decarboxylation of leucine, while Ni/TiO<sub>2</sub> catalyst is effective in terms of deamination of leucine to produce leucic acid. However, both products are preferred to relocate in aqueous phase, thereby decreasing the bio-oil yield. In comparison, Pt Ni/TiO<sub>2</sub> promotes both deamination and decarboxylation of leucine producing methylbutanal that preferably partitioned to the oil phase. As a result of this, the bio oil yield slightly increased with respect to the blank experiment. Furthermore, it contains less nitrogen containing compounds.

Even though the deamination product, leucic acid, is mainly transferred to the aqueous phase, this approach could be considered as an alternative route for the producing  $\alpha$ -hydroxycarboxylic acid. A special application of  $\alpha$ -hydroxycarboxylic acid could be possibility to create polymers when using them as monomers in a condensation reaction [119].

The methods to prepare  $\alpha$ -hydroxycarboxylic acids encompass, for instance, an asymmetric dihydroxylation, asymmetric reduction of 2-oxo acids, hydroxylation of carboxylic acids, addition of cyanide to aldehydes and nitrile hydrolysis or enzymatic deracemization [120].

General drawbacks of these reactions are the requirement of often expensive, chiral metal-complex catalysts, the contamination of the end product with catalysts.

Producing  $\alpha$ -hydroxycarboxylic acids from amino acids under hydrothermal conditions should be further optimized. Moreover, the separation is needed, since isopentylamine is a by-product in aqueous phase. Regarding the acidity and basicity of the main compounds presented in the aqueous phase (amines and acids), ion-exchange basic separation can be a good solution for isolation of leucic acid from the reaction mixture.

### 4.3.3 Conclusion

Several catalysts have been employed to investigate their effect on the deamination rate of leucine under hydrothermal conditions. Using catalysts results in the reduction of solid residue and nitrogen content of the bio-oil. Moreover, there is an increase in the bio-oil in the presence of Ni Pt/TiO<sub>2</sub> and Ru/TiO<sub>2</sub>.

In the case of Ni/TiO<sub>2</sub> leucine is converted to leucic acid with 53 wt. % yield, thus demonstrating a promising alternative approach for the production of  $\alpha$ -hydroxycarboxylic acid that can be considered as a commercially attractive product.

Further work could be done on the possibility to convert different amino acid hydrothermal conditions and further optimize the process by adjusting the reaction operating parameters.

#### 4.4 HTL of oleaginous yeast

Sections 4.1 and 4.2 report the possibility of co-feeding of protein rich biomass with the lipids to increase the energy yields and prevent the formation of heterocyclic nitrogen compounds. As lipids waste cooking oils or microbial oils can be employed.

Regarding this, oleaginous yeasts can be considered as a promising platform for the production of lipids. There have been two possible options for bio-oils recovery from oleaginous yeasts: cell disruption followed by lipid extraction with organic solvents and hydrothermal liquefaction. In the present section two processes were studied and compared in terms of bio-oil yields and chemical composition.

##### 4.4.1 HTL product yields, element analyses and HHV of

In order to release oil from inside a cell, cell disruption was performed by thermal treatment at 120 °C for 1 hour followed by solvent extraction using octane, while HTL experiment was carried out as described in Section 3.3.

Table 17 reports the bio-oil yields and element analyses of bio-oil produced from two processes. HTL of yeast biomass resulted in higher bio-oil yield in comparison to that produced from solvent extraction. However, the bio-oil obtained through solvent extraction showed lower nitrogen and oxygen contents and hence higher HHV value.

**TABLE 17.** Bio-oil yields, elemental analysis, HHV and ER of bio-oil products of oleaginous yeasts

	<b>HTL</b>	<b>Solvent extraction</b>
Bio-oil yield, %	69.7	62.5
	<i>Element analysis, %</i>	
C	70.8	75.3
N	0.7	0.1
H	11.2	11.9
O	15	12.6
HHV, Mj/kg	36.3	38.9
ER, %	84.88	81.5

It is worth mentioning that HTL of yeast resulted in a higher bio-oil yield (69.7%) than the starting lipid content (67.2 %) of the feedstock. This is due to the transformation of proteins and carbohydrates into bio-oil phase under hydrothermal conditions.

#### 4.4.2 Chemical composition of bio-oils

The chemical composition of bio-oils produced from solvent extraction and HTL of oleaginous yeast is presented in Table 18. According to the results, the bio-oil from solvent extraction contained mainly mono-, di-, and triglycerides. The presence of aromatic and heterocyclic compounds was not observed.

In comparison, free fatty acids were the main components of HTL oil. About 5.8 % components related to aromatic and heterocyclic compounds were determined by GC-FID.

HTL of vegetable oils is known as a homogeneous reaction consisting of three reversible stepwise reactions that convert triglycerides into diglycerides, monoglycerides, and glycerol [121]. The rate of hydrolysis is typically slow at first and then increases as fatty acids (FA) are released, decreasing the pH of the reaction medium [78], [79]. This increase in the hydrolysis rate is attributed to the autocatalytic effect of FA.

**TABLE 18.** Chemical composition of bio-oils from oleagineous yeast

Compounds	HTL	Solvent extraction
FA (C16 and C18)	74.9 %	2 %
Mono- and diglycerides	1.3 %	4.0 %
Triglycerides	ND	82.5 %
Others	5.8 %	ND

FT-ICR MS was used for further characterization of nitrogen containing compounds in the bio-oil. According to the results, N2 is the most abundant heteroatom class, followed by N1, O2N1 and O1N1 classes in the bio-oil (Figure 48).

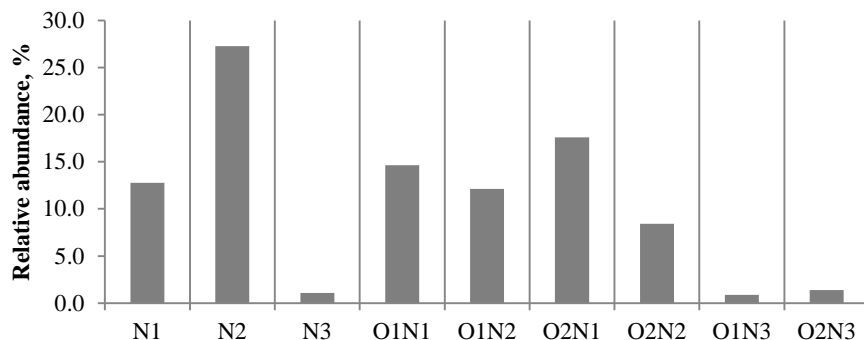


**FIGURE 48.** Nitrogen species presented in HTL oil from oleaginous yeast

According to the abundance-contoured plots of DBE versus  $C_n$  for main O2N1 class compounds, the main compounds are spread at DBE of 10 with a broad distribution of  $C_n$  of 18-26 (Figure 49). Because of their high DBE value, these compounds are likely aromatic amides, oxygenated imidazoles.

For main N2 class components of the bio-oil from the blank experiment are distributed at DBE=5-11 with  $C_n$ =15-25. These components can be assigned as imidazole or pyrazine derivatives [122].

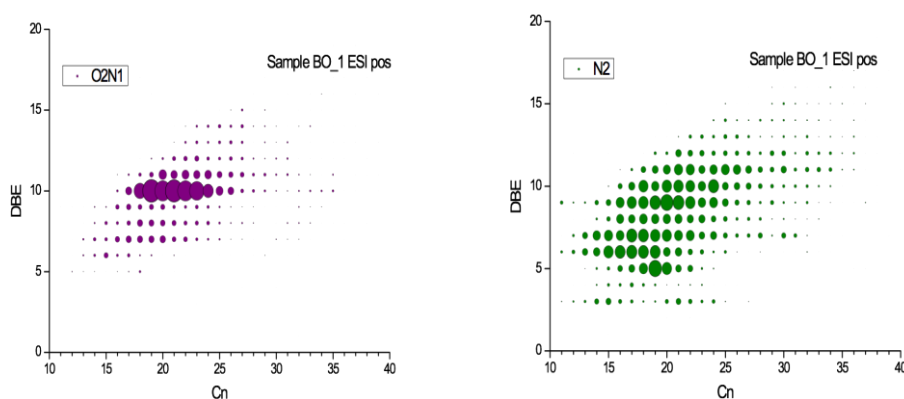


**FIGURE 49.** DBE versus  $C_n$  for N2 and O2N1 class compounds in bio-oil products

### 4.3.3 Conclusion

In this study, hydrothermal liquefaction of oleaginous yeast was investigated and compared to the solvent extraction approach in terms of quantity and quality of bio-oils. HTL resulted in higher oil yield (67.9 %) than the lipid content of initial feedstock (67.2%) due to the release of other cellular metabolites, such as carbohydrates and protein under hydrothermal conditions.

Conversely, the oil yield (62.5 %) was lower when solvent extraction was employed; however, the nitrogen content was significantly lower (0.7 % vs 0.1% by HTL). Regarding the chemical composition of bio-oils, triglycerides were abundant in the oil produced from solvent extraction, while HTL oil contained mainly free fatty acids, thus increasing the TAN value of HTL oil.

These results indicate that the oil obtained via solvent extraction demonstrates better properties. Therefore, it is more suitable for a replacement of vegetable oils.

However, further investigations are still needed to determine the best strategy to produce oil intermediate suitable for upgrading fuel by hydrotreatment, considering the catalyst poisoning, life cycle of hydroprocessing catalysts, and the blending specifications of upgraded oils.

## 4.5 HTL of Liamocins

The concept of using lignocellulosic biomass as a source for commodity chemicals has been a promising solution to alleviate dependence on the petroleum market. Regarding this, lignocellulosic biomass derived liamocins may serve as a precursor to fuels and chemicals that are currently derived in an unsustainable way.

Considering this, in the present section methods for the conversion of liamocins to natural  $\sigma$ -lactones containing alkyl chain, such as 6-Pentyl-5,6-dihydropyran-2-one, 3-hydroxy-5-decanolide and decalactone, are demonstrated through a hydrothermal process or by employing heterogeneous catalysts. The obtained molecules can integrate directly into current industrial chemical markets or undergo further chemical catalytic upgrading to produce diverse end products that can serve as replacements of petrochemicals.

### 4.5.1 Characterization of the liamocins

In order to characterize the lipophilic and hydrophilic components of liamocins and isolate some monomeric components the saponification has been performed. After saponification, the mixture of the lipids gave several spots on TLC after charring with 50 %  $H_2SO_4$  (Figure 50). The spots were divided into two groups; designated the upper and lower parts. Decanoic acid was used as a reference and gave similar spots at the upper part on TLC, thus suggesting that these components at upper part are likely fatty acid components, while at bottom part the spots are likely mannitol and arabitol linked lipids.

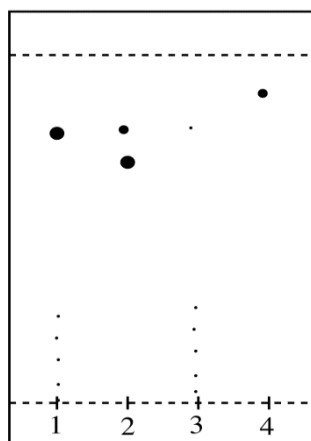


**FIGURE 50.** TLC of liamocins before and after saponification  
1)Liamocins, 2) Fatty acids in ether, 3)ether insoluble fraction, 4) Decanoic acid

The mixture of the fatty acid components was subjected to column chromatography (30:70% Hexane:Ethyl acetate) to separate the monomers. Around 0.5 % and 3.9 % were isolated from liamocins and are found to be **massoia lactone (ML)** ( $^1H$  NMR: 0.96 (3H, t), 1.2-1.85 (9 H, m), 2.31 (2H, m), 4.40 (1H, m), 5.99 (1H, m), 6.86 (1H, m).  $^{13}C$ -NMR: 13.97 (CH<sub>3</sub>), 22.48, 24.45, 29.38, 31.52, 34.82 (CH<sub>2</sub>), 78.03 (HCO), 121.39, 145.09 (=CH), 164.61 (C=O) and **3-hydroxy-5-decanolide 2 (BHDL)** ( $^1H$  NMR: 0.96 (3H, t), 1.3-1.96 (10H, m), 2.62 (1H, m), 2.75 (1H-OH, s), 4.36 (1H, m), 4.69 (1H, m);  $^{13}C$ -NMR: 13.98 (CH<sub>3</sub>), 22.51, 24.51, 31.77, 35.51, 35.86, 38.61 (CH<sub>2</sub>), 62.60 (HCOH), 76.17 (HCO), 171.12 (C=O)), respectively. The presence of the lactones ML and BHDL is also confirmed by GC-MS analysis.

The lipophilic fraction of liamocins is known to consist of 3,5-dihydroxydecanoic acids (3,5-DHDA); however, after the saponification, most of them must have been lactonized to ML and BHDL during solvent extraction and evaporation of extraction solvent.

The hydrophilic components of the liamocins are found to be mannitol and arabitol according to the HPLC analysis of aqueous phase after extraction with ether.

#### 4.5.2 Characterization of bio-oil

Based on the data obtained from previous chapters on HTL of model compounds as well as the real oleaginous yeast biomass, under hydrothermal conditions liamocins were expected to undergo molecular breakdown to form monomers, such as mannitol, arabitol, acetic acid and 3, 5-dihydroxydecanoic acids, being latter difficult to detect by traditional GC and HPLC analyses. Therefore,  $^1H$ ,  $^{13}C$ , COSY, HSCQ, HMBC NMR were performed for the elucidation of the composition of one of the bio-oil samples produced at 200 °C.

The NMR spectrum of the ML and BHDL lactones (Figure 51) isolated from the liamocins saponification was compared to the bio-oil components and the main resonance signals were assigned.

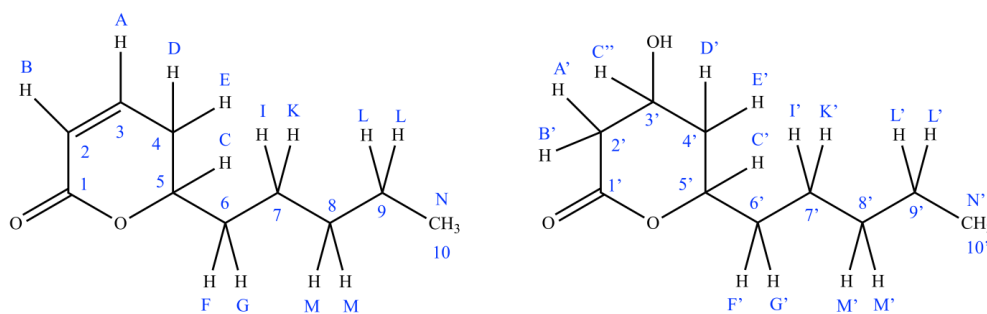


**FIGURE 51.** The structure of ML and BHDL

ML showed characteristic enoyl signals at 5.99 ppm/121.4 ppm (*B*) and 6.86 ppm/145.1 ppm (*A*), position-4 CH<sub>2</sub> protons at 2.31 ppm (*D*, *E*), and a position-5 CH proton at 4.40 ppm (*C*), which is shifted upfield by the attached 5-O-lactone ester linkage (Figure 52).

BHDL showed characteristic signals at 4.1 ppm/62.6 and 4.6/76.2 (*C''* and *C'*, respectively) and *D'* and *E'* shifted upfield at 2.87. Since the protons in alkyl chains were overlapped, therefore, the quantification of lactone 2 was done by means of proton at 4.6 ppm.

It should be pointed out that BHDL and 3,5-DHDA are not easily distinguished from each other; however, based on HBMBC, both C3 and C5 showed a strong correlation with C1, while in case of 3,5-dihydroxydecanoic acid only C3 should have shown a correlation with C1. According to the assignments obtained, the main components of bio-oil were 1 and 2, while the presence of 3, 5-hydroxydecanoic acids were not identified. Supplementary analysis on GC also confirms the presence of only ML and BHDL.

Also the signal at 5.08/72 ppm, which is attributed to C5 ester linkage between 3,5-dihydroxydecanoate groups, is not observed, thus assuming a full hydrolysis of liamocins at 200 °C.

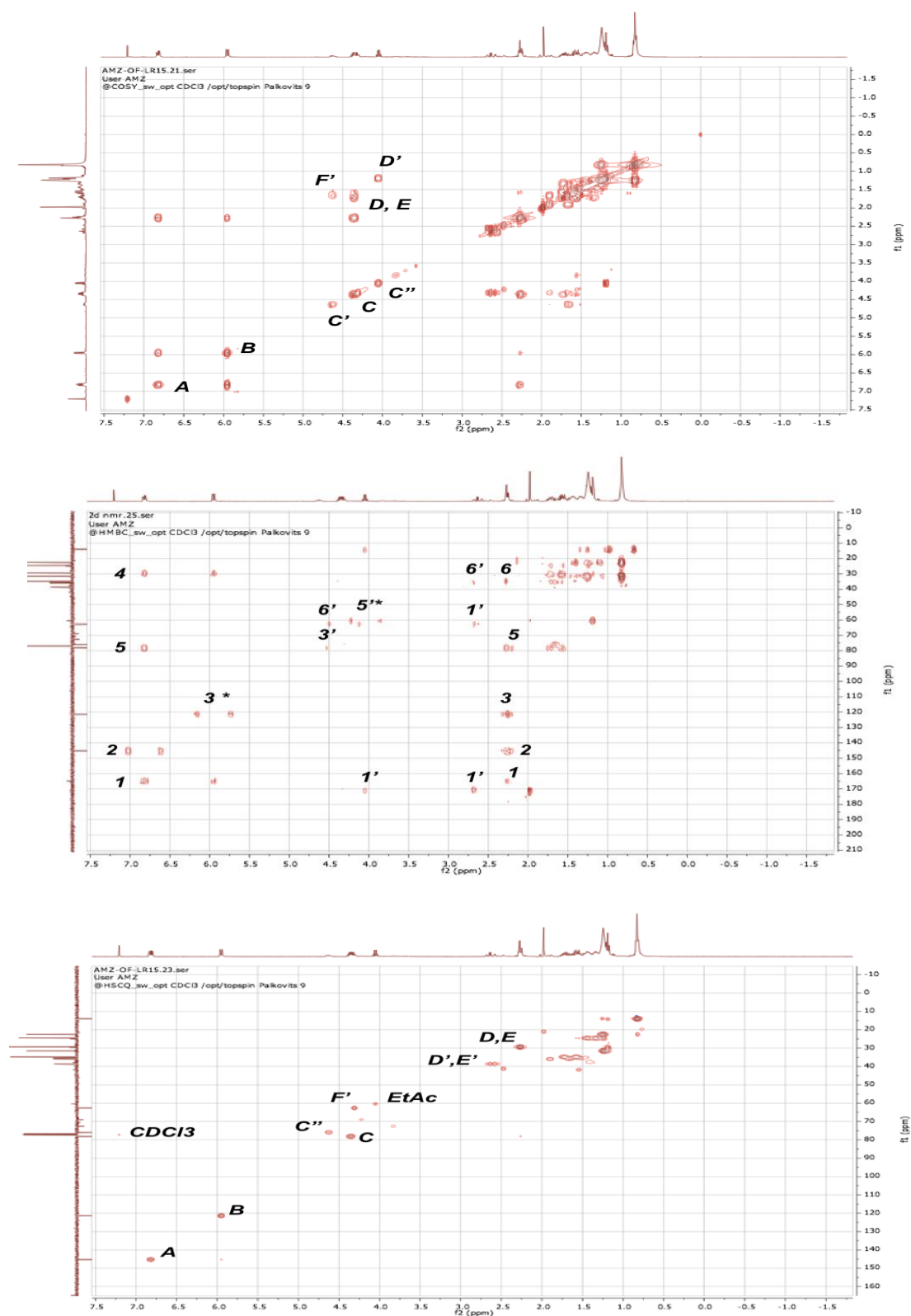


**FIGURE 52.** COSY, HMBC, HSCQ NMR of bio-oil produced from HTL of liamocins at 200 °C

It should be pointed out that the interconversion of the component BHDl into ML could happen during the GC-FID analysis. For instance, the yield of ML quantified by GC-FID analysis was always higher about 5-7% than those quantified by HPLC analysis for the same bio-oil sample. This may be explained by previous findings of Versonder et al. [123] who performed the GC-MS analysis of 3,5-DHDA. They found that the spectrum of 3,5-DHDA was identical to the one of massoia lactone. It suggests that 3,5-DHDA undergoes an easy Versonder type dehydration to the lactone of 5-hydroxy 2-decenoic acid during GC analysis because of the increase in temperature during GC analysis. So the quantification of the compounds ML and BHDl on HPLC or NMR is preferred to GC analysis, since, at higher temperature 3,5-DHDL or BHDl could be dehydrated to yield massoia lactone, thus increasing the standard error.

#### 4.5.3 HTL of Liamocins

The quantification of the reaction products has been performed separately in the aqueous phase and oil phase. According to the results obtained, in the first step liamocins hydrolysis to form monomers. As expected, mannitol, arabitol, acetic acid were transferred into the aqueous phase, while 3,5-DHDL undergoes lactonization quantitatively contributing into bio-oil phase (Figure 53).

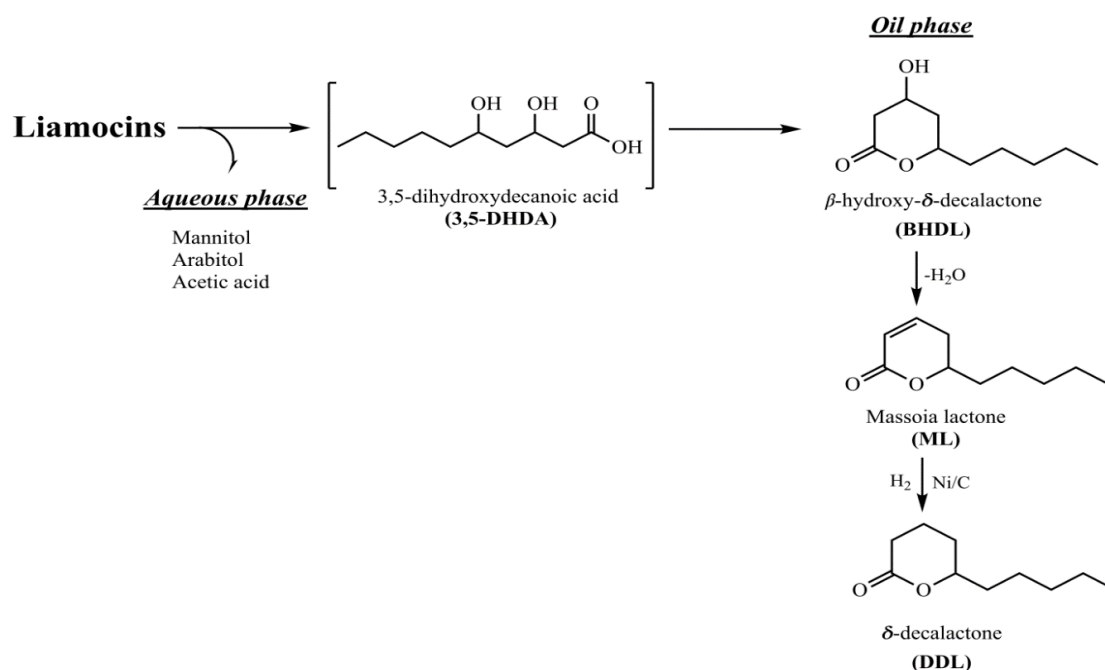


**FIGURE 53.** Reaction pathway of liamocins HTL

It is important that hydrolysis and lactonization occur at the same reaction conditions.

The supplementary experiments on the effect of pH on the lactonization were carried out using  $\text{Na}_2\text{CO}_3$  and  $\text{H}_3\text{PO}_4$  at pH=9 and pH=3, respectively, and compared to the standard experiment performed in water without any additives, where the pH was always around pH=5 after reaction.

Based on the results obtained, there was no formation of lactones at pH=3 and pH=9, while lactonization always occurred at pH=5. Similarly, in the study [124] the hydrolysis and lactonization rate of poly( $\alpha$ -hydroxyacrylic acid) reaction rates coincided approximately at pH 5.3, yet the rates were very low.

The conversion of 3,5-DHDL form to lactone proceeds via a proton transition from hydroxyl to carboxylic oxygen followed by elimination of  $\text{H}_2\text{O}$ . Under alkaline conditions (pH=9), once the free acid is formed it is immediately converted to the carboxylate anion ( $\text{ROONa}$  salt), which is not further attacked by  $[\text{OH}^-]$ . In the lower pH region (pH=3) the lactonization rate is decreased because of the increasing distance between the functional groups available for lactonization reaction [124]. This kind of pH dependent behavior of the lactonization is caused by the protonation and deprotonation of the carboxylic or hydroxyl group, which may have an effect on all other electrons in the molecule, thus slightly changing the bond lengths.

It is worth mentioning that an increased temperature is another parameter for hydrolysis acceleration. There is a gradual increase in sugars yields with the temperature, which is due to the continuous hydrolysis of liamocins. At 250 °C, the aldol cleavage products of sugars, such as glyceraldehyde 1.3-dihydroxyacetone, is observed in trace amount (less than 1%) (Table 19).

However, a decrease in oil yield as well as the massoia lactone yield at higher temperature (225-250°C) suggests a low thermal stability of lactone 1. The maximum yields of 1 and 2 are obtained at 200 °C. The total yield of ML and BHDL fully corresponded to the yield of the oil fraction (fraction after the evaporation of the solvent), suggesting that they are the major components of the bio-oil.

**TABLE 19.** Hydrothermal decomposition of liamocins in water

T (° C)	Conv. (wt.%)	Oil yield (wt.%)	Yield of 1 (wt.%)	Yield of 2 (wt.%)	Yield of C4 acid (wt.%)	Yield of mannitol (wt.%)	Yield of arabitol (wt.%)
175	89	45	16.7	-	16.5	8.5	0.6
200	89	35	17.6	15	15.7	8.5	0.7
225	91	4.0	2.36	-	12.1	9.8	0.8
250	93	3.8	-	-	13.7	10.3	1.5

*Reacton conditions: 2h, 10 bar N<sub>2</sub>, 0.01 g/ml Liamocins in water as feed.*

Simultaneous high oil yield and lower yield of 1 at 175 °C in comparison to those at 200 °C is due to incomplete hydrolysis of liamocins at lower temperature. This is confirmed by ESI MS analysis of the oil fraction obtained at 175 °C (Appendix B), showing higher molecular ions that are hardly amenable for the detection by traditional GC or HLPC analyses .

The extracted oil at 175 °C was analyzed in both positive and negative ions in the mass range 200-850 Da, in which dominant ones were M/z=335, 371, 451, 746,827 in negative mode and M/z=241, 393 in positive mode.

In negative mode m/z (ion [576+K]) were non-acetylated liamocins with three 3,5-dihydroxydecanoate acyl chains connected via 1,5-polyester bonds., while the m/z 827 is an acetylated liamocins with four 3,5-DBHA chains [804+Na]. Under the negative operation mode of ESI, ML was accordingly ionized by its adduction of corresponding anion to the lactone. The m/z 335 in negative mode is suggested to be a dimer of ML ions [M+M].

Water is known to be a good reaction medium for biomass deconstruction; however, the thermal decomposition of biomass in water should be done under subcritical conditions (above 200 till 374 °C). Accordingly, the hydrolysis of liamocins should be carried out at a temperature above 200 °C.

However, the lactones ML and BHDL are thermally instable at a higher temperature than 200°C. The supplementary reactions performed with ML HTL at 250 °C showed the full conversion, while the conversion of 1 at 200 °C was about 54%. Instead, the formation of gas phase was observed. The gas phase was subsequently quantified using an internal standard of acetylene and was found to consist of about 30.1 % of C<sub>1</sub>-C<sub>4</sub>. The presence of CO<sub>2</sub> became evident; however, it was not quantified.

Since GC-MS did not show any peaks except massoia lactone in the bio-oil after the reaction, it was analyzed by  $^1\text{H}$  and  $^{13}\text{C}$  NMR analyses (Figure 54). The  $^{13}\text{C}$  NMR spectra of massoia lactone after the HTL at 250 °C showed the shift of ester group of 1 at 164-165 ppm to acid group at 171 and 175 ppm. Moreover, the presence of multiple resonances in the region 110-138 ppm/4.9-7.0 are observed that are related to the formation of  $-\text{CH}=\text{CH}-$  bonds. According to  $^1\text{H}$  NMR spectra, the shifts of  $\text{CH}-\text{OH}$  at 4.40 ppm to 4.0 ppm and  $-\text{CH}_2$  protons at 4-position of massoia lactone at 2.31 ppm to 2.5 ppm are observed. All these facts suggests that massoia lactone could undergo ring-opening to form four different geometrical isomers of 2,4-decadienoic acid (trans-2, cis-4-; cis-2-trans-4-; cis-2-cis-4; trans-2, trans-4-), some of them could attach the water at the position of  $-\text{C}3$  (4.00 ppm) to form 3-hydroxy-4-decenoic acid. The high boiling point (290 °C) of 2,4-decadienoic acid and the presence of the OH-group in the structure of 3-hydroxy-4-decenoic acid make these compounds amenable for the detection of GC analysis, while on HPLC instrument 2,4-decadienoic acid and massoia lactone have shown the same response factor.

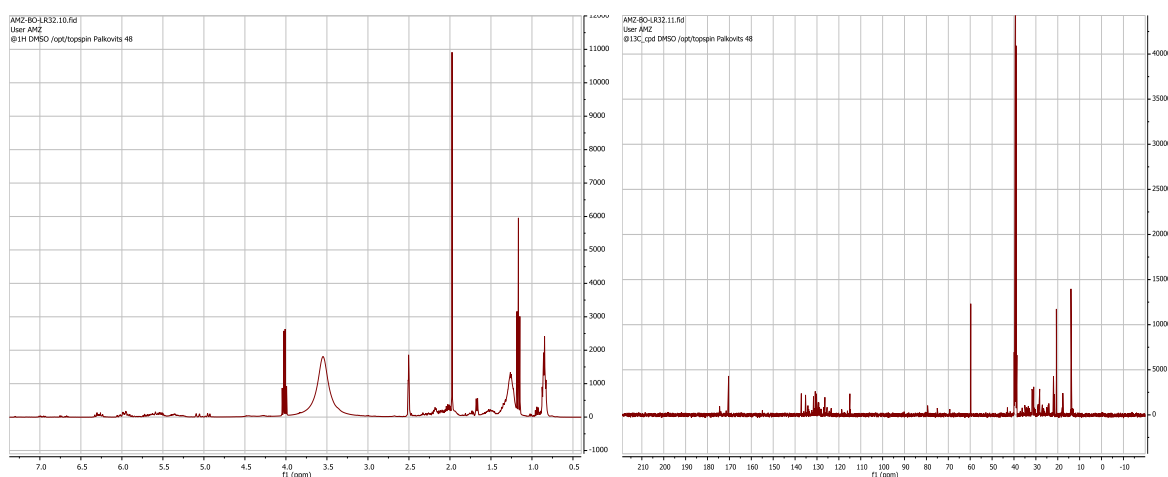


**FIGURE 54.**  $^1\text{H}$  and  $^{13}\text{C}$  NMR analyses of ML HTL at 250 °C

Mei Chia and co-workers [125] performed a thermodynamic calculation using the Gaussian software to predict ring-opening of d-hexalactone to hexenoic acid. Regarding their estimates, the ratio of dienoic acid to lactone increases with reaction temperature, which is consistent with the results of the present study.

Since the main target of the present study is to optimize the process of liamocins HTL in order to increase the yield of lactone, the quantification of by-products, such as 2,4-decadienoic acid and 3-hydroxy-4-decenoic acids were not done because of the complexity of

the analysis. However, it could be done by isolation of bio-oil components on column chromatography and subsequent derivatization of interesting products or by a method described elsewhere [126].

#### 4.5.4 Solvolytic liquefaction

Due to the susceptibility of lactones 1 and 2 to undergo ring-opening in the presence of water at higher temperatures, thermal decomposition of liamocins were performed in organic solvents. Using organic solvents are known to stabilize the reaction intermediate fragments, thus improving the stability of desired products [127].

Therefore, several solvents with different polarity, such as hexane, 1,4-dioxane, tetrahydrofuran (THF) were selected and the results are presented in Table 20. Since liamocins hydrolysis is not complete at lower temperatures than 175 °C, the following experiments were performed at 200 °C.

**TABLE 20.** Hydrothermal decomposition of liamocins in organic solvents

Solvent	Conv. (wt.%)	Yield of ML (wt.%)	Yield of 2-butanol (wt.%)	Yield of others (wt.%)
Hexane	97.8	51	5.3	-
Dioxane	76.9	26	-	5.9
THF	88	29.1	5.9	21.8
Isopropanol	98.6	31.3	10.29	-
Water	91.3	3.3	-	14.7

*Reaction conditions: 5h, 200 °C, 20 bar N<sub>2</sub>, 0.01 g/ml*

Notably, the yield of ML in the presence of all organic solvents was higher than that obtained when the water was the solvent. The formation of BHDL was not observed, probably due to affinity of 2 to dehydration in the presence of organic solvents and/or due to the longer time. The highest yield of ML is obtained in the presence of hexane. The following dependence was observed: ML yields are higher with lower solvent surface tensions; hexane (18.4 mN) > isopropanol (23 mN) > THF (28 mN) > 1,4-dioxane (40 mN) > water (72.7 mN).

The reason behind this yield increase is not completely understood. However, changes in interactions between the solvent and solute that occur because of changes in hydrogen bonding and differing dipole moments can significantly alter the solubility and the thermodynamic state of reactants, transition states, etc. [128].

In the water 3,5-DHDA molecules are bounded strongly by intermolecular hydrogen bonds, while in hexane the intramolecular hydrogen bonds are predominant which enhances the lactonization (Figure 55). Intermolecular hydrogen force increases the intermolecular attraction between molecules, thus increasing the boiling point, surface tension, etc., while intramolecular H-bond results in lower surface tension.

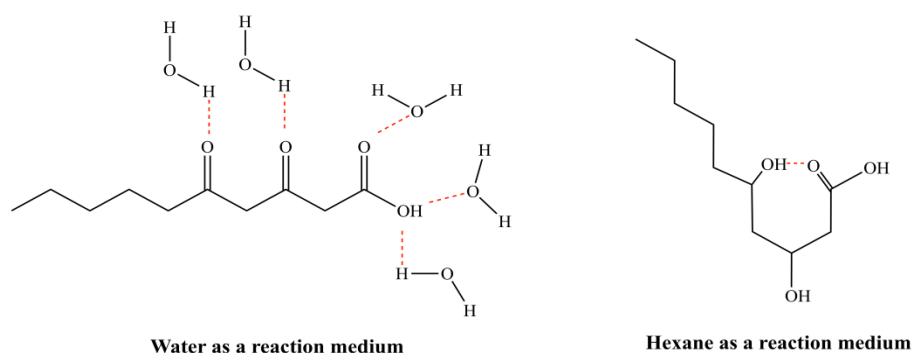


**FIGURE 55.** Pictorial view of the solvation of 3,5-DHDA in water and hexane solvents

However, other factors could play a significant role in enhancing the yields of ML. The combination of improved computational chemistry methods and increasing amount of experimental data will help to gain mechanistic insights into these solvent effects.

Interestingly, a relatively different reaction pathway of liamocins under hydrothermal conditions is observed in the presence of THF. The formation of around 6.4 % of  $\gamma$ -butyrolactone (GBL), 9.1 % of 1,3-octadiene and 6.4 % of ethyl formate is detected. An increase in 1,3-Octadiene and GBL up to 16.3 % and 9.8 %, respectively is observed at 250°C (Table 21).

**TABLE 21.** Hydrothermal decomposition of liamocins in THF

T, °C	Conv. wt. %	Yield of 1, wt. %	Yield of 2-butanol, wt. %	Yield of 1,3-octadiene, wt. %	Yield of GBL, wt. %	Yield of ethyl formate, wt. %
175	86.8	20.9	3.4	8.4	3.4	-
200	88.9	29.1	5.91	9.1	6.2	6.4
225	98.4	35.3	8.5	10.7	6.0	1.86
250	99.2	21.3	4.1	16.3	9.8	12.2

*Reaction conditions: 5h, 200 °C, 20 bar N<sub>2</sub>, 0.01 g/ml Liamocins in THF*

1,3-octadiene is a decarboxylation product of ML after cleavage of C1 in the alkyl chain, while GBL could be formed after relactonization of d-lactone into g-lactone followed by cleavage of C6 of the alkyl chain (Figure 56).

The group of James A. Dumesic observed that 40 % and 23 % of d-valerolactone and ε-caprolactone reacted to form g-lactones, suggesting that larger, less stable lactones undergo ring-opening to form an alkene acid, which can isomerize and subsequently close, forming more stable g-lactone [129].

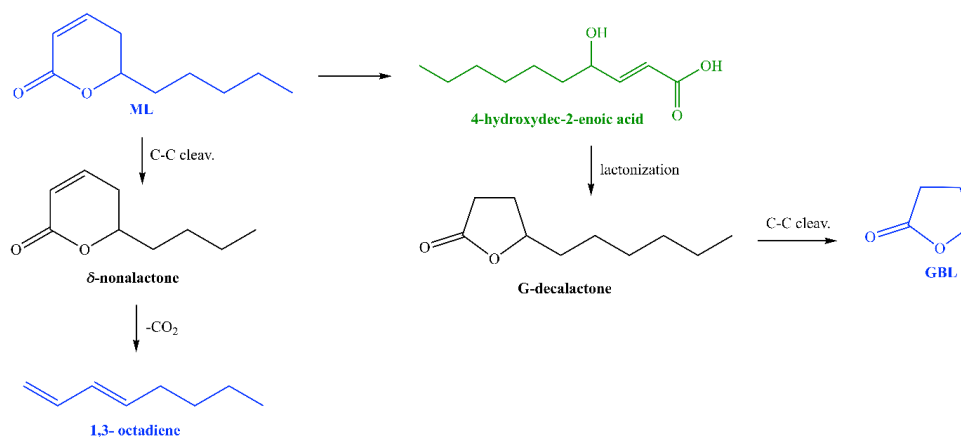


**FIGURE 56.** The possible formation of GBL and 1,3-octadiene

*\*blue products have been quantified, black products are detected in trace amount, green product is not detected*

1,3-Octadiene is obtained by naphtha cracking and is useful for making resins, plastics, etc. [130]. GBL also has widespread industrial use [131].

#### 4.5.5 Catalytic hydrothermal liquefaction

To produce DDL from liamocins, one-pot catalytic hydrothermal liquefaction of liamocins has been performed. As shown in Table 23, also in this case the highest DDL yield is obtained with hexane as solvent. The yield of DDL was higher than that of ML by 8%, suggesting that unsaturated lactones are less stable than their saturated counterparts under hydrothermal conditions.

The reaction medium has a significant influence on the yield. For hexane the DDL yield is more than two times higher than for water indicating that DDL in the presence of water also tends to undergo ring opening to form decenoic acid. In the presence of hydrogen decenoic acid is partially further hydrogenated to decanoic acid over Ni/C.

**TABLE 22.** Catalytic treatment of liamocins

Solvent	t, h	Conv. wt.%	Yield of DDL, wt.%	Yield of C10 acid, wt.%	Yield of C6-C9 wt.%	Yield of sugars, wt.%
H2O	3	99	23	-	2	13.8
H2O	5	99	26	3.95	1.6	17.8
Hexane	3	78.3	33	-	-	-
Hexane	5	93	58	-	-	-

*Reaction conditions: T=200°C, 30 bar H<sub>2</sub>, 0.01 g/ml Liamocins in Hexane, 1:10 (wt/wt) Ni/C:Liamocins*

Even though the carbon balance is not completed due to the initial complex composition of liamocins and difficulties in the detection of the reaction products by traditional analytical instruments (GC, HLPC), the findings of the present study offer a promising approach to the production of families of commodity products from liamocins.

In future work, identification and quantification of by-products will be developed further utilizing powerful techniques, for instance FTICR MS, which is devoted to more complex compounds with higher molecular mass and with high heteroatom content.

#### 4.5.6 Purification of liamocins

One of the challenges with using *A. pullulans* for bio-product formation is that most strains produce dark melanin-associated pigments that contaminate the final desired product.

Although the downstream process normally accounts for the major part of a bioprocess costs, only limited attention has been placed on the amelioration of lipid extraction protocols. A classical solvent-based method has been largely used to perform lipid extraction from various biological materials. The Folch method [132] consists in using chloroform–methanol, and then the extracted solvent (chloroform) is washed with water to remove non-lipid substances. Bligh and Dyer [133] later proposed a method based on Folch's combining chloroform, methanol and water, for lipid extraction from a wide range of biological materials.

The Folch method has the advantage of being simpler, applicable to any scale desired, substantially decreasing the losses of lipids incidental to the washing process.

Approximately 1.05 g of liamocins were mixed with 20 ml of chloroform:methanol (2:1) and centrifuged at 3,000 for 10 min. About 5 ml of water was added to the filtrate and was shaking vigorously about 5 min. After centrifugation at 3000 for 10 min, the upper bottom was eliminated and MgSO<sub>4</sub> was added to the bottom part. Then the oil part was filtrated and the solvent was evaporated. The yield of lipids extracted reached 86%. The colour of purified liamocins was changed from dark brown to yellowish brown, thus assuming the purification of liamocins from melanin-derived intermediates and different inorganic substances used as a cultivation medium. The conversion and yield produced from purified liamocins clearly exceeded (95.7% and 31%, respectively) the results obtained in the case of non-purified liamocins (100% and 40.9%, respectively) in the presence of hexane at 200 °C for 3h.

During the liquefaction in water these impurities automatically are transferred to the aqueous phase, thus avoiding the necessity of prior purification. However, in the presence of the solvents, the purification of liamocins is recommended.

#### **4.5.6 Conclusion**

It was demonstrated that a wide range of commercially valuable chemicals, such as pentyl-5,6-dihydropyran-2-one, 3-hydroxy-5-decanolide and decalactone can be obtained from liamocins via thermal decomposition in organic solvents or using heterogeneous catalyst. The main experimental evidences resulting from this study can be summarized as follows:

-For the production of lactones from liamocins via hydrothermal liquefaction, the hydrolysis and lactonization should occur at the same pH, which is likely pH=5. At lower pH values (pH=3) the distance between the functional groups (OH, COOH) that are available for lactonization increases, so inhibiting the lactonization. At higher pH values (pH=9), the acid intermediate forms immediately carboxylate anion which does not react with OH<sup>-</sup>.

-Temperature plays a significant role in both hydrolysis and thermal stability of lactones ML. The hydrolysis does not proceed below 175 °C, while at higher than 200 °C the lactone is not stable. Therefore, the optimal temperature for both liamocins hydrolysis and lactonization is 200 °C.

-Using organic solvent possessing lower surface tension increase the stability of ML. The maximum yield (51%) of 1 is observed in the presence of hexane.

-The production of decalactone with 58% in one-pot catalytic hydrothermal liquefaction process in the presence of hexane and Ni/C and 30 bar of H<sub>2</sub> is obtained. It is shown that the stability of unsaturated lactones is less in comparison to saturated ones.

-Purification of liamocins from different impurities can be done by Folch method. Obviously, the product yields as well as the conversion of the process are significantly higher.

Further work is needed for development of methods for the quantification of by-products in order to optimize further the liquefaction process.

## Chapter 5. Conclusion and Future work

In this study the behavior of different model compounds and microbial biomass, namely oleaginous yeasts and liamocins, under hydrothermal conditions is studied. The product distribution, reaction pathways and mechanisms for these systems were investigated. The findings of the present study showed that HTL process is a promising tool to obtain bio-oils with valuable technological properties and commercially attractive products that can serve as feasible alternatives to fossil fuels and petrochemicals.

In the first part of this study (Section 4.1) the choice of monomeric model compounds, representative of protein, polysaccharide and lipid fractions of waste biomass, has made possible to simplify the spectrum of the products, thus allowing the identification of the main chemical pathways under hydrothermal conditions.

It is confirmed that lipids are the main contributors to the bio oil yield. They also display the synergistic effect on the protein contribution into bio-oil yield by the reactive extraction of hydrophilic species (amines). Lipids also exert the reduction of nitrogen content in the bio-oil by mass effect, thus making the resulting product less critical for the co-feeding in the refinery upgrading processes. More importantly, in the presence of lipids, amides formation is in the competition with the generation of nitrogen containing heterocyclic species, observed in the presence of carbohydrates.

Then, these results were verified using complex biomass polymers (albumin, starch, tripalmitin), since they move closer to mimicking the true chemistry of HTL of waste biomass (Section 4.2). The effect of lipid dosage on the HDN reactivity of the nitrogen compounds was also confirmed by determining the ratio of fatty acid amides and heterocyclic nitrogen components of the bio-oils produced from the feedstocks with the different lipid contents (33 and 25%). This conclusion is crucial in terms of upgrading process, since nitrogen presented as FFAs could be easily reduced by the hydrotreatment, while the nitrogen contained in heterocyclic compounds is less amenable and cause catalyst deactivation (Section 1.6).

The results of the present study shed light on the advanced understanding the chemical reaction mechanism of the HTL process of waste biomass and demonstrates a potential for tailoring the chemical composition of the feedstock for the production of advanced transport fuel from the waste.

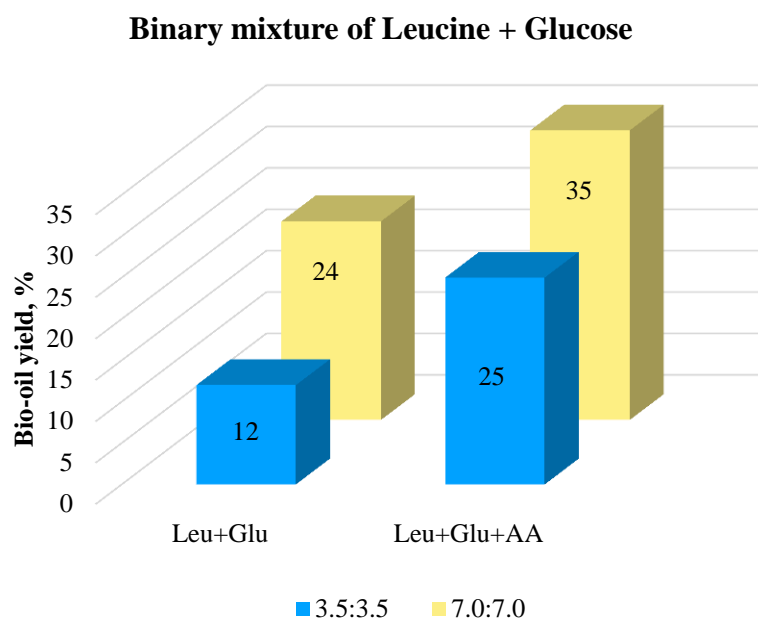
Another important implication of this study was the demonstration of an alternative method for the production of  $\alpha$ -hydroxycarboxylic acid from leucine under hydrothermal conditions. In Section 4.3 several catalysts have been employed to investigate their effect on the deamination rate of leucine under hydrothermal conditions. It is shown that leucine can be converted to leucic acid with overall 53 % yield using 15% Ni/TiO<sub>2</sub>.

In Section 4.4 HTL has been demonstrated as an effective approach for oil recovery from oleaginous yeasts. HTL of oleaginous yeasts resulted in significantly higher yield of bio-oil (67.2%) than that obtained from solvent extraction (performed without a co-solvent (62.5 %). However, the nitrogen content of HTL oil was higher compared to those from solvent extraction (0.7 % vs 0.1%). This was due to the tendency of HTL to transform not only lipids, but also carbohydrates, protein degradation products into the oil phase.

Furthermore, in this study a method for the transformation of liamocins into massoia lactone and d-decalactone via hydrothermal liquefaction is demonstrated in Section 4.5. Massoia lactone and d-decalactone produced with maximum yields of 51 and 58 %, respectively.

Overall, the HTL process could be considered as an innovative tool to limit the reliance on petroleum-based products and produce the energy in a sustainable way.

Further work could be performed on the optimization of liamocins and catalytic hydrothermal liquefaction of amino acids in order to increase the yields of desired products.

**Appendix A. Supporting information to Section 4.1.4.**

## Appendix B. Supporting information to Section 4.5.3.

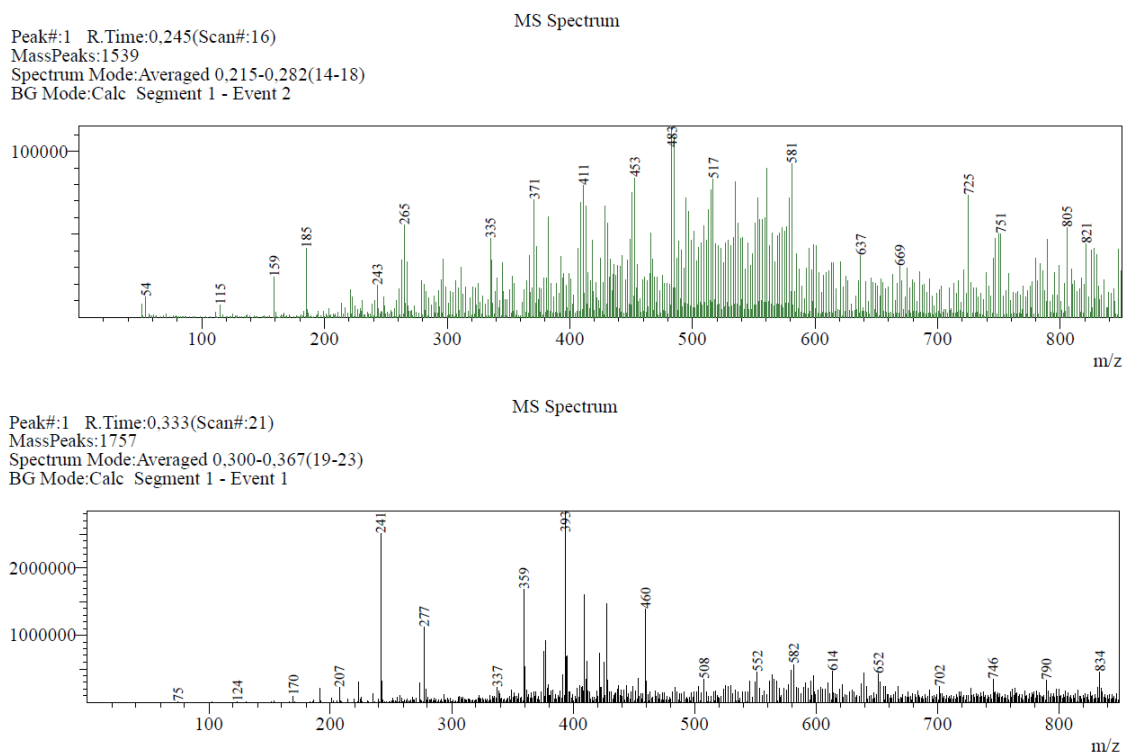


FIGURE A.1. ESI spectra for bio-oil produced at 175 °C: a) ESI+ b)ESI-

## References

- [1] W. N. R. W. Isahak, M. W. M. Hisham, M. A. Yarmo, and T. Yun Hin, "A review on bio-oil production from biomass by using pyrolysis method," *Renew. Sustain. Energy Rev.*, vol. 16, pp. 5910–5923, 2012.
- [2] "Renewable Energy Directive 2009/28/CE." [Online]. Available: <https://eur-lex.europa.eu/legal-content/EN/TXT/PDF/?uri=CELEX:32009L0028&from=EN>. [Accessed: 27-Aug-2018].
- [3] P. Zhao, Y. Shen, S. Ge, Z. Chen, and K. Yoshikawa, "Clean solid biofuel production from high moisture content waste biomass employing hydrothermal treatment," *Appl. Energy*, vol. 131, pp. 345–367, 2014.
- [4] "Waste atlas 2013. Report 2013," 2013. [Online]. Available: <http://www.atlas.d-waste.com>.
- [5] U. Jena, K. C. Das, and J. R. Kastner, "Effect of operating conditions of thermochemical liquefaction on biocrude production from *Spirulina platensis*," *Bioresour. Technol.*, vol. 102, no. 10, pp. 6221–6229, 2011.
- [6] P. Duan, B. Wang, and Y. Xu, "Catalytic hydrothermal upgrading of crude bio-oils produced from different thermo-chemical conversion routes of microalgae," *Bioresour. Technol.*, vol. 186, pp. 58–66, 2015.
- [7] C. Hognon *et al.*, "Comparison of pyrolysis and hydrothermal liquefaction of *Chlamydomonas reinhardtii*. Growth studies on the recovered hydrothermal aqueous phase," *Biomass and Bioenergy*, vol. 73, pp. 23–31, 2015.
- [8] H. P. Blaschek and T. C. Ezeji, "Biofuels from Agricultural Wastes," in *Biofuels from Agricultural Wastes*, 2010, pp. 3–9.
- [9] M. Déniel, G. Haarlemmer, A. Roubaud, E. Weiss-Hortala, and J. Fages, "Energy valorisation of food processing residues and model compounds by hydrothermal liquefaction," *Renew. Sustain. Energy Rev.*, vol. 54, pp. 1632–1652, 2016.
- [10] A. Dimitriadis and S. Bezergianni, "Hydrothermal liquefaction of various biomass and waste feedstocks for biocrude production: A state of the art review," *Renew. Sustain. Energy Rev.*, vol. 68, pp. 113–115, 2017.
- [11] M. Kumar, A. O. Oyedun, and A. Kumar, "A review on the current status of various hydrothermal technologies on biomass feedstock," *Renew. Sustain. Energy Rev.*, vol. 81, pp. 1742–1770, 2018.
- [12] S. R. Villadsen *et al.*, "Development and Application of Chemical Analysis Methods for Investigation of Bio-Oils and Aqueous Phase from Hydrothermal Liquefaction of Biomass," *Energy and Fuels*, vol. 26, pp. 6988–6998, 2012.
- [13] M. T. Timko, A. F. Ghoniem, and W. H. Green, "Upgrading and desulfurization of heavy oils by supercritical water," *J. Supercrit. Fluids*, vol. 96, pp. 114–123, 2015.
- [14] D. P. Fernández, Y. Mulev, A. R. H. Goodwin, and J. M. H. L. Sengers, "A Database for the Static Dielectric Constant of Water and Steam," *Journal of Physical and Chemical Reference Data*, vol. 24, no. 1, pp. 33–70, 1995.
- [15] P. Duan, Y. Xu, F. Wang, B. Wang, and W. Yan, "Catalytic upgrading of pretreated algal bio-oil over zeolite catalysts in supercritical water," *Biochem. Eng. J.*, vol. 116, pp. 105–112, 2016.
- [16] R. Campuzano and S. González-Martínez, "Characteristics of the organic fraction of municipal solid waste and methane production: A review," *Waste Manag.*, vol. 54, pp. 3–12, 2016.
- [17] P. Biller, R. Riley, and A. B. Ross, "Catalytic hydrothermal processing of microalgae: Decomposition and upgrading of lipids," *Bioresour. Technol.*, vol. 102, no. 7, pp. 4841–4848, 2011.
- [18] W. Bühler, E. Dinjus, H. J. Ederer, A. Kruse, and C. Mas, "Ionic reactions and pyrolysis of glycerol as competing reaction pathways in near- and supercritical water," *J. Supercrit. Fluids*, vol. 22, no. 1, pp. 37–53, 2002.
- [19] C. Tian, B. Li, Z. Liu, Y. Zhang, and H. Lu, "Hydrothermal liquefaction for algal biorefinery:

- A critical review,” *Renew. Sustain. Energy Rev.*, vol. 38, pp. 933–950, 2014.
- [20] M. Daroch, S. Geng, and G. Wang, “Recent advances in liquid biofuel production from algal feedstocks,” *Appl. Energy*, vol. 102, pp. 1371–1381, 2013.
- [21] S. S. Toor, L. Rosendahl, and A. Rudolf, “Hydrothermal liquefaction of biomass: A review of subcritical water technologies,” *Energy*, vol. 36, no. 5, pp. 2328–2342, 2011.
- [22] P. Biller and A. B. Ross, “Potential yields and properties of oil from the hydrothermal liquefaction of microalgae with different biochemical content,” *Bioresour. Technol.*, vol. 102, no. 1, pp. 215–225, 2011.
- [23] Y. Gao, X. H. Wang, H. P. Yang, and H. P. Chen, “Characterization of products from hydrothermal treatments of cellulose,” *Energy*, vol. 42, no. 1, pp. 457–465, 2012.
- [24] Y. Dote, S. Inoue, T. Ogi, and S. Y. Yokoyama, “Distribution of nitrogen to oil products from liquefaction of amino acids,” *Bioresour. Technol.*, vol. 64, no. 2, pp. 157–160, 1998.
- [25] D. R. Vardon *et al.*, “Chemical properties of biocrude oil from the hydrothermal liquefaction of *Spirulina* algae, swine manure, and digested anaerobic sludge,” *Bioresour. Technol.*, vol. 102, no. 17, pp. 8295–8303, 2011.
- [26] A. A. Peterson, F. Vogel, R. P. Lachance, M. Fröling, M. J. Antal, Jr., and J. W. Tester, “Thermochemical biofuel production in hydrothermal media: A review of sub- and supercritical water technologies,” *Energy Environ. Sci.*, vol. 1, no. 1, p. 32, 2008.
- [27] Y. Zhang, “Hydrothermal Liquefaction to Convert Biomass into Crude Oil,” in *Biofuels from Agricultural Wastes and Byproducts*, 2010, pp. 201–232.
- [28] D. Klingler, J. Berg, and H. Vogel, “Hydrothermal reactions of alanine and glycine in sub- and supercritical water,” *J. Supercrit. Fluids*, vol. 43, no. 1, pp. 112–119, 2007.
- [29] H. Chen, D. Zhou, G. Luo, S. Zhang, and J. Chen, “Macroalgae for biofuels production: Progress and perspectives,” *Renew. Sustain. Energy Rev.*, vol. 47, pp. 427–437, 2015.
- [30] Y. Guo, T. Yeh, W. Song, D. Xu, and S. Wang, “A review of bio-oil production from hydrothermal liquefaction of algae,” *Renew. Sustain. Energy Rev.*, vol. 48, no. June 2016, pp. 776–790, 2015.
- [31] S. M. Changi, J. L. Faeth, N. Mo, and P. E. Savage, “Hydrothermal Reactions of Biomolecules Relevant for Microalgae Liquefaction,” *Ind. Eng. Chem. Res.*, vol. 54, no. 47, pp. 11733–11758, 2015.
- [32] B. E. O. Eboibi, D. M. Lewis, P. J. Ashman, and S. Chinnasamy, “Hydrothermal liquefaction of microalgae for biocrude production: Improving the biocrude properties with vacuum distillation,” *Bioresour. Technol.*, vol. 174, pp. 212–221, 2014.
- [33] C. Jazrawi *et al.*, “Two-stage hydrothermal liquefaction of a high-protein microalga,” *Algal Res.*, vol. 8, pp. 15–22, 2015.
- [34] Y. F. Yang, C. P. Feng, Y. Inamori, and T. Maekawa, “Analysis of energy conversion characteristics in liquefaction of algae,” vol. 43, pp. 21–33, 2004.
- [35] A. B. Ross, P. Biller, M. L. Kubacki, H. Li, A. Lea-Langton, and J. M. Jones, “Hydrothermal processing of microalgae using alkali and organic acids,” *Fuel*, vol. 89, no. 9, pp. 2234–2243, 2010.
- [36] N. Neveux *et al.*, “Biocrude yield and productivity from the hydrothermal liquefaction of marine and freshwater green macroalgae,” *Bioresour. Technol.*, vol. 155, pp. 334–341, 2014.
- [37] P. J. Valdez, M. C. Nelson, H. Y. Wang, X. N. Lin, and P. E. Savage, “Hydrothermal liquefaction of *Nannochloropsis* sp.: Systematic study of process variables and analysis of the product fractions,” *Biomass and Bioenergy*, vol. 46, pp. 317–331, 2012.
- [38] Y. Dote, S. Inoue, T. Ogi, and S. Y. Yokoyama, “Studies on the direct liquefaction of protein-contained biomass: The distribution of nitrogen in the products,” *Biomass and Bioenergy*, vol. 11, no. 6, pp. 491–498, 1996.
- [39] \* a Krzysztof Stanczyk a, Hak Soo Kim b, C. Sayag b, Dominique Brodzki b and G´erald Dj´ega-Mariadassou b, “HDN of 1-4 tetrahydroquinoline over MoN<sub>x</sub>O<sub>y</sub> and NbN<sub>x</sub>O<sub>y</sub>: Effect of transition metal, solvent and ammonia,” *CEUR Workshop Proc.*, vol. 53, pp. 59–64, 1998.
- [40] D. Canelas, “Basic concepts of chemical Bonding,” in *Chemistry: The Central Science (13th Edition)*, 2015, pp. 326–329.
- [41] K. L. Kim, N. H. Chung, and K. S. Choi, “A study of hydrodenitrogenation of pyridine catalyzed by sulfided Ni-Mo/ $\gamma$ -Al<sub>2</sub>O<sub>3</sub>,” *Korean J. Chem. Eng.*, vol. 4, no. 1, pp. 61–65, 1987.

- [42] G. C. Hadjiloizou, J. B. Butt, and J. S. Dranoff, "Pyridine hydrogenation and piperidine hydrogenolysis on a commercial hydrocracking catalyst I. Reaction and deactivation kinetics," *J. Catal.*, vol. 131, no. 2, pp. 545–572, 1991.
- [43] T. Zhang *et al.*, "Transformation of nitrogen compounds in deasphalted oil hydrotreating: Characterized by electrospray ionization fourier transform-ion cyclotron resonance mass spectrometry," *Energy and Fuels*, vol. 27, no. 6, pp. 2952–2959, 2013.
- [44] H. F. Silver and N. H. Wang, "a Comparison of Shale Gas O I L Denitrification Reactions," *Prepr Pap Present Am Chem Soc Div Fuel Chem*, vol. 19, no. 2, pp. 147–155, 1974.
- [45] "EST." [Online]. Available: [https://www.eni.com/docs/en\\_IT/enicom/publications-archive/company/operations-strategies/refining-marketing/eni\\_EST\\_esecutivo.pdf](https://www.eni.com/docs/en_IT/enicom/publications-archive/company/operations-strategies/refining-marketing/eni_EST_esecutivo.pdf). [Accessed: 27-Aug-2018].
- [46] E. M. Giuseppe Bellussi, Giacomo Rispoli, Daniele Molinari, Alberto Landoni, Paolo Pollesel, Nicoletta Panariti, Roberto Millini, "The role of MoS<sub>2</sub> nano-slabs in the protection of the heterogeneous cracking catalyst for the total conversion of heavy oils to good quality distillates," *Catal. Sci. Technol.*, vol. 3, p. 176, 2013.
- [47] D. C. Elliott, P. Biller, A. B. Ross, A. J. Schmidt, and S. B. Jones, "Hydrothermal liquefaction of biomass: Developments from batch to continuous process," *Bioresour. Technol.*, vol. 178, pp. 147–156, 2015.
- [48] Y. Xue, H. Chen, and Y. Zhao, "A review on the operating conditions of producing bio-oil from hydrothermal liquefaction of biomass," *Int. J. energy Res.*, vol. 40, pp. 865–877, 2015.
- [49] C. Jazrawi, P. Biller, A. B. Ross, A. Montoya, T. Maschmeyer, and B. S. Haynes, "Pilot plant testing of continuous hydrothermal liquefaction of microalgae," *Algal Res.*, vol. 2, no. 3, pp. 268–277, 2013.
- [50] T. M. Brown, P. Duan, and P. E. Savage, "Hydrothermal Liquefaction and Gasification of *Nannochloropsis* sp .," *Energy Fuels*, vol. 24, pp. 3639–3646, 2010.
- [51] X. Peng, X. Ma, Y. Lin, X. Wang, X. Zhang, and C. Yang, "Effect of process parameters on solvolysis liquefaction of *Chlorella pyrenoidosa* in ethanol-water system and energy evaluation," *Energy Convers. Manag.*, vol. 117, pp. 43–53, 2016.
- [52] B. E. Eboibi, D. M. Lewis, P. J. Ashman, and S. Chinnasamy, "Effect of operating conditions on yield and quality of biocrude during hydrothermal liquefaction of halophytic microalga *Tetraselmis* sp.," *Bioresour. Technol.*, vol. 170, pp. 20–29, 2014.
- [53] J. L. Faeth, P. J. Valdez, and P. E. Savage, "Fast Hydrothermal Liquefaction of *Nannochloropsis* sp. To Produce Biocrude," *Energy Fuels*, vol. 27, no. 3, pp. 1391–1398, 2013.
- [54] A. Demirbaş, M. Balat, and K. Bozbaş, "Direct and catalytic liquefaction of wood species in aqueous solution," *Energy Sources*, vol. 27, pp. 271–277, 2005.
- [55] L. Zhang, C. (Charles) Xu, and P. Champagne, "Overview of recent advances in thermochemical conversion of biomass," *Energy Convers. Manag.*, vol. 5, pp. 969–982, 2010.
- [56] A. Hammerschmidt *et al.*, "Catalytic conversion of waste biomass by hydrothermal treatment," *Fuel*, vol. 90, no. 2, pp. 555–562, 2011.
- [57] M. Watanabe, T. Iida, and H. Inomata, "Decomposition of a long chain saturated fatty acid with some additives in hot compressed water," *Energy Convers. Manag.*, vol. 47, pp. 3344–3350, 2006.
- [58] U. Jena, K. C. Das, and J. R. Kastner, "Comparison of the effects of Na<sub>2</sub>CO<sub>3</sub>, Ca<sub>3</sub>(PO<sub>4</sub>)<sub>2</sub>, and NiO catalysts on the thermochemical liquefaction of microalga *Spirulina platensis*," *Appl. Energy*, vol. 98, pp. 368–375, 2012.
- [59] Z. Shuping, W. Yulong, Y. Mingde, I. Kaleem, L. Chun, and J. Tong, "Production and characterization of bio-oil from hydrothermal liquefaction of microalgae *Dunaliella tertiolecta* cake," *Energy*, vol. 35, no. 12, pp. 5406–5411, 2010.
- [60] T. O. Matsui, A. Nishihara, C. Ueda, M. Ohtsuki, N. O. Ikenaga, and T. Suzuki, "Liquefaction of micro-algae with iron catalyst," *Fuel*, vol. 76, no. 11, pp. 1043–1048, 1997.
- [61] C. Yang, L. Jia, C. Chen, G. Liu, and W. Fang, "Bio-oil from hydro-liquefaction of *Dunaliella salina* over Ni/REHY catalyst," *Bioresour. Technol.*, vol. 102, no. 6, pp. 4580–4584, 2011.
- [62] Y. Xu, P. Duan, and B. Wang, "Catalytic upgrading of pretreated algal oil with a two-component catalyst mixture in supercritical water," *Algal Res.*, vol. 9, pp. 186–193, 2015.

- [63] X. Bai, P. Duan, Y. Xu, A. Zhang, and P. E. Savage, "Hydrothermal catalytic processing of pretreated algal oil: A catalyst screening study," *Fuel*, vol. 120, no. March, pp. 141–149, 2014.
- [64] P. Duan and P. E. Savage, "Hydrothermal liquefaction of a microalga with heterogeneous catalysts," *Ind. Eng. Chem. Res.*, vol. 50, pp. 52–61, 2011.
- [65] G. Van Rossum, W. Zhao, M. C. Barnes, J. P. Lange, and S. R. A. Kersten, "Liquefaction of lignocellulosic biomass: Solvent, process parameter, and recycle oil screening," *ChemSusChem*, vol. 7, no. 1, pp. 253–259, 2014.
- [66] X. Yuan *et al.*, "Comparative studies of thermochemical liquefaction characteristics of microalgae using different organic solvents," *Energy*, vol. 36, no. 11, pp. 6406–6412, 2011.
- [67] H. Huang *et al.*, "Thermochemical liquefaction characteristics of microalgae in sub- and supercritical ethanol," *Fuel Process. Technol.*, vol. 92, no. 1, pp. 147–153, 2011.
- [68] N. Sato, A. T. Quitain, K. Kang, H. Daimon, and K. Fujie, "Reaction Kinetics of Amino Acid Decomposition in High-Temperature and High-Pressure Water," *Ind. Eng. Chem. Res.*, vol. 43, no. 13, pp. 3217–3222, 2004.
- [69] D. K. Alargov, S. Deguchi, K. Tsujii, and K. Horikoshi, "Subcritical Water Conditions," vol. 1981, pp. 1–12, 2001.
- [70] M. Faisal, N. Sato, A. T. Quitain, H. Daimon, and K. Fujie, "Reaction kinetics and pathway of hydrothermal decomposition of aspartic acid," *Int. J. Chem. Kinet.*, vol. 39, no. 3, pp. 175–180, 2007.
- [71] Y. F. and K. Yamamoto, "Hydrothermal synthesis of oligoglycines with adiabatic expansion cooling," vol. 33, pp. 269–274, 2005.
- [72] N. Lee, D. I. Foustoukos, D. A. Sverjensky, G. D. Cody, and R. M. Hazen, "The effects of temperature, pH and redox state on the stability of glutamic acid in hydrothermal fluids," *Geochim. Cosmochim. Acta*, vol. 135, pp. 66–86, 2014.
- [73] Y. Chen, Y. Huang, J. Xie, X. Yin, and C. Wu, "Hydrothermal reaction of phenylalanine as a model compound of algal protein," *J. Fuel Chem. Technol.*, vol. 42, no. 1, pp. 61–67, 2014.
- [74] S. Changi, M. Zhu, and P. E. Savage, "Hydrothermal reaction kinetics and pathways of phenylalanine alone and in binary mixtures," *ChemSusChem*, vol. 5, no. 9, pp. 1743–1757, 2012.
- [75] W. Abdelmoez, T. Nakahasi, and H. Yoshida, "Amino acid transformation and decomposition in saturated subcritical water conditions," *Ind. Eng. Chem. Res.*, vol. 46, no. 16, pp. 5286–5294, 2007.
- [76] M. Nagamori and T. Funazukuri, "Glucose production by hydrolysis of starch under hydrothermal conditions," *J. Chem. Technol. Biotechnol.*, vol. 79, no. 3, pp. 229–233, 2004.
- [77] T. Miyazawa, S. Ohtsu, Y. Nakagawa, and T. Funazukuri, "Solvothetical treatment of starch for the production of glucose and maltooligosaccharides," *J. Mater. Sci.*, vol. 41, no. 5, pp. 1489–1494, 2006.
- [78] E. Minami and S. Saka, "Kinetics of hydrolysis and methyl esterification for biodiesel production in two-step supercritical methanol process," vol. 85, pp. 2479–2483, 2006.
- [79] R. Alenezi, G. A. Leeke, R. C. D. Santos, A. R. Khan, U. D. Division, and P. O. Box, "Chemical Engineering Research and Design Hydrolysis kinetics of sunflower oil under subcritical water conditions," vol. 7, no. May, pp. 867–873, 2008.
- [80] R. L. Orozco, M. D. Redwood, G. A. Leeke, A. Bahari, R. C. D. Santos, and L. E. Macaskie, "Hydrothermal hydrolysis of starch with CO<sub>2</sub> and detoxification of the hydrolysates with activated carbon for bio-hydrogen fermentation," *Int. J. Hydrogen Energy*, vol. 37, no. 8, pp. 6545–6553, 2012.
- [81] G. Teri, L. Luo, and P. E. Savage, "Hydrothermal Treatment of Protein, Polysaccharide, and Lipids Alone and in Mixtures," *Energy Fuels*, vol. 28, pp. 7501–7509, 2014.
- [82] A. Croce, E. Battistel, S. Chiaberge, S. Spera, F. De Angelis, and S. Reale, "A Model Study to Unravel the Complexity of Bio-Oil from Organic Wastes," *ChemSusChem*, vol. 10, pp. 171–181, 2017.
- [83] J. Sun, J. Yang, and M. Shi, "Review of Denitrogenation of Algae Biocrude Produced by Hydrothermal Liquefaction," *Trans. Tianjin Univ.*, vol. 23, no. 4, pp. 301–314, 2017.
- [84] M. G. Al-Shaal, P. J. C. Hausoul, and R. Palkovits, "Efficient, solvent-free hydrogenation of  $\alpha$ -angelica lactone catalysed by Ru/C at atmospheric pressure and room temperature," *Chem.*

- Commun.*, vol. 50, no. 71, pp. 10206–10209, 2014.
- [85] S. Mussatto and J. Teixeira, “Lignocellulose as raw material in fermentation processes,” *Appl. Microbiol. an Microb. Biotechnol.*, vol. 2, pp. 897–907, 2010.
- [86] Z. Anwar, M. Gulfraz, and M. Irshad, “ScienceDirect Agro-industrial lignocellulosic biomass a key to unlock the future bio-energy : A brief review,” *J. Radiat. Res. Appl. Sci.*, vol. 7, pp. 163–173, 2014.
- [87] B. Dalecka, M. Strods, and L. Mezule, “Production of fermentation feedstock from lignocellulosic biomass : applications of membrane separation,” vol. 13, no. 2, pp. 287–293, 2015.
- [88] D. Ghosh *et al.*, “Fuels and Chemicals from Lignocellulosic Biomass : An Integrated Biorefinery Approach,” *Energy Fuels*, vol. 29, pp. 3149–3157, 2015.
- [89] A. B. Chhetri, K. C. Watts, and M. R. Islam, “Waste Cooking Oil as an Alternate Feedstock for Biodiesel Production,” *Energies* 2, vol. 1, pp. 3–18, 2008.
- [90] G. Jin, F. Yang, C. Hu, H. Shen, and Z. K. Zhao, “Bioresource Technology Enzyme-assisted extraction of lipids directly from the culture of the oleaginous yeast *Rhodospiridium toruloides*,” *Bioresour. Technol.*, vol. 111, pp. 378–382, 2012.
- [91] I. Espinosa-gonzalez, A. Parashar, and D. C. Bressler, “Hydrothermal treatment of oleaginous yeast for the recovery of free fatty acids for use in advanced biofuel production,” *J. Biotechnol.*, vol. 187, pp. 10–15, 2014.
- [92] Y. Liang, Y. Cui, J. Trushenski, and J. W. Blackburn, “Bioresource Technology Converting crude glycerol derived from yellow grease to lipids through yeast fermentation,” *Bioresour. Technol.*, vol. 101, no. 19, pp. 7581–7586, 2010.
- [93] P. E. Hegel, S. Camy, P. Destrac, and J. S. Condoret, “The Journal of Supercritical Fluids Influence of pretreatments for extraction of lipids from yeast by using supercritical carbon dioxide and ethanol as cosolvent,” *J. Supercrit. Fluids*, vol. 58, no. 1, pp. 68–78, 2011.
- [94] U. Jena *et al.*, “Oleaginous yeast platform for producing biofuels via co-solvent hydrothermal liquefaction,” *Biotechnol. Biofuels*, vol. 8, no. 1, pp. 1–19, 2015.
- [95] N. P. Price, K. M. Bischoff, T. D. Leathers, A. A. Cossé, and P. Manitchotpisit, “Polyols, not sugars, determine the structural diversity of anti-streptococcal liamocins produced by *Aureobasidium pullulans* strain NRRL 50380,” *J. Antibiot. (Tokyo)*, vol. 70, no. 2, pp. 136–141, 2016.
- [96] N. P. J. Price, P. Manitchotpisit, K. E. Vermillion, M. J. Bowman, and T. D. Leathers, “Structural characterization of novel extracellular liamocins (mannitol oils) produced by *Aureobasidium pullulans* strain NRRL 50380,” *Carbohydr. Res.*, vol. 370, pp. 24–32, 2013.
- [97] P. Manitchotpisit *et al.*, “*Aureobasidium pullulans* as a source of liamocins (heavy oils) with anticancer activity,” *World J. Microbiol. Biotechnol.*, vol. 30, no. 8, pp. 2199–2204, 2014.
- [98] E. Kendrick, “A Mass Scale Based on  $CH_2 = 14.0000$  for High Resolution Mass Spectrometry of Organic Compounds,” *Anal. Chem.*, vol. 35, no. 13, pp. 2146–2154, 1963.
- [99] S. Chiaberge *et al.*, “Investigation of Asphaltene Chemical Structural Modification Induced by Thermal Treatments,” vol. 89, no. 18, pp. 4486–4495, 2009.
- [100] S. K. Panda, J. T. Andersson, and W. Schrader, “Characterization of Supercomplex Crude Oil Mixtures : What Is Really in There ?,” *Angew Chem Int Ed Engl.*, vol. 48, no. 10, pp. 1788–1791, 2009.
- [101] M. Wu, J. Long, A. Huang, Y. Luo, S. Feng, and R. Xu, “Microemulsion-mediated hydrothermal synthesis and characterization of nanosize rutile and anatase particles,” *Langmuir*, vol. 15, no. 26, pp. 8822–8825, 1999.
- [102] M. Andersson, L. Osterlund, S. Ljungstrom, and a Palmqvist, “by Hydrothermal Treatment of Microemulsions and Their Activity for Photocatalytic Wet Oxidation of Phenol,” *J. Phys. Chem. B*, vol. 106, pp. 10674–10679, 2002.
- [103] T. Kurosawa, K. Sakai, T. Nakahara, Y. Oshima, and T. Tabuch, “Extracellular accumulation of the polyol lipids, 3,5-dihydroxydecanoyl and 5-hydroxy-2-decenoyl esters of arabitol and mannitol, by *aureobasidium* sp.,” *Biosci. Biotechnol. Biochem.*, vol. 58, no. 11, pp. 2057–2060, 1994.
- [104] T. Minowa, S.-Y. Yokoyama, M. Kishimoto, and T. Okakurat, “Oil production from algal cells of *Dunaliella tertiolecta* by direct thermochemical liquefaction,” *Fuel*, vol. 74, no. 12, pp.

- 1735–1738, 1995.
- [105] R. Shakya, J. Whelen, S. Adhikari, R. Mahadevan, and S. Neupane, “Effect of temperature and Na<sub>2</sub>CO<sub>3</sub> catalyst on hydrothermal liquefaction of algae,” *ALGAL*, vol. 12, pp. 80–90, 2015.
- [106] G. Yoo, M. S. Park, J. W. Yang, and M. Choi, “Lipid content in microalgae determines the quality of biocrude and Energy Return On Investment of hydrothermal liquefaction,” *Appl. Energy*, vol. 156, pp. 354–361, 2015.
- [107] K. Anastasakis and A. B. Ross, “Hydrothermal liquefaction of the brown macro-alga *Laminaria Saccharina*: Effect of reaction conditions on product distribution and composition,” *Bioresour. Technol.*, vol. 102, no. 7, pp. 4876–4883, 2011.
- [108] H. I. Hwang, T. G. Hartman, R. T. Rosen, and C. T. Ho, “Formation of Pyrazines from the Maillard Reaction of Glucose and Glutamine-amide-15N,” *J. Agric. Food Chem.*, vol. 41, no. 11, pp. 2112–2115, 1993.
- [109] H. I. Hwang, T. G. Hartman, and C. T. Ho, “Relative Reactivities of Amino Acids in the Formation of Pyridines, Pyrroles, and Oxazoles,” *J. Agric. Food Chem.*, vol. 43, no. 11, pp. 2917–2921, 1995.
- [110] J. D. Campbell, J. A. Allaway, F. Teymour, and M. Morbidelli, “High-Temperature Polymerization of Styrene: Mechanism Determination with Preparative Gel Permeation Chromatography, Matrix-Assisted Laser Desorption / Ionization Time-of-Flight Mass Spectrometry, and <sup>13</sup>C Nuclear Magnetic Resonance,” *J. Appl. Polym. Sci.*, vol. 94, pp. 890–908, 2004.
- [111] A. A. Peterson, R. P. Lachance, and J. W. Tester, “Kinetic Evidence of the Maillard Reaction in Hydrothermal Biomass Processing: Glucose - Glycine Interactions in High-Temperature, High-Pressure Water,” *Ind. Eng. Chem. Res.*, vol. 49, no. 5, pp. 2107–2117, 2010.
- [112] L. Luo, L. Dai, and P. E. Savage, “Catalytic Hydrothermal Liquefaction of Soy Protein Concentrate,” *Energy Fuels*, vol. 29, no. 5, pp. 3208–3214, 2015.
- [113] A. N. Adams, V. Polizzi, M. Van Boekel, and N. De Kimpe, “Formation of pyrazines and a novel pyrrole in Maillard model systems of 1,3-dihydroxyacetone and 2-oxopropanal,” *J. Agric. Food Chem.*, vol. 56, no. 6, pp. 2147–2153, 2008.
- [114] V. A. Yaylayan and A. Keyhani, “Elucidation of the mechanism of pyrrole formation during thermal degradation of (<sup>13</sup>C)-labeled L-serines,” *Food Chem.*, vol. 74, no. 1, pp. 1–9, 2001.
- [115] ROBERT L. FRANK AND RAYMOND P., “Pyridines. IV. A Study of the Chichibabin Synthesis,” vol. 71, pp. 2629–2635, 1949.
- [116] A. Naidja and B. Siffert, “Glutamic acid deamination in the presence of montmorillonite,” *Clay Miner.*, vol. 24, no. 4, pp. 649–661, 1989.
- [117] D. J. Ager and I. Prakash, “Reductions of Aromatic Amino Acids and Derivatives,” *Org. Process Res. Dev.*, vol. 7, no. 2, pp. 164–167, 2003.
- [118] S. Bagheri, N. Muhd Julkapli, and S. Bee Abd Hamid, “Titanium dioxide as a catalyst support in heterogeneous catalysis,” *ScientificWorldJournal*, vol. 2014, p. 727496, 2014.
- [119] X. Zhang, R. Luo, Z. Wang, Y. Deng, and G. Q. Chen, “Application of (R)-3-hydroxyalkanoate methyl esters derived from microbial polyhydroxyalkanoates as novel biofuels,” *Biomacromolecules*, vol. 10, no. 4, pp. 707–711, 2009.
- [120] E. Busto, N. Richter, B. Grischek, and W. Kroutil, “Biocontrolled formal inversion or retention of L- $\alpha$ -amino acids to enantiopure (R)- or (S)-hydroxyacids,” *Chem. - A Eur. J.*, vol. 20, no. 35, pp. 11225–11228, 2014.
- [121] R. B. Levine, T. Pinnarat, and P. E. Savage, “Biodiesel Production from Wet Algal Biomass through in Situ Lipid Hydrolysis and Supercritical Transesterification,” *Energy Fuels*, vol. 24, pp. 5235–5243, 2010.
- [122] N. Sudasinghe *et al.*, “High resolution FT-ICR mass spectral analysis of bio-oil and residual water soluble organics produced by hydrothermal liquefaction of the marine microalga *Nannochloropsis salina*,” *Fuel*, vol. 119, pp. 47–56, 2014.
- [123] A. W. K. R. F. VESONDER, F. H. STODOLA, “Formation of the  $\alpha$ -Lactone of 3,5-Dihydroxydecanoic Acid by the Fungus *Cephalosporium recifei*,” *Can. J. Biochem.*, vol. 50, pp. 363–365, 1972.
- [124] H. Virkki, A. Vuori, and T. Vuorinen, “Intramolecular Lactonization of Poly ( $\alpha$ -hydroxyacrylic acid): Kinetics and Reaction Mechanism,” *J. Polym.*, vol. 2015, pp. 1–9, 2015.

- [125] M. Chia, T. J. Schwartz, B. H. Shanks, and J. A. Dumesic, "Triacetic acid lactone as a potential biorenewable platform chemical," *Green Chem.*, vol. 14, no. 7, pp. 1850–1853, 2012.
- [126] J. Devine, "The composition of stillingia oil and the presence therein of 2:4-decadienoic acid," *J. Sci. Food Agric.*, vol. 1, no. 3, pp. 88–92, 1950.
- [127] B. P. Pinto, A. L. L. Fortuna, C. P. Cardoso, and C. J. A. Mota, "Hydrogenation of Levulinic Acid (LA) to  $\gamma$ -Valerolactone (GVL) over Ni–Mo/C Catalysts and Water-Soluble Solvent Systems," *Catal. Letters*, vol. 147, no. 3, pp. 751–757, 2017.
- [128] L. Shuai and J. Luterbacher, "Organic Solvent Effects in Biomass Conversion Reactions," *ChemSusChem*, vol. 9, no. 2, pp. 133–155, 2016.
- [129] J. Q. Bond, D. Martin Alonso, R. M. West, and J. A. Dumesic, " $\gamma$ -valerolactone ring-opening and decarboxylation over SiO<sub>2</sub>/Al<sub>2</sub>O<sub>3</sub> in the presence of water," *Langmuir*, vol. 26, no. 21, pp. 16291–16298, 2010.
- [130] "1,3-octadiene." [Online]. Available: <http://www.hmdb.ca/metabolites/HMDB0040966>. [Accessed: 28-Aug-2018].
- [131] "butyrolactone." [Online]. Available: [http://www.who.int/medicines/areas/quality\\_safety/4\\_3\\_EPR\\_1.pdf](http://www.who.int/medicines/areas/quality_safety/4_3_EPR_1.pdf). [Accessed: 28-Aug-2018].
- [132] J. Folch, M. Lees, and G. H. Sloane Stanley, "A simple method for the isolation and purification of total lipides from animal tissues," *Send to J Biol Chem*, vol. 55, no. 5, pp. 999–1033, 1957.
- [133] E. . Bligh and W. . Dyer, "A rapid method of total lipid extraction and purification," *J. Biochem. Physiol.*, vol. 37, no. 8, pp. 911–917, 1959.

## **Report of the academic activities**

### Mobility's scheme:

- Bologna University: November 01, 2015 - May 01, 2016
- Renewable Energy and Environmental R&D Center, Instituto Eni Donegani: May 02, 2016 - May 01, 2017
- Bologna University: May 02, 2017 - January 12, 2018
- RWTH Aachen University: January 15, 2018 - July 15, 2018
- Bologna University: July 18, 2018 - November 01, 2018

### Conferences and schools attendance, results dissemination:

- The 2-nd EFCATS-CNRS European Summer School on Catalyst Preparation. 12-17 June, 2016. France. (Poster).
- The 3rd International Conference of the Cluster of Excellence Tailor Made fuel from biomass (TMFB). 21-23 June 2016. Germany. (Poster).
- 13<sup>th</sup> European Congress (Europacat 2017). 27-31 August 2017. Italy. (Poster).
- DGMK International Conference "International Conference. Petrochemistry and Refining in a Changing Raw Materials Landscape." 9-12 October 2017. Germany. (Oral presentation).
- SINCHEM & Phototrain winter school. 12/02-14/02/2018. Department of Industrial Chemistry, "Toso Montanari", University of Bologna. Italy.
- 7th International Conference on Engineering for waste and Biomass Valorisation. 2-5 June 2018. Czech Republic (Oral presentation).
- "Green Chemistry (GRS)" Gordon Research Seminar and Conference. 28 July-3 August 2018. Spain. (Poster).

### **The list of publications**

1. A. Matayeva, F. Basile, F. Cavani, D. Bianchi, S. Chiaberge. Bio-oil upgrading via HTL and pyrolysis. (2018). Horizons in Sustainable Industrial Chemistry and Catalysis. Elsevier.
2. A. Matayeva, D. Bianchi, S. Chiaberge, F. Cavani, F. Basile. Elucidation of reaction pathways of nitrogenous species by hydrothermal liquefaction process of model compounds. Fuel 240 (2019) 169–178.